

TERMINATION OF THE SOLAR WIND IN THE HOT,  
PARTIALLY IONIZED INTERSTELLAR MEDIUM

NASA Grant NGR 05-020-330

A DISSERTATION  
SUBMITTED TO THE DEPARTMENT OF APPLIED MECHANICS  
AND THE COMMITTEE ON GRADUATE STUDIES  
OF STANFORD UNVIERSITY  
IN PARTIAL FULFILLMENT OF THE REQUIREMENTS  
FOR THE DEGREE OF  
DOCTOR OF PHILOSOPHY

(NASA-CR-140699) TERMINATION OF THE  
SOLAR WIND IN THE HOT, PARTIALLY IONIZED  
INTERSTELLAR MEDIUM Ph.D. Thesis  
(Stanford Univ.) 152 p HC \$6.25

N75-10893

Unclas  
52658

CSCL 03B G3/92

By

Charles Klem Lombard

November 1974

## Acknowledgments

The author wishes to express particular appreciation to Professor John R. Spreiter for suggesting the thesis topic and for his warm friendship and helpful guidance throughout its development. Special thanks are also due to Professors Krishnamurty Karamcheti and Peter A. Sturrock in whose courses the author found preparation and who kindly consented to serve as readers.

The author also wishes to thank Mr. Harvard Lomax and Mrs. Audrey Summers of NASA - Ames Research Center for useful suggestions with respect to the numerical computations. Mr. Ray Reynolds kindly made facilities available at Ames.

The author is personally indebted to Mrs. Theofana Hegis for her patient typing of the manuscript.

This research was partially supported by the National Aeronautics and Space Administration under Grant NGR 05-020-330 administered by NASA Headquarters as part of their Physics and Astronomy Program and by the Atmospheric Sciences Section of the National Science Foundation under Grant GA-3761 as part of their Solar-Terrestrial Research Program.

## TABLE OF CONTENTS

Chapter		Page
I.	The Problem	1
	1. Introduction - Physical and Historical Perspective	1
	a. Static, heat conducting corona	2
	b. Dynamic, polytrope corona	6
	2. Shock Termination of the Solar Wind	16
	3. Heating and Flowfield Temperature	34
	4. Modern Developments - Particle Interactions	44
	a. Photoionization	46
	b. Charge exchange	50
	c. Linear theory for the supersonic region	61
	d. Lyman- $\alpha$ scattering and radiation pressure on hydrogen	70
II.	A Mathematical Model	75
	1. Distribution Functions, Boltzmann's Equations, and the Plasma Transport Equations	75
	2. The Magnetohydrodynamic Description	90
	a. Maxwell's equations and the MHD approximation	90
	b. Discontinuity relations of the MHD formulation	97
	c. Equations of quasi-one-dimensional compressible flow	104
	3. Transport of Hydrogen of Interstellar Origin and Moments of the Distribution Function	109
III.	Numerical Results - Interplanetary Neutral Hydrogen and the Speed of the Interstellar Wind	118
	1. Algorithm for Computing Moments of the Hydrogen Distribution Function	118
	2. Axial Profiles of Hydrogen Number Density	122

TABLE OF CONTENTS (cont.)

Chapter

III. (cont.)

3. Predicted Intensity of Solar Lyman- $\alpha$  Backscatter from Hydrogen 127

4. Estimates of the Mach Number and Speed of the Interstellar Wind 134

IV. Summary and Discussion 136

References

## List of Figures

Figure		Page
1	Streamlines of flowfield described by the extended Parker solution for the termination of the solar wind.	32
2	Geometry of the hydrogen transport problem.	113
3	Ellipsoid-cylinder approximation to the figure of the heliopause boundary.	121
4	Hydrogen number density profiles computed on the upstream and downstream axes of flow for $N_0 = 0.1 \text{ cm}^{-3}$ , $V_0 = 16.6 \text{ km/s}$ .	123
5	Hydrogen number density profiles computed on the upstream and downstream axes of flow for $N_0 = 0.1 \text{ cm}^{-3}$ , $V_0 = 8 \text{ km/s}$ .	124
6	Comparison of profiles of hydrogen number density for $N_0 = 0.1 \text{ cm}^{-3}$ , $T_0 = 10^4 \text{ }^\circ\text{K}$ , and $V_0 = 8 \text{ km/s}$ and $16.6 \text{ km/s}$ .	126
7	Derivative of the Lyman- $\alpha$ backscatter intensity function for line of sight along upstream and downstream axes of flow.	128
8	Plot of velocity of the interstellar wind vs. computed upstream to downstream Lyman- $\alpha$ backscatter intensity ratio for parameter temperature.	131
9	Universal plot of ratio of interstellar wind velocity to most probable thermal speed vs. ratio of computed upstream to downstream Lyman- $\alpha$ backscatter intensities.	133

## List of Tables

Table		Page
1	Properties of the local interstellar medium	2
2	Properties of two polytropic solutions for dynamic expansion of the solar corona.	14
3	Properties of the solar wind observed at 1 a.u.	16
4	Nominal values for parameters of solar wind and interstellar wind flow regimes.	47
5	Parameters of formulae for primitive rate coefficients for charge exchange.	54
6	Mean free paths for charge exchange and characteristic flowfield dimensions by region.	59
7	Synopsis of computer runs with model predicting Lyman- $\alpha$ backscatter on upstream and downstream axes of flow.	130
8	Maximum and Minimum intensity of Lyman- $\alpha$ backscatter measured by earth satellite at 1 a.u.	134

## Abstract

Theoretical foundations of our understanding of the problem of the termination of the solar wind are reexamined in the light of most recent findings concerning the states of the solar wind and the local interstellar medium. The investigation suggests that a simple extension of Parker's (1961) analytical model provides a useful approximate description of the combined solar wind, interstellar wind plasma flowfield under conditions presently thought to occur. A linear perturbation solution exhibiting both the effects of photoionization and charge exchange is obtained for the supersonic solar wind. The solution demonstrates the point that the addition of mass and decrease of velocity as the result of photoionization in the supersonic region of the solar wind has no effect on the momentum flux and, thus, the location of the shock surface. The effect of charge exchange, however, serves to reduce by about 14% the estimate of the shock radius provided by Parker's solution as extended. Finally, investigation along lines of the one dimensional compressible flow equation and heating associated with polytrope solutions brings to light further theoretical evidence that the classical coefficients of thermal conductivity for an ionized gas may be too high - perhaps by as much as a factor of five - to describe the flow of the supersonic solar wind beyond earth.

Derived from its roots in kinetic theory and the plasma transport equations a la Braginskii (1965), a model for the combined flow of the solar wind with the ionized component of the interstellar wind is formulated on the level of one-fluid magnetohydrodynamics. The model features quasi-normal, strong shock relations on a closed surface surrounding the sun and imbedded in the solar wind. Tangential discontinuity relations apply at the free surface between the solar wind and ionized interstellar

## Chapter I. - The Problem

### 1. Introduction - Physical and Historical Perspective

From the theoretical point of view the termination of the solar wind is the problem of finding a model for the extended solar corona such that admissible boundary conditions match conditions in the perturbed local interstellar medium. Taken in its full physical and attendant mathematical generality the problem is so complex that the pioneer analyst in the subject Parker (1963) quickly and, by events, correctly pronounced that "real progress can come only ad hoc".

After a brief statement of conditions in the local interstellar medium as best they are known to astronomers, we bring forth in this introductory section two such ad hoc models of the corona. The models which combine the virtues of mathematical tractability with broad phenomenological richness serve to illuminate the character of the problem and exhibit important qualitative and semi-quantitative features of its solution. The models are the static, heat conducting corona and the dynamic polytrope corona.

The former model has its roots in the earliest description (Chapman, 1957) of the far corona but a solution satisfying a boundary condition of greater physical content has been found by the present author and is given here. The latter model incorporates the prediction of the interplanetary supersonic solar wind (Parker, 1958). The material, which includes the critical polytrope solution chosen by Parker, is treated in the concise, explicit manner due to Bondi (1952) who had invoked the other member of the family of critical polytrope solutions earlier in the study of stellar accretion.

Axford (1972), Wentzel (1972), and Silk (1973) have recently summarized theory and observation concerning the state of the interstellar



medium in the vicinity of the sun. Neglecting infrequent small dense clouds whose inhomogeneous effect is not the subject of concern here, the picture that emerges is of a tenuous, partially ionized, weakly magnetized, hot hydrogen gas. Typical numbers on which the discussion is based herein appear in Table 1.

Table 1. Properties of the local interstellar medium.

TEMPERATURE	$10^3 - 10^4$ ° K
PARTICLE DENSITY	
NEUTRAL HYDROGEN	$0.1 - 0.2 \text{ cm}^{-3}$
PROTON OR ELECTRON	$0.01 - 0.025 \text{ cm}^{-3}$
MAGNETIC FIELD STRENGTH	$3 \times 10^{-6}$ gauss

a. Static, heat conducting corona

The model assumes a spherically symmetric corona of fully ionized hydrogen gas. The equation of static equilibrium yields

$$\frac{dp}{dr} = - GM_{\odot} m \frac{n}{r^2} \quad (1.1a-1)$$

where at  $r$  the radial distance from the center of the sun  $p$  is the pressure,  $m$  is the mass of a proton and an electron,  $n$  is the number density of protons or electrons,  $M_{\odot}$  is the solar mass, and  $G$  is the universal gravitational constant.

Starting at some high temperature  $T_0$  at  $r_0$  very close to the sun, a constant heat flux is assumed satisfying the energy equation

$$\text{div}(\underline{q}) = 0 \quad (1.1a-2)$$

where  $\underline{q}$  is the conduction heat flux density vector given by

$$\underline{q} = -\kappa \frac{dT}{dr} \quad (1.1a-3)$$

In equation (3) the coefficient of thermal conductivity  $\kappa$  appropriate to fully ionized hydrogen can be expressed as

$$\kappa = A T^{5/2} \quad (1.1a-4)$$

where  $A$  is a constant whose value as computed by Chapman (1954) is  $4 \times 10^{-7}$  in cgs units when the temperature is measured in  $^{\circ}\text{K}$ .

With the spherically symmetric form of the divergence operator, equation (2) with equations (3) and (4) provides the first integral

$$-Ar^2 T^{5/2} \frac{dT}{dr} = q_0 r_0^2 \quad (1.1a-5)$$

Equation (5) is integrated over the interval  $r_0$  to  $r$  yielding

$$T^{7/2} = T_0^{7/2} - \frac{7}{2} \frac{q_0 r_0}{A} \left(1 - \frac{r_0}{r}\right) \quad (1.1a-6)$$

Letting the temperature asymptotically approach the temperature  $T_{\infty}$  of the interstellar medium permits the evaluation of the constant  $\frac{7}{2} \frac{q_0 r_0}{A}$  in equation (6). (Here Chapman (1957) arbitrarily took the temperature to vanish at infinity.)

As the result, equation (6) may be represented

$$T^{7/2} = T_{\infty}^{7/2} + \left(T_0^{7/2} - T_{\infty}^{7/2}\right) \frac{r_0}{r} \quad (1.1a-7)$$

Solving for  $T$  we have

$$T = T_0 \left( \frac{r_0}{r} \right)^{2/7} \left[ 1 + \left( \frac{T_\infty}{T_0} \right)^{7/2} \left( \frac{r}{r_0} - 1 \right) \right]^{2/7} \quad (1.1a-8)$$

When  $T_\infty \ll T_0$  equation (8) predicts that for a vary wide range in  $r$  such that  $\frac{r}{r_0} \ll \left( \frac{T_0}{T_\infty} \right)^{7/2}$  the temperature in the corona drops off as  $r^{-2/7}$ .

Equation (8) and the equation of state

$$p = 2 k n T \quad (1.1a-9)$$

permit the equation of equilibrium (1) to be cast

$$\frac{dp}{dr} = - \epsilon_0 p \left[ \chi + \left( \frac{T_\infty}{T_0} \right)^{7/2} \frac{r}{r_0} \right]^{-2/7} r_0^{5/7} r^{-12/7} \quad (1.1a-10)$$

where  $\epsilon_0 = \frac{GM_0 m}{2kT_0 r_0}$  and  $\chi = 1 - \left( \frac{T_\infty}{T_0} \right)^{7/2}$ .

With the change of variable  $r' = r/r_0$ , equation (10) may be rewritten in the form

$$\frac{dp}{p} = - \epsilon_0 \left[ \frac{\chi}{r'} + \left( \frac{T_\infty}{T_0} \right)^{7/2} r' \right]^{-2/7} \frac{dr'}{r'} \quad (1.1a-11)$$

Equation (11) is integrated over the interval 1 to  $r'$  yielding the solution

$$\begin{aligned}
 p &= p_0 \exp \left[ -\frac{7}{5} \frac{\epsilon_0}{x} \left\{ 1 - \left[ \frac{x}{r} + \left( \frac{T_\infty}{T_0} \right)^{7/2} \right]^{5/7} \right\} \right] \\
 &= p_0 \exp \left[ -\frac{7}{5} \frac{\epsilon_0}{x} \left\{ 1 - \left[ \frac{r_0}{r} + \left( \frac{T_\infty}{T_0} \right)^{7/2} \left( 1 - \frac{r_0}{r} \right) \right]^{5/7} \right\} \right]. \quad (1.1a-12)
 \end{aligned}$$

In the limit as  $r \rightarrow \infty$ ,

$$p_\infty = 2 k n_0 T_0 \exp \left[ -\frac{7}{5} \frac{1 - \left( \frac{T_\infty}{T_0} \right)^{5/2}}{1 - \left( \frac{T_\infty}{T_0} \right)^{7/2}} \epsilon_0 \right] \quad (1.1a-13)$$

The corresponding number density is

$$n_\infty = n_0 \frac{T_0}{T_\infty} \exp \left[ -\frac{7}{5} \frac{1 - \left( \frac{T_\infty}{T_0} \right)^{5/2}}{1 - \left( \frac{T_\infty}{T_0} \right)^{7/2}} \epsilon_0 \right] \quad (1.1a-14)$$

Estimating  $r_0$  by  $R_0 = 7 \times 10^{10}$  cm the radius of the visible disc and taking  $T_\infty = 10^4$  °K from Table 1,  $T_0 = 2 \times 10^6$  °K,  $n_0 = 2 \times 10^8$  cm<sup>-3</sup>, and  $M_0 = 2 \times 10^{33}$  gm, we find that  $\epsilon_0$  is 5.5 approximately. Equations (13) and (14) then predict the pressure far from the sun should have the value  $5 \times 10^{-5}$  dyne/cm<sup>2</sup> and the number density  $2 \times 10^7$  cm<sup>-3</sup>. Since in the solution we have matched temperature in the interstellar medium, the density given by equation (14) being eight orders of magnitude higher than that measured in the interstellar medium implies that the pressures are out of balance by a like amount. (The pressure of the interstellar magnetic field being at best of the order of  $10^{-12}$  dyne/cm<sup>2</sup> offers no help in supporting the static corona.) The model thus grossly failing the condition for static equilibrium, we conclude that the only available mechanism for dropping the inexorable pressure of the solar corona is via action against the inertia forces of dynamic expansion.

Before considering in the next model the consequences of such expansion we close this discussion by noting that at earth distance from the sun the temperature given by equation (8)  $T_e = 4.34 \times 10^5 \text{ }^\circ\text{K}$  is comparable with though larger than the electron temperature  $1.5 \times 10^5 \text{ }^\circ\text{K}$  measured by earth satellites (Montgomery, 1972). Since heat conduction is a process that is defined in the local rest frame of a gas, the process is not inhibited by dynamic expansion but in fact enhanced by the larger temperature gradients resulting from expansion. We therefore expect heat conduction to play a significant role in any comprehensive model of the solar corona.

b. Dynamic, polytrope corona

The model assumes steady, spherically symmetric flow with mass conservation leading to the first integral of the continuity equation the constant mass flux

$$\dot{m} = \rho v r^2 \quad (1.1b-1)$$

where  $v$  is the bulk velocity and where  $\rho$  is the mass density.

The equation of motion is

$$\rho v \frac{dv}{dr} = - \frac{dp}{dr} - G M_o \frac{\rho}{r^2} \quad (1.1b-2)$$

The polytrope law

$$p = \frac{p_o}{\rho_o^\alpha} \rho^\alpha \quad (1.1b-3)$$

where  $\alpha$  is a free parameter is taken to replace the energy equation. Use of the law with equations (1) and (2) serves both to make a tractable mathematical problem and a useful tool in analyzing the nature of solutions of the physical problem being modeled.

After dividing by the mass density  $\rho$  and substituting equation (3), we integrate equation (2) over the interval  $r_0$  to  $r$  yielding

$$\frac{v^2}{2} - \frac{v_0^2}{2} = -\frac{\alpha}{\alpha-1} \frac{p_0}{\rho_0^\alpha} \left[ \rho^{\alpha-1} - \rho_0^{\alpha-1} \right] - G M_0 \left( \frac{1}{r_0} - \frac{1}{r} \right). \quad (1.1b-4)$$

We define at the base of the corona the characteristic speed  $c_0$  by the relation  $c_0^2 = \alpha p_0 / \rho_0$  and the nondimensional parameter  $\epsilon_0 = \frac{G M_0 \rho_0}{p_0 r_0}$ , which is seen to reduce to the same expression as for the static corona. Thence making the changes of variable

$$x = \frac{\alpha}{\epsilon_0} \frac{r}{r_0}, \quad y = \frac{v}{c_0}, \quad z = \rho / \rho_0 \quad (1.1b-5)$$

permits recasting equation (4) in the canonical form

$$\frac{y^2}{2} + \frac{1}{\alpha-1} z^{\alpha-1} = \frac{1}{x} - \frac{1}{x_0} + \frac{y_0^2}{2} + \frac{1}{\alpha-1}. \quad (1.1b-6)$$

Equation (1) may be represented equivalently as

$$y z x^2 = \lambda = \left( \frac{\alpha}{\epsilon_0} \right)^2 \frac{\varphi}{\rho_0 c_0 r_0^2}. \quad (1.1b-7)$$

Since in equations (6) and (7)  $x$  is an explicit function of  $r$ , the problem is to solve the equations for  $y$  and  $z$  as explicit functions of  $x$ .

The solution is obtained with the aid of the substitution

$$\bar{M} = \left[ \frac{y^2}{z^{\alpha-1}} \right]^{1/2} \equiv \frac{v}{c}. \quad (1.1b-8)$$

Solving equations (7) and (8) for  $z$  we get

$$z = \left[ \frac{\lambda}{x^2} \right]^{\frac{2}{\alpha+1}} \bar{M}^{-\frac{2}{\alpha+1}} \quad (1.1b-9)$$

while combining equations (7) and (9) gives

$$y = \left[ \frac{\lambda}{x^2} \right]^{\frac{\alpha-1}{\alpha+1}} \bar{M}^{\frac{2}{\alpha+1}} \quad (1.1b-10)$$

When equations (9) and (10) are substituted in equation (6) there results with some arranging of terms

$$\frac{\bar{M}}{2} \frac{4}{\alpha+1} + \frac{\bar{M}}{\alpha-1} \frac{-2(\alpha-1)}{\alpha+1} = \left( \frac{1}{x} - \frac{1}{x_0} + \frac{y_0^2}{2} + \frac{1}{\alpha-1} \right) \left( \frac{x^2}{\lambda} \right)^{\frac{2(\alpha-1)}{\alpha+1}} \quad (1.1b-11)$$

Equation (11) is of the form

$$f(\bar{M}) = \lambda^{\frac{-2(\alpha-1)}{\alpha+1}} g(x) \quad (1.1b-12)$$

In equation (3)  $\alpha = 1$  describes an isothermal corona which does not admit finite heat conduction and therefore requires a heat source which is unidentifiable except near the sun. Since  $\alpha = \gamma = 5/3$  describes the adiabatic corona, i.e. no heating at all, we are led to investigate the topology of continuous solutions  $\bar{M}(x)$  of equation (11) for  $\alpha$  between 1 and  $5/3$ . To clear up a point of confusion in Bondi's related discussion, in the solutions to be obtained for general  $\alpha$  the characteristic speed  $c = (\alpha p/\rho)^{1/2}$  is not the speed of sound  $a$  and accordingly, equation (8),  $\bar{M}$  is not the Mach number  $M$  but these objects are related by

$$c = \sqrt{\frac{\alpha}{\gamma}} a \quad \text{and} \quad M = \sqrt{\frac{\alpha}{\gamma}} \bar{M} \quad (1.1b-13)$$

To begin the analysis, since  $\bar{M}$  is positive the left hand side of equation (11)  $f(\bar{M})$  is positive definite. The constant  $\lambda$  (related to the mass flux) being positive, solutions of equation (11) require that the function  $g(x)$  be positive definite also. Since  $\frac{1}{x}$  approaches zero as  $r$  approaches infinity, solutions only exist when

$$\frac{y_0^2}{2} + \frac{1}{\alpha-1} > \frac{1}{x_0} \quad (1.1b-14)$$

As we shall confirm by the solution the flow starts out very slowly in relatively dense gas and  $y_0^2/2$  is a very small number compared to  $\frac{1}{\alpha-1}$ . Consequently with  $x_0 = \alpha/\epsilon_0$ , from relation (5), the condition (14) effectively requires

$$\alpha < \frac{\epsilon_0}{\epsilon_0 - 1} \quad (1.1b-15)$$

Since as we have seen in the discussion of the static corona model  $\epsilon_0$  has the value 5.5 approximately, relation (15) indicates that  $\alpha$  should be less than 1.22+.

Analysis of  $f(\bar{M})$  reveals that at  $\bar{M} = 1$  the function has a minimum of value

$$f_m = \frac{\alpha+1}{2(\alpha-1)} \quad (1.1b-16)$$

The function  $g(x)$  also has a minimum of value

$$\epsilon_m = \frac{1}{4} \frac{\alpha+1}{\alpha-1} \left[ \frac{4 \left( 1 + \frac{\alpha-1}{2} y_0^2 - \frac{\alpha-1}{\alpha} \epsilon_0 \right)}{5-3\alpha} \right] \frac{5-3\alpha}{\alpha+1} \quad (1.1b-17)$$



The minimum of the function  $g$  is located at

$$x_m = \frac{5-3\alpha}{4(1 + \frac{\alpha-1}{2} y_o^2 - \frac{\alpha-1}{\alpha} \epsilon_o)} \quad (1.1b-18)$$

Taking differentials of both sides of equation (12) provides the relation

$$f' d\bar{M} = \lambda \frac{-2(\alpha-1)}{\alpha+1} g' dx \quad (1.1b-19)$$

Equation (12) together with the differential relation (19) suggest two kinds of physically meaningful solutions to equation (11).

The first type is the "critical solution" obtained when  $\lambda$  is so chosen that the minima of  $f$  and  $g$  jointly satisfy equation (12). In this case  $f'$  and  $g'$  both change from negative to positive through zero at the same point in the flow and the fluid accelerates smoothly through the critical point leading eventually to supersonic flow. The critical value of  $\lambda$  is denoted by  $\lambda_c$  and is given by

$$\lambda_c = \left( \frac{g_m}{f_m} \right)^{\frac{\alpha+1}{2(\alpha-1)}} = \left( \frac{1}{2} \right)^{\frac{\alpha+1}{2(\alpha-1)}} x_m^{\frac{-(5-3\alpha)}{2(\alpha-1)}} \quad (1.1b-20)$$

Combining equations (20), (10), and (5) we have that the velocity at the critical point is

$$v_c = c_o \left[ \frac{2(1 + \frac{\alpha-1}{2} y_o^2 - \frac{\alpha-1}{\alpha} \epsilon_o)}{5-3\alpha} \right]^{1/2} \quad (1.1b-21)$$

Similarly with equation (9) the critical point density is

$$\rho_c = \rho_o \left[ \frac{2(1 + \frac{\alpha-1}{2} y_o^2 - \frac{\alpha-1}{\alpha} \epsilon_o)}{5-3\alpha} \right]^{\frac{1}{\alpha-1}} \quad (1.1b-22)$$

The corresponding pressure follows from equation (2) as

$$p_c = p_o \left[ \frac{2(1 + \frac{\alpha-1}{2} y_o^2 - \frac{\alpha-1}{\alpha} \epsilon_o)}{5-3\alpha} \right]^{\frac{\alpha}{\alpha-1}} \quad (1.1b-23)$$

Thence the perfect gas law gives for the temperature

$$T_c = T_o \left[ \frac{2(1 + \frac{\alpha-1}{2} y_o^2 - \frac{\alpha-1}{\alpha} \epsilon_o)}{5-3\alpha} \right] \quad (1.1b-24)$$

To exhibit the solution far from the sun, equation (11) approaches asymptotically

$$\bar{M}^{\frac{4}{\alpha+1}} = \lambda^{\frac{-2(\alpha-1)}{\alpha+1}} \left( y_o^2 + \frac{2}{\alpha-1} - \frac{2\epsilon_o}{\alpha} \right) x^{\frac{4(\alpha-1)}{\alpha+1}} \quad (1.1b-25)$$

Combining equations (5), (10), and (25) gives the asymptotic velocity

$$v_\infty = c_o \left[ y_o^2 + \frac{2}{\alpha-1} - \frac{2\epsilon_o}{\alpha} \right]^{1/2} \quad (1.1b-26)$$

which is seen to be a constant.

The critical mass flux from equations (7), (18), and (20) is

$$\psi_c = \left( \frac{1}{2} \right)^{\frac{\alpha+1}{2(\alpha-1)}} \left[ \frac{4(1 + \frac{\alpha-1}{2} y_o^2 - \frac{\alpha-1}{\alpha} \epsilon_o)}{5-3\alpha} \right]^{\frac{5-3\alpha}{2(\alpha-1)}} \frac{\epsilon_o^2}{\alpha^2} \rho_o c_o r_o^2 \quad (1.1b-27)$$

The density at large distance from the sun then varies as

$$\rho = \frac{\varphi_c}{v_\infty} r^{-2} \quad (1.1b-28)$$

Accordingly the pressure approaches asymptotically

$$p = p_0 \left( \frac{\varphi_c}{\rho_0 v_\infty} \right)^\alpha r^{-2\alpha} \quad (1.1b-29)$$

and the temperature varies like

$$T = T_0 \left( \frac{\varphi_c}{\rho_0 v_\infty} \right)^{\alpha-1} r^{-2(\alpha-1)} \quad (1.1b-30)$$

The polytrope solution of the second kind, the subcritical solution, obtains when  $\lambda < \lambda_c$  and the minimum in  $g$  is reached before  $f$  reaches minimum. In this case going through  $x_m$  the derivative  $g'$  changes from negative to positive while  $f'$  remains negative. Consequently  $\frac{d\bar{M}}{dx}$  changes from positive to negative and  $\bar{M}$  is caused to retreat back along the lower branch of  $f$  from the maximum value  $\bar{M}^*$  obtained as the solution of

$$f(\bar{M}^*) = \frac{\alpha+1}{4(\alpha-1)} \lambda^{\frac{-2(\alpha-1)}{\alpha+1}} x_m^{\frac{-5+3\alpha}{\alpha+1}} \quad (1.1b-31)$$

On the lower branch of  $f(\bar{M})$ ,  $\bar{M}$  approaches zero as  $f(\bar{M})$  approaches infinity, corresponding in this solution to  $g$  approaching infinity with  $x$  on the upper branch of  $g$ . Thus in the subcritical solution far from the sun equation (11) approaches asymptotically

$$\bar{M}^{\frac{-2(\alpha-1)}{\alpha+1}} = \lambda^{\frac{-2(\alpha-1)}{\alpha+1}} \left( 1 + \frac{\alpha-1}{2} y_0^2 - \frac{\alpha-1}{\alpha} \epsilon_0 \right) x^{\frac{4(\alpha-1)}{\alpha+1}} \quad (1.1b-32)$$

Solving equation (32) for  $\bar{M}^{\frac{2}{\alpha+1}}$  and combining the results with equations (10) and (5) gives for the far field velocity.

$$v = c_o \lambda \frac{\epsilon_o^2}{\alpha^2} \left( 1 + \frac{\alpha-1}{2} y_o^2 - \frac{\alpha-1}{\alpha} \epsilon_o \right)^{-\frac{1}{\alpha-1}} \frac{r_o^2}{r} \quad (1.1b-33)$$

Inspection of equation (33) in the light of equations (7) and (5) shows that the density far from the sun approaches the constant limit

$$\rho_\infty = \rho_o \left( 1 + \frac{\alpha-1}{2} y_o^2 - \frac{\alpha-1}{\alpha} \epsilon_o \right)^{\frac{1}{\alpha-1}} \quad (1.1b-34)$$

Accordingly from equation (3), the pressure is seen to approach the constant value

$$p_\infty = p_o \left( 1 + \frac{\alpha-1}{2} y_o^2 - \frac{\alpha-1}{\alpha} \epsilon_o \right)^{\frac{\alpha}{\alpha-1}} \quad (1.1b-35)$$

Finally, the temperature also approaches a constant

$$T_\infty = T_o \left( 1 + \frac{\alpha-1}{2} y_o^2 - \frac{\alpha-1}{\alpha} \epsilon_o \right) \quad (1.1b-36)$$

In summary of the character of the two kinds of solutions, the critical solution admits a flow that accelerates continuously approaching a constant supersonic velocity far from the sun. The density correspondingly decreases as  $r^{-2}$  and the pressure and temperature both similarly approach zero far from the sun. Given conditions in the corona, the critical solution for any given  $\alpha$  uniquely defines a mass flux from the sun.

The subcritical solution admits a flow that accelerates continuously to some maximum velocity less than the speed of sound and thence slows continuously approaching zero velocity far from the sun. The velocity history is carried out in such a manner that the density, pressure, and temperature

monotonically drop throughout, approaching constant minimum values far from the sun. Choosing a value of  $\alpha$  does not uniquely define the mass flux since a solution exists for all values of the mass flux less than that prescribed by the critical solution. Since the velocity far from the sun depends linearly on the mass flux and varies inversely with the square of the distance from the sun, the asymptotic values for the density, pressure, and temperature do not depend on the mass flux in the subcritical solution.

Table 2 sets forth values for both types of solution for  $\alpha = 1.15$  and  $\alpha = 1.22$  at salient points in the flows. The value  $\alpha = 1.15$  was chosen because it best reproduces in the critical solution the supersonic velocity measured in the solar wind at earth distance from the sun. The value  $\alpha = 1.22$  was chosen because it best matches in the subcritical solution the pressure in the local interstellar medium.

Comparing both the values of mass flux and velocity in the critical solution at  $\alpha = 1.15$  and the subcritical solution at  $\alpha = 1.22$

Table 2. Properties of two polytrope solutions for dynamic expansion of the solar corona.

	critical	subcritical
$\alpha$	1.15	1.22
$r_c/R_o$	6.6	2.15
$\lambda_c$	$1.4 \times 10^{-3}$	$2.4 \times 10^{-7}$
$f$	$1 \times 10^{12} \text{ gm s}^{-1} \text{ ster}^{-1}$	$1.7 \times 10^8 \text{ gm s}^{-1} \text{ ster}$
$v_c$	$1.2 \times 10^7 \text{ cm s}^{-1}$	$2.1 \times 10^6 \text{ cm s}^{-1}$
$v_\infty$	$4 \times 10^7 \text{ cm s}^{-1}$	0
$T_\infty$	0	$10^4 \text{ }^\circ\text{K}$
$n_\infty$	0	$0.03 \text{ cm}^{-3}$
$P_\infty$	0	$10^{-13} \text{ dyne cm}^{-2}$

evidences the dramatic nature of the labels coined by Parker, "The Solar Wind", and Chamberlain, "The Solar Breeze", in their now famous competitive advocacy of the respective solutions to describe the state of the solar corona (Parker, 1960, 1963; Chamberlain, 1960, 1961).

In the perspective of conditions as measured by instrumented satellites in the interplanetary region, Parker had the better of it, for from the coronal base to earth the solar wind undoubtedly follows a solution close to the critical polytrope. However, at large distances from the sun the critical solution which predicts vanishing density, pressure, and temperature suffers a catastrophic failure and there a chamberlain-like solution is appropriate.

Parker resolved this apparent paradox in a third ad hoc model which we take up in the next section. From the point of view of results developed in the present section, the model provides a synthesis featuring discontinuous branching via a shock transition from a supersonic (critical) solution to a subsonic (subcritical) one. An additional feature of the third model providing greater physical content is that the sun is permitted to move relative to the interstellar gas.

## 2. Shock Termination of the Solar Wind

The model to be presented follows the development brought forth by Parker (1961,1963) to demonstrate characteristic phenomena of the combined flow field resulting from the clash of the supersonic solar wind with the interstellar medium. As the result of certain bold idealizations of the physics of the problem made in the interest of obtaining a tractable mathematical formulation, Parker emphasized the "qualitative" nature of his results, disclaiming "quantitative and definitive" accuracy.

The supersonic character of the flow admitting such a formulation, here and throughout the remainder of the thesis the discussion is from the point of view of an initial value problem beginning at 1 a.u. There the properties of the flow are now thoroughly established by observation. (See for example reviews by Wolf, 1972; Gosling, 1972; Montgomery, 1972; and Schatten, 1972.) Typical numbers used in subsequent computations appear in Table 3.

Table 3. Properties of the solar wind observed at 1 a.u.

TEMPERATURE	
ELECTRONS	$1.5 \times 10^5 \text{ } ^\circ\text{K}$
PROTONS	$5 \times 10^4 \text{ } ^\circ\text{K}$
PARTICLE DENSITY ELECTRONS or PROTONS	$5 \text{ cm}^{-3}$
MAGNETIC FIELD STRENGTH	$5 \times 10^{-5} \text{ Gauss}$

Parker's analysis is reviewed below with considerable amplification and one important extension. Here the material will serve the original

expository intent. But in later sections it will serve as an analytical tool in conjunction with theory to guide the development of and to explore features of the solution to be expected from a considerably more detailed physical model whose construction and analysis are among the major subjects and purposes of this thesis. As the result of the interplay useful light will be shed on the question of the accuracy available in the approximate solution of Parker's model as extended, the analytical solution being presently the only general description of the flowfield extant. Finally, while not a task taken up in the thesis, the results of the analysis are expected to be useful in guiding the future development and application of numerical procedures to obtain a full solution for the flowfield described by the more exact model.

Following ideas suggested in papers by Clauser (1960) and Weymann (1960) Parker constructed a solution for the termination of the solar wind by explicitly assuming the existence of a shock transition. The shock provides a stable mechanism by which the very low pressure in the supersonic regime of the far interplanetary solar wind can be raised to match the much higher pressures of the local interstellar medium in the vicinity of the boundary where the two media must ultimately interact. Steady flow modeling average conditions is assumed in a non-rotating heliocentric reference frame.

Parker made the following assumptions. The weakly magnetized gas of the interstellar medium is taken to be incompressible, implying the flow is subsonic in its passage of the sun. Also, the flow of the interstellar gas, termed "the interstellar wind", is assumed to be non-viscous, irrotational, and to form a sharp, mutually impenetrable boundary with the magnetized post-shock solar wind.



To decouple the transonic flow problem governing the location, the geometry, and the conditions over the shock surface from the solution of the ensuing subsonic flow problem in the solar wind, a spherical shock surface is assumed across which the uniform conditions on either side should obey the Rankine-Hugoniot normal shock relations. Since the Mach number of the preshock supersonic solar wind is very high, the strong shock relations are invoked. Across a strong shock a highly supersonic flow becomes a moderately subsonic flow and the post shock solar wind can be treated as an incompressible fluid to a fair approximation. Finally, the subsonic solar wind is assumed non-viscous and irrotational, also.

With the above assumptions, both the post shock solar wind and the interstellar wind satisfy the relations of ideal fluid flow

$$\text{div } (\underline{v}) = 0, \quad \rho = \text{constant} \quad (1.2-1)$$

$$\underline{\text{curl}} (\underline{v}) = 0, \quad \text{and} \quad (1.2-2)$$

$$\rho \frac{v^2}{2} + p = \text{constant} . \quad (1.2-3)$$

Since the density  $\rho$  in either regime is constant the velocity  $\underline{v}$  in equations (1) and (2) may be replaced by  $(\rho^{1/2} \underline{v} \equiv \underline{v}')$ . The substitution results in the equivalent set of equations

$$\text{div } (\underline{v}') = 0, \quad (1.2-4)$$

$$\underline{\text{curl}} (\underline{v}') = 0, \quad \text{and} \quad (1.2-5)$$

$$\frac{v' \cdot v'}{2} + p = \text{constant} . \quad (1.2-6)$$

In these equations, no density explicitly appears and the constant of the Bernoulli equation is the same over all stream lines of both flow regimes, the constant being the stagnation pressure of the interstellar wind. Consequently there is nothing in the equations to distinguish them between either flow regime and they represent the flow in both. The problem mathematically then has been reduced to that of a single ideal fluid of unit density flowing in both regimes subject to certain boundary conditions at  $\infty$  and at the shock surface where the solar wind part of the flow field first becomes subsonic.

To recover the solutions for the real fluids in either regime from the solution of the ideal fluid equations one simply applies the inverse transformation

$$\tilde{v} = \rho^{-1/2} v^* \quad (1.2-7)$$

with appropriate density in corresponding regions of the ideal fluid solution. Since the pressure  $p$  in the Bernoulli equation (6) was not affected by the transformation of the original equations, the pressures obtained in the solution of the ideal fluid problem carry back unchanged to the respective regimes of the real fluid problem.

Equations (4) and (5) admit a velocity potential that is the solution of Laplace's equation. The solution of the equation is effected by superposition.

At large distances from the sun (infinity) the effects of the solar wind are no longer felt and the fluid appears as an incompressible uniform parallel flow. At the spherical shock surface by assumption the solar wind flows radially with uniform subsonic velocity and hence is indistinguishable from the flow of an incompressible point source

matching conditions at the distance of the shock radius. The flowfield of the combined subsonic flows is, then, to be constructed as the superposition of the appropriate parallel and source flows to which the combined flow is assumed asymptotic at the boundaries. By the vanishing nature of the source flow at infinity, there the solution so obtained will be exact. Since the parallel flow does not vanish identically at the shock surface, but depending on parameters may be small there compared to the source flow, the solution in the vicinity of the shock will only be an approximation more or less in keeping with the assumed sphericity of the shock surface and other idealizations of the problem.

To solve the subsonic flow problem as indicated above requires the location of and determination of conditions at the shock surface. This is accomplished using the integral of the continuity equation, with constant velocity in the supersonic region, to project conditions at the earth to the shock; using the strong normal shock relations to carry conditions across the shock; and using the incompressible Bernoulli equation to project conditions imposed by the interstellar medium back onto the shock to achieve a match up as detailed below.

The integral of the continuity equation in the preshock interplanetary solar wind gives

$$\rho v r^2 = \rho_1 v_1 R^2 = \rho_e v_e r_e^2, \quad v = v_1 = v_e \quad (1.2-8)$$

where subscript 1 refers to conditions immediately on the supersonic side of the shock and subscript e refers to conditions in the solar wind at earth distance from the sun. The radial distance of the shock surface from the sun is  $R$ . With the constancy of the velocity beyond

the orbit of earth, the density in the supersonic solar wind is seen to vary with the reciprocal of the square of the radial distance from the sun.

The Rankine-Hugoniot normal shock relations are

$$\rho_1 v_1 = \rho_2 v_2 \quad (1.2-9)$$

$$p_1 + \rho_1 v_1^2 = p_2 + \rho_2 v_2^2 \quad (1.2-10)$$

$$\frac{v_1^2}{2} + \frac{\gamma}{\gamma-1} \frac{p_1}{\rho_1} = \frac{v_2^2}{2} + \frac{\gamma}{\gamma-1} \frac{p_2}{\rho_2} \quad (1.2-11)$$

where the subscript 2 refers to conditions immediately on the subsonic side of the shock. In the case of strong shocks  $M_1 \gg 1$ ,  $p_2 \approx \rho_1 v_1^2 \gg p_1$  and the derived relations

$$\frac{v_1}{v_2} = \frac{\rho_2}{\rho_1} = \frac{\gamma+1}{\gamma-1} \quad \text{apply} \quad (1.2-12)$$

Since for a monoatomic gas such as the fully dissociated and ionized hydrogen of the solar wind  $\gamma = 5/3$ , the right hand side of relation (12) has the value 4. Substitution of relations (12) in (10) and dropping the negligible pressure  $p_1$  gives for the post shock pressure in the solar wind

$$p_2 = \frac{2}{\gamma+1} \rho_1 v_1^2 \quad (1.2-13)$$

Beyond the shock the incompressible Bernoulli equation holds in the subsonic solar wind so that immediately after the shock

$$p_2 + \rho_2 \frac{v_2^2}{2} = \text{constant} = p_s \quad (1.2-14)$$

where  $p_s$  is the pressure at the stagnation point.

But the stagnation point pressure also obeys the incompressible Bernoulli equation in the interstellar wind region where

$$p_s = p_i + \frac{1}{2} \rho_i v_i^2 = p_{i\infty} + \frac{1}{2} \rho_i v_o^2 \quad (1.2-15)$$

In equation (15)  $v_o$  is the velocity of the sun with respect to the undisturbed interstellar medium and the pressure of the undisturbed medium is of the order

$$p_{i\infty} = \frac{B_i^2}{8\pi} + \rho_i R T_i \quad (1.2-16)$$

taking account both of the scalar pressure due to the interstellar magnetic field  $B_i$  and the thermodynamic pressure of the interstellar gas treated as atomic hydrogen.

In the light of relations (15) and (16), the right hand side of relation (14) is a constant dependent only on the properties of the undisturbed interstellar medium and the motion of the sun through the medium.

Substitution of relations (12) and (13) in the left hand side of (14) then gives

$$\frac{\gamma+3}{\gamma+1} \rho_1 \frac{v_1^2}{2} = p_s \quad (1.2-17)$$

Relation (17) is viewed as selecting the place in the supersonic solar wind flow where the momentum flux is such that if the shock occurs there the post shock conditions will match up with a subsonic solar wind solution the constant of whose Bernoulli equation is  $p_s$  as given by relation (15) with (16). Finally, substituting for  $\rho_1$  in relation (17) the value in terms of the parameters at earth and the radial distance from the sun through relation (8) we get that the radial distance of the shock from the sun may be found as

$$R = r_e \left[ \left( \frac{\gamma+3}{\gamma+1} \right) \frac{\rho_e v_e^2}{2 p_{i\infty} + \rho_1 v_o^2} \right]^{1/2} \quad (1.2-18)$$

With  $R$  as given by relation (18), the immediate post shock velocity and density obtained from relations (12) and (8) are

$$v_2 = \left( \frac{\gamma-1}{\gamma+1} \right) v_e \quad \text{and} \quad (1.2-19)$$

$$\rho_2 = \left( \frac{\gamma+1}{\gamma-1} \right) \frac{r_e^2}{R^2} \rho_e \quad (1.2-20)$$

For the source flow representation of the post shock solar wind the source strength is given by

$$Q = 4\pi R^2 v'_{sR} \quad (1.2-21)$$

where  $v'_{sR}$  is the velocity of the source component of the ideal fluid at the point  $R$  and is given by

$$v'_{sR} = \rho_2^{1/2} v_2 \quad (1.2-22)$$

Combining relations (19), (20), and (22) in (21) yields the source strength as a function of  $R$

$$Q = 4\pi r_e R \left( \frac{\gamma-1}{\gamma+1} \right)^{1/2} \rho_e^{1/2} v_e \quad (1.2-23)$$

The potential function and Stokes stream function for the source component of the ideal fluid flow are respectively

$$\varphi_s = - \frac{Q}{4\pi r} \quad \text{and} \quad (1.2-24)$$

$$\psi_s = \frac{Q}{2} (1 - \cos \theta) \quad (1.2-25)$$

where  $\psi_s$  is the flux in a cone of given semivertex angle  $\theta$  measured with the axis of flow in the direction of motion of the sun through the interstellar medium, i.e. in the direction upstream of the sun with respect to the interstellar wind.

For the parallel flow representation of the far interstellar wind the velocity of the parallel flow component of the fictitious fluid is

$$-U \equiv v_p' = -\rho_i^{1/2} v_o \quad (1.2-26)$$

The corresponding components of the potential function and Stokes stream function for the ideal fluid are

$$\varphi_p = -U x \quad \text{and} \quad (1.2-27)$$

$$\psi_p = -\pi U y^2 \quad (1.2-28)$$

In the equations,  $x$  is a cartesian vector component measured along the axis of flow, positive in the upstream direction with respect to the interstellar wind, and  $y$  is orthogonal to  $x$ .

Adding components for the source and parallel flows gives the potential function

$$\varphi = -Ux - \frac{Q}{4\pi r} \quad (1.2-29)$$

Similarly the Stokes stream function for the ideal fluid representation of the combined flows of the solar and interstellar winds is

$$\psi = \frac{Q}{2} (1 - \cos \theta) - \pi U y^2 \quad (1.2-30)$$

Differentiating equation (29) with respect to  $x$  and setting the result to zero on the upstream axis of the flow places the stagnation point at

$$x_o = \left( \frac{Q}{4\pi U} \right)^{1/2} \quad (1.2-31)$$

From relations (23) and (26) we find for the stagnation point location

$$x_o^* = (R^*)^{1/2} \left( \frac{\gamma-1}{\gamma+1} \frac{\rho_e v_e^2}{\rho_1 v_o^2} \right)^{1/4} \quad (1.2-32)$$

In the equation the asterisks signify quantities measured in astronomical units, i.e. normalized by  $r_e$  (See equation (18).)



Combining equations (30) and (31) we find the streamlines in the  $x, y$  plane corresponding to the intersections with streamsurfaces of constant velocity flux  $\psi$  are given by

$$y^2 = 2x_0^2 (1 - \cos \theta) + \text{constant}. \quad (1.2-33)$$

The regions of the flowfield corresponding to the solar and interstellar winds are separated by the stagnation point streamline obtained from equation (33) with the constant set equal to zero. Streamlines in the interstellar wind regime correspond to positive constants and those in the solar wind regime to negative constants. The most negative constant yielding a real streamline is  $(-4 x_0^2)$  corresponding to the axial streamline in the downwind direction. At large distances downstream of the sun the streamlines become asymptotically parallel corresponding to circular cylindrical stream surfaces. In particular the radius of the stagnation point stream surface approaches asymptotically

$$y_0 = 2x_0 \quad (1.2-34)$$

With equation (31), equation (29) may be represented as

$$\varphi = -U \left( x + \frac{x_0^2}{r} \right) \quad (1.2-35)$$

Then the ideal fluid velocity components obtained by differentiating equation (35) are

$$v'_x = U \left( \frac{x_o^2}{r^3} x - 1 \right) \quad \text{and} \quad (1.2-36)$$

$$v'_y = U \frac{x_o^2 y}{r^3} \quad (1.2-37)$$

Finally, making use of equation (7) and (26) we have the real fluid velocity components

$$v_x = v_o \left( \frac{\rho_i}{\rho} \right)^{1/2} \left( \frac{x_o^2}{r^3} x - 1 \right) \quad \text{and} \quad (1.2-38)$$

$$v_y = v_o \left( \frac{\rho_i}{\rho} \right)^{1/2} \frac{x_o^2 y}{r^3} \quad (1.2-39)$$

where setting  $\rho = \rho_i$  gives the velocity in the interstellar medium and  $\rho = \rho_2 = \frac{\gamma+1}{\gamma-1} \left( \frac{r_e}{R} \right)^2 \rho_e$  gives the velocity in the subsonic solar wind. Equation (38) predicts that at large distances downstream of the sun the velocity in the subsonic solar wind should approach the constant value

$$v_x = v_o \left( \frac{\gamma-1}{\gamma+1} \frac{\rho_i}{\rho_e} \right)^{1/2} R^* \quad (1.2-40)$$

The speed with which the sun moves relative to the local interstellar gas is presently quite uncertain. Astronomical measurements put the speed of the sun with respect to the nearby stars at 20 km/s (Allen, 1963). In the absence of other better indications, this value has been the standard interstellar wind speed for purposes of calculations and physical inquiry.

However, consistent with both the expanded knowledge of the temperature and density in the interstellar medium and the developing model for the interaction of the solar wind with interstellar neutral hydrogen, recent interpretation of measurements of interplanetary Lyman -  $\alpha$

radiation provide both grounds (Bertaux and Blamont, 1972) and a method (Thomas 1972) for making a new, more direct estimate. In the reference cited, Thomas finds the speed of the interstellar wind to be on the order of 6 km/s .

Since the model used by Thomas is somewhat incomplete, for the present, we regard the value given as indicative. The subject of Lyman -  $\alpha$  scattering with inferences to be drawn from it is discussed further in section 4. and again in Chapter III. in conjunction with calculations of interstellar wind speed based on our own model.

We now explore the possibility of using the foregoing solution of Parker to provide a rough approximate description of the combined solar wind - interstellar wind flow field under conditions typifying current estimates. To point up a separate major difficulty in the model as originally formulated and directly interpreted we initially push the assumption of Incompressibility in the interstellar medium to the limit by assuming the sun to move with sonic speed (  $\sim 16$  km/s ) relative to the ionized component of the interstellar gas. Later, with the model reinterpreted when we reduce the assumed interstellar wind speeds toward the substantially subsonic estimate of Thomas, reasonable consistency is achieved in the incompressibility assumption.

To proceed accordingly, we choose from Table I the particle density of the interstellar neutral gas to be  $0.1 \text{ cm}^{-3}$ , the density of the ionized fraction to be  $0.01 \text{ cm}^{-3}$ , and the interstellar magnetic field strength to be  $3 \times 10^{-6}$  gauss. Putting numbers in equation (18) where  $\rho_i$  and  $p_{i\infty}$  include contributions of the ionized as well as neutral interstellar gas, we find 125 a.u. as the estimate of the distance to the shock termination. If the same procedure is followed for equation (32) using the foregoing result

for  $R^*$ , the stagnation point is found to be at 100 a.u., well within the shock radius. The latter is an obviously absurd result from which we infer that some assumption of Parker's model must be grossly inconsistent with the physics of the problem to which the model is being applied. Understanding of the difficulty is promoted through a relation for  $x_o^*/R^*$  obtained from equations (18) and (32).

The relation is

$$\frac{x_o^*}{R^*} = \left[ \frac{2(\gamma-1)}{\gamma+3} \frac{P_{i\infty} + 1/2 \rho_i v_o^2}{\rho_i v_o^2} \right]^{1/4} \quad (1.2-41)$$

Viewed as representing an ordinary gas dynamics problem, equation (40) may be recast

$$\frac{x_o^*}{R^*} = \left[ \frac{\gamma-1}{\gamma+3} \left( \frac{2}{\gamma} \frac{1}{M_\infty^2} + 1 \right) \right]^{1/4} \quad (1.2-42)$$

With  $\gamma$  given the value  $5/3$ , the coefficients  $\frac{\gamma-1}{\gamma+3}$  and  $2/\gamma$  have the values  $1/7$  and  $6/5$  respectively. Hence in order that the model place the stagnation point outside the shock surface ( $\frac{x_o^*}{R^*} > 1$ ), equation (41) requires that  $M_\infty^2 < \frac{1}{5}$  or the free stream Mach number  $M_\infty < 0.45$ .

Based on Thomas' estimate of  $v_o$ , the Mach number of the sun through the neutral interstellar gas is 0.5. Quite evidently then Parker's model in the purely gas dynamic interpretation of the problem predicts that in the upstream direction the assumed incompressible source flow of the solar wind will be deflected back and around the flow of the interstellar gas before the source flow ever reaches the

place where the shock in the real supersonic solar wind ought to be. Parker himself noted (1961) that the representation should apply only for very slow passage of the sun through the interstellar gas.

Somewhat ironically but fortunately for the vitality of his model, in fact, the bulk of the interstellar wind does not flow as Parker originally hypothesized. As recognized by Holzer and Axford (e.g., Axford, 1972) and as we shall see in more detail in the next section where we discuss particle interactions, outside the shock the mean free path for a neutral hydrogen atom to interact with anything is much greater than the characteristic dimension of the flowfield, as measured by  $R^*$  for example. Consequently the neutral hydrogen is not deflected as a continuum fluid forming a definable boundary with and flowing around the solar wind in accordance with Parker's model. But the numerically much weaker ionized component of the interstellar wind being a magnetized plasma of short gyro-radius interacting with another similar plasma does form such a boundary and is deflected to flow in such a way. To the zeroth order approximation of the present discussion, then, the neutral hydrogen is regarded as passing without effect through both the ionized interstellar wind and the subsonic solar wind.

If we now examine the assumptions of Parker's model in the light of the foregoing, we note that the relations for the location of the shock distance are a statement about exchanges of momentum between the two media. As the result of momentum conservation in the  $x$  direction in single particle collisions, it does not appear that on the axis in the forward direction it should make too much difference whether a fraction of the overall momentum flux of the interstellar wind is

exchanged with the solar wind within the shock as in the case of the neutral hydrogen or whether it is all stopped at a stagnation point as in Parker's assumption.

On the other hand, given the location of the shock the location of the stagnation point in Parker's model can be seen to derive from kinematical relations and is a statement about the conservation of velocity flux in the flow of two incompressible, irrotational fluids that must evade each other. Evidently the two such fluids here should be the solar wind, in principle augmented by the ionization of neutral hydrogen transported into the solar wind, and the ionized interstellar wind.

Consequently while in equation (18) it is reasonable to take  $\rho_i$  as the sum of the mass densities of the neutral and ionized components of the interstellar wind, in equation (32)  $\rho_i$  should reflect only the density of the ionized component. When this is done in equation (32) the prediction is that the solar wind be bounded at 185 a.u., a distance well outside the shock.

Following the corrected procedure but with Thomas' estimate of the interstellar wind speed (6 km/s) we find 145 a.u. for the shock radius and 328 a.u. for the distance to the stagnation point. Streamlines of the flow field are sketched in Figure 1.

An indication of the internal consistency of the model as extended is available from equation (38) evaluated on the upstream axis of flow in the subsonic solar wind. With equation (32) and  $x$  and  $r$  taken equal to  $R$ , it may be seen that the first term of equation (38) gives the post shock velocity, equation (19); and accordingly the second term represents the error at the shock. The relative error in the subsonic solar wind velocity in the vicinity of the shock is hence measured by  $R^2/x_0^2$ , about 20% for  $v_0 = 6$  km/s.

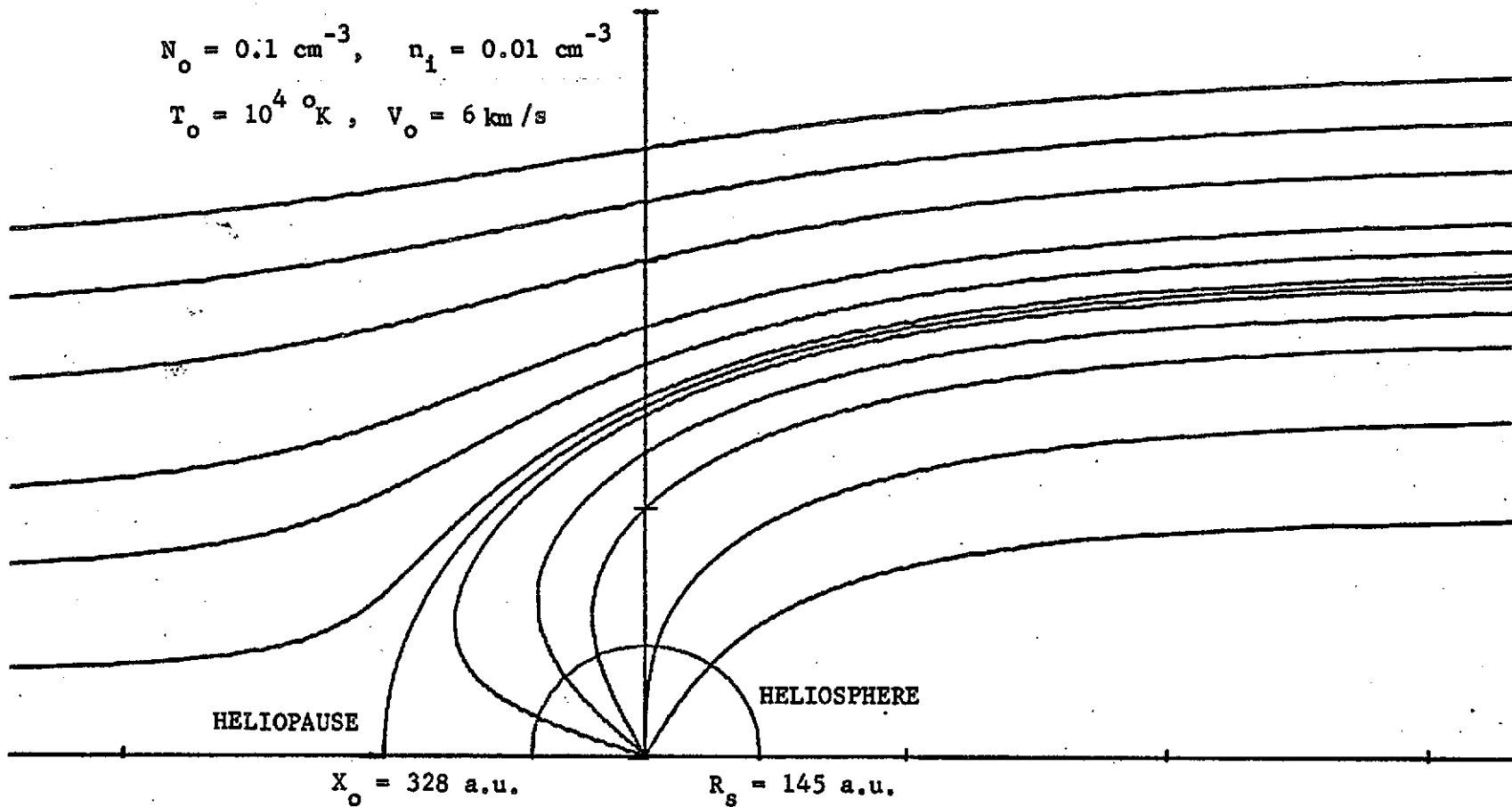


Figure 1. Streamlines of flowfield described by the extended Parker solution for the termination of the solar wind.

Using the value for the shock radius 145 a.u., we see from equation (40) that the velocity in the subsonic solar wind downstream of the sun is of the order of  $3 v_0$  or  $2 \times 10^6$  cm/sec. We recall the speed  $v_0$  of the sun to be equivalent to about Mach 0.5 in the interstellar gas. Thus downstream of the sun the flow of the solar wind has the character of a transonic jet in the interstellar medium.



### 3. Heating and Flowfield Temperature

We now complete the gross characterization of the flowfield beyond earth orbit with a discussion of the temperature. The extended shock termination solution provides the general description of the flowfield on which the analysis is based.

In the supersonic regime of the solar wind flow the temperature is governed by a competition between heating by conduction and cooling by expansion. Use can be made of the heat conduction and critical polytrope solutions examined in the previous section to get a qualitative view of the situation. The polytrope solution predicts constant velocity and resulting density and temperature functions that vary as  $r^{-2}$  and  $r^{-2(\alpha-1)}$  respectively.

The volume rate of heating  $\dot{Q}$  associated with any prescribed flow can be got from a representation of the first law of thermodynamics, the heat equation for steady flow

$$\dot{Q} = p \operatorname{div} \underline{v} + \rho \underline{v} \cdot \underline{\operatorname{grad}} e \quad (1.3-1)$$

Expressing  $\operatorname{div} \underline{v}$  in the radial coordinate with spherical symmetry, the internal energy  $e$  by  $\frac{1}{\gamma-1} (p/\rho)$ ,  $p$  by the polytrope law  $p = p_e (\rho/\rho_e)^\alpha$  and invoking the critical polytrope solution yields the result

$$\dot{Q} = \frac{2p_e v_e}{r_e} \left( \frac{\gamma-\alpha}{\gamma-1} \right) \left( \frac{r_e}{r} \right)^{2\alpha+1} \quad (1.3-2)$$

Evidently the requirement for heating is substantially reduced both with increasing  $\alpha$  and distance from the sun. For  $\alpha = \gamma$ , the adiabatic solution, there is no heating.

The heating available from conduction is given by

$$\dot{Q} = - \operatorname{div} \underline{q} = \frac{1}{r^2} \frac{d}{dr} (r^2 \kappa \frac{dT}{dr}) \quad (1.3-3)$$

Neglecting for the moment the effect of the interplanetary magnetic field on conductivity in using equation (1.1-4) and again assuming the polytrope dependence for  $T$  leads to the result

$$\dot{Q} = \frac{2AT_e^{7/2}}{r_e} (\alpha-1) (7\alpha-8) \left(\frac{r_e}{r}\right)^{7\alpha-5} \quad (1.3-4)$$

Inspection of equation (4) reveals no heating ( $\dot{Q} > 0$ ) is available from conduction when  $1 \leq \alpha \leq 8/7$ . When the upper limit of the range is substituted in  $r^{-2(\alpha-1)}$  the temperature dependence of the accorded polytrope solution is found to be the  $r^{-2/7}$  variation of the constant heat flux solution of Chapman.

Solutions in the range  $8/7 < \alpha < \gamma = 5/3$  can derive heating from conduction. It is interesting to note that the effective polytrope index best representing the flow of the solar wind from the base of the corona to earth  $\alpha = 1.15$  lies rather closer to the lower end of the range indicating the system adopts gradual heating of the flow from slow attenuation of the conduction heat flux. Indeed if one equates the expressions for heat supply and demand, equations (2) and (4), to get the exponents of  $r$  in consonance one finds  $\alpha = 1.2$ , furthering the conjecture. The transport coefficient of thermal conductivity  $A$  required to bring the coefficients of the two expressions to equality is found to be  $5.6 \times 10^{-7}$  c.g.s. units, a value consistent with theoretical estimates.

In the vicinity of the solar poles where the interplanetary magnetic field lines make only small angles with the radial direction, the state of the system should be essentially as we have just described. But near the solar equatorial plane the situation is more complicated.

There it is now well established the magnetic field lines follow an Archimedes spiral approximately according to the law

$$\zeta = \tan^{-1} \frac{r_e}{r} \quad (1.3-5)$$

where  $\zeta$  is the angle the field direction makes with the azimuthal direction.

As presently understood theoretically and as we shall see in the next chapter, the consequences of the magnetic field becoming more azimuthal is to rapidly lower (by  $\sin^2 \zeta$ ) the effective coefficient of thermal conductivity in the radial direction. Beyond several earth radii from the sun the heat flux is effectively blocked. Qualitatively the result is a temperature profile that falls off faster than  $r^{-.4}$  (for  $\alpha = 1.2$ ) which was found in the absence of the field.

The effect of cutting off the heat flux can be partially analyzed through the dynamical form of the heat equation

$$\text{div} \left[ \rho v \left( \frac{v^2}{2} + \frac{\gamma}{\gamma-1} p/\rho - \frac{GM_o}{r} \right) \right] = - \text{div} \underline{q} \quad (1.3-6)$$

Assuming spherical symmetry and conservation of mass (equation 1.1b-1) we get from equation (6) the integral

$$\frac{2\gamma}{\gamma-1} R(T - T_e) + \frac{1}{2} (v^2 - v_e^2) + \frac{GM_o}{r_e} \left( 1 - \frac{r_e}{r} \right) = \frac{q_e}{\rho_e v_e} \quad (1.3-7)$$

Equation (7) is seen to embody a prediction of the temperature in the supersonic region provided consistent estimates are available for the second and last terms.

Since at earth the angle which the interplanetary magnetic field makes with the radial direction has only reached about  $45^\circ$ , heat conduction from the base of the corona has not yet been greatly effected. Hence for purposes of estimating the heat conduction flux at earth we take the temperature profile locally to have the  $r^{-.4}$  dependence found in the absence of the field. Then taking account of the local inhibition of conductivity by the field the heat flux is given by

$$q_e = .4 \sin^2 \zeta_e A \frac{T_e^{7/2}}{r_e} \quad (1.3-8)$$

Taking  $T_e$  to be the electron temperature  $1.5 \times 10^5$  °K measured at 1 a. u. gives the value  $3.12 \times 10^{13}$  erg/gm for the right hand side of equation (7). Out near the shock ( $r \sim 125$  a. u.) the gravitational term has the value  $.88 \times 10^{13}$  erg/gm. Taking  $T_e$  in the first term of the left hand side to have the average value  $1. \times 10^5$  °K of the electron and proton temperatures measured at 1 a. u., one finds the term  $\frac{2\gamma}{\gamma-1} R T_e = 4.16 \times 10^{13}$  erg/gm.

The term  $v_e^2/2$  has the value  $8 \times 10^{14}$  erg/gm which is substantially larger than the others. Hence if we are to use equation (7) to estimate the temperature we must be able to gauge the dynamics rather closely. The extent to which the latter may be accomplished depends on the importance of heating to the remainder of the dynamical trajectory. To investigate the question we invoke the one dimensional compressible flow equation (Chapter II) in radial symmetry.

$$\frac{(a^2 - v^2)}{v} \frac{dv}{dr} = -\frac{2a^2}{r} + \frac{GM_o}{r^2} + (\gamma-1) \frac{\dot{Q}}{\rho v} \quad (1.3-9)$$

Using the relation for the speed of sound

$$a^2 = 2 \gamma R T \quad (1.3-10)$$

we find at earth  $a_e^2 = 2.77 \times 10^{13} \text{ cm}^2 \text{ s}^{-2}$  which is much less than  $v^2$ . Consequently the left hand side of equation (9) is  $-\frac{d}{dr} \left( \frac{v^2}{2} \right)$  and making use of the constant mass flux relation we write

$$\frac{d}{dr} \left( \frac{v^2}{2} \right) = \frac{2a^2}{r} - \frac{GM_o}{r^2} - (\gamma-1) \frac{\dot{Q}}{\rho_e v_e} \frac{r^2}{r_e^2} \quad (1.3-11)$$

At earth the first term on the r.h.s. has the value  $3.7 \text{ erg gm}^{-1} \text{ cm}^{-1}$  compared to  $-.59 \text{ erg gm}^{-1} \text{ cm}^{-1}$  for the gravitational term.

Beyond earth the thermal conductivity diminishing factor  $\sin^2 \zeta$  has the approximate dependence

$$\sin^2 \zeta \approx \left( \frac{r_e^2}{r^2} \right) \begin{cases} \sin^2 \zeta_e & | r \sim r_e \\ \tan^2 \zeta_e & | r > r_e \end{cases} \quad (1.3-12)$$

Using the  $r$  functional dependence of equation (12) and again assuming the polytrope temperature dependence we find

$$\dot{Q} = \frac{2(\alpha-1)(7\alpha-6) A T_e^{7/2}}{r_e^2} \left( \frac{r_e}{r} \right)^{7\alpha-3} \begin{cases} \sin^2 \zeta_e \\ \tan^2 \zeta_e \end{cases} \quad (1.3-13)$$

for the volume rate of heating by conduction. Comparing equations (4) and (13) we see that the relative effect of the interplanetary magnetic

field is to increase heating near earth ( $\alpha \sim 1.2$ ) but rapidly to diminish heating (by  $r_e^2/r^2$ ) farther away.

At earth the heating term on the right hand side of equation (11) then has the value  $-3.33 \text{ erg gm}^{-1} \text{ cm}^{-1}$  which is comparable with the value of the first term on the right hand side. Hence as a result of the closing magnetic field lines in the solar equatorial plane heating is important, in a relative sense, in the dynamics of the supersonic solar wind near earth. However substituting equations (13) and (10), with the polytrope law, in equation (11) we see that the terms on the right hand side vary with  $r$  respectively as  $r^{-(2\alpha-1)}$ ,  $r^{-2}$ ,  $r^{-(7\alpha-5)}$ . Then beyond earth, where  $\alpha \geq 1.2$  is assumed, the heating term diminishes with respect to the first at least as fast as  $r^{-2}$ . Hence for purposes of estimating from equation (7) the temperature out near the shock ( $r \sim 145 \text{ a. u.}$ ) we can get a fair estimate of the integral of equation (11) by neglecting heating.

The integral is formally available to us in the adiabatic polytrope solution ( $\alpha = \gamma = 5/3$ ) already developed (section 1.1b). The solution is given relevance to the present problem by basing the initial point parameters  $x_0$ ,  $y_0$ ,  $\rho_0$ , and  $\epsilon_0$  on conditions measured at earth.

Since for the adiabatic solution  $c_e$  is the speed of sound  $a_e$ ,  $y_e \equiv \bar{M}_e = M_e$  the Mach number which is  $\sim 7.7$  at earth. The Mach number being greater than one, the solution is on the ascending branch of  $f(M)$ .

The initial value for the non-dimensional distance  $x_e$  has the value 3.12 which is greater than zero, the location of the minimum of  $g(x)$  for the adiabatic solution. Hence  $x_e$  is on the ascending branch of  $g(x)$ , also.

The initial values for  $x$  and  $M$  both being on ascending branches of their respective function curves, the solution we seek to equation (1.1b-11) belongs to the class of critical solutions. Since out near the shock  $x$  and  $M$  have values of the order of 400 and 20 respectively, the asymptotic formulas are appropriate. Then the result we seek, equation (1.1b-26) gives  $v^2/2 = 8.33 \times 10^{14} \text{ cm}^2 \text{ s}^{-2}$  for  $v = 4.08 \times 10^7 \text{ cm s}^{-1}$ , an increase in velocity of only 2% beyond earth. Since by equation (11) the effect of heating a supersonic flow is to retard the velocity, the result given is an upper bound.

Thus the second term of equation (7) has the value  $3.3 \times 10^{13} \text{ erg gm}^{-1} \text{ cm}^{-1}$ . Accumulating numbers found for the other terms previously, we find 74,000 °K for the estimate of the temperature at the shock. But the polytrope law even with  $\alpha = 1.14$ , i.e. unattenuated heat conduction, gives a temperature of only 25,000 °K; and for  $\alpha = 1.2$ , gives 14,000 °K. Evidently the estimate of the temperature that we have derived from equation (7) is much too high.

The source of difficulty lies not with the equation itself, which is fundamental, or with the estimate of the terms on the left hand side, the least well known one being an upper bound. Hence the problem must lie with the right hand side of the equation.

Two possibilities suggest themselves. The first is that the classical transport coefficient of heat conduction  $6 \times 10^{-7} \text{ c.g.s. units}$  (and the resulting estimate of heat flux  $1.04 \times 10^{-2} \text{ erg cm}^{-1} \text{ s}^{-1}$  at earth) is too large. The second is that the hypothesis of effective extinction of the heat conduction flux at large distances beyond earth by the closing magnetic field lines is too severe.

That the former is true has been inferred previously on a variety of different empirical and solar wind- theoretical grounds by Montgomery

(1972), Scudder (1972), Barnes and Hartle (1972), Whang (1972), and Cuperman and Harten (1972). Estimates of the required reduction based on solar wind theory range from a factor of 2 to 5.5. Numbers at the high end of the range are consistent both with the predictions of the polytrope law and Scudder's interpretation of the conduction heat flux in the steady solar wind derived from measured electron distributions. Corresponding in our calculation to a reduction factor of five, the heat flux  $2 \times 10^{-3} \text{ erg cm}^{-2} \text{ s}^{-1}$  is typical of the numbers quoted by Scudder in the "convergence region", i.e. the third moment of the distribution function cut off between 200 and 300 ev. (With regard to the cut off point, it is noted that the r.m.s. value of the Maxwellian distribution for the electron temperature at 1 a. u. is 40 ev.) If using the quoted reduced heat flux at earth, we recompute from equation (7) the estimate of the temperature at the shock we find 14,000 °K, the prediction of the polytrope law for  $\alpha = 1.2$ .

In the reference cited, Scudder also has observations relevant to the possibility that the effective coefficient of heat conduction transverse to the interplanetary magnetic field is not greatly reduced with respect to the coefficient in the field free or field parallel case. Looking at the directional distribution of the heat flux vector about the magnetic field lines, he finds that the flux due to unsteady injections of high temperature electrons into the solar wind is ducted by about a factor of three by the magnetic field lines. But for the steady electron population in the convergence region the direct interpretation of the data presented is that conduction transverse to the field is not greatly reduced, apparently only by a factor of about 0.7, with respect to the field aligned component.



If in addition to the reduced heat flux at earth we accept the direct interpretation of Scudder's data, namely that the steady component of the electron heat flux transverse to the magnetic field is transmitted with only a factor of 0.3 attenuation, the estimate of the temperature out near the shock is reduced to only 400 °K . We take this value to be a lower bound on the temperature and the previous estimate 14,000 °K to be an upper bound. It is noted that the temperature predicted by the strictly adiabatic polytrope expansion is 130 °K .

Thus in the present state of uncertainty the range of temperature estimates in the supersonic solar wind near the shock essentially duplicates that in the interstellar medium. Hence we can take as a rule of thumb that the temperature in the far supersonic solar wind is comparable with that in the interstellar medium. Accordingly, the speed of sound is at most 20 km s<sup>-1</sup> and the preshock Mach number is at least of the order of 20 .

Because the Mach number in the preshock supersonic solar wind is so high, the post shock pressure and temperature are only very weakly dependent on the preshock pressure and temperature through the strong shock relations. Making use of the relations developed in section 1.2 we find that the post shock and stagnation pressures are given respectively by

$$P_2 = \frac{2}{\gamma+1} \rho_e v_e^2 \left( \frac{r_e}{R} \right)^2 \quad \text{and} \quad (1.3-14)$$

$$P_s = \frac{\gamma+3}{2(\gamma+1)} \rho_e v_e^2 \left( \frac{r_e}{R} \right)^2 \quad (1.3-15)$$

The coefficients in equations (14) and (15) differ only by about 12%. Then the subsonic solar wind is only slightly compressible, the post shock density being given by equation (1.2-20). Hence the temperature in the subsonic solar wind may be considered isothermal with value given by

$$T_2 = \frac{\gamma-1}{(\gamma+1)} \frac{v_e^2}{R} \approx 1.8 \times 10^{+6} \text{ } ^\circ\text{K} . \quad (1.3-16)$$

Thus we close this section by noting as a second rule of thumb that the temperature in the subsonic solar wind replicates that at the base of the corona.

#### 4. Modern Developments - Particle Interactions

In the historical context, one can equate the early development of the subject with the establishment of the flowfield by classical continuum methods, the focus of our discussion to this point. This phase spanned six years culminating in the publication of Parker's (1963) book.

Signaled by the publication in the same year of papers by Axford, Dessler, and Gottlieb (1963) and Patterson, Johnson, and Hanson (1963), the modern development is characterized by the occupation with filling in a wealth of physical detail missing in the early macroscopic models. Much of the effort has been concerned with identifying the important microscopic physical processes underlying bulk behavior within and between the solar wind and the interstellar medium. The progress of research, involving of practical necessity the rather piecemeal testing of concepts in the evolving corporate model, has now led to the point of understanding where it is timely to enter a new era of analysis from synthesis.

Thus the present section summarizes, unifies and in some particulars clarifies the contributions to the physical model made in the recent literature. The remainder of the thesis is then concerned with producing a coherent mathematical model adequate to explore features of the combined flow problem with the increased accuracy and for the subtlety of detail the added physics portends.

The paper by Axford, et al. (1963) touched on many noteworthy topics including the role of the interplanetary magnetic field in the dynamics of the solar wind, a subject we treat in Chapters II. and IV. But the point of greatest significance to the present development, at least, is the recognition of the compelling likelihood of the charge exchange interaction between solar wind protons and atoms of neutral hydrogen. The neutral hydrogen

is of interstellar origin and is able to invade the cavity occupied by the solar wind in the galactic magnetic field. The authors also tentatively estimated the effect of photoionization of atomic hydrogen by solar ultra-violet radiation in the Lyman continuum.

Patterson, et al. then introduced the important notion of using measurements of extraterrestrial Lyman- $\alpha$  radiation to infer both properties of the interstellar medium and structure of the solar wind through correspondence with predictions of an interdependent physical model. As the result of large wavelength dispersion, the Lyman- $\alpha$  was considered to originate in backscatter of solar radiation from hot interplanetary neutral hydrogen. The hot interplanetary hydrogen, in turn, was supposed to be the product of charge exchange reactions between hot solar wind protons and interstellar hydrogen which at that time was thought to be cold ( $\sim 100$  °K). Following Axford, et al., the reactions were assumed to take place in a thin shell subsonic region.

Hundhausen (1968) recognized the thin shell assumption to be fallacious on grounds of the large mean free path for charge exchange. In a more systematic model, he then showed that the assumption the Lyman- $\alpha$  scattering should come from secondary hydrogen leads to an unreconcilable theoretical contradiction in the location of the shock surface in the solar wind.

Semar (1970), following the work of Biermann, Brosowski, and Schmidt (1967) for cometary flow, pioneered numerical calculations of solar wind flow using one dimensional gas dynamic equations. The equations featured source terms for mass, momentum, and energy additions based on photoionization and charge exchange reactions with interstellar hydrogen.

Blum and Fahr (1970,1971), Fahr 1972, Holzer and Axford (1970 a,b) Holzer (1972) and others have elaborated various aspects of the transport of interstellar neutral hydrogen into the supersonic solar wind region, the influence of charge exchange with this hydrogen on the location of the shock, and the interpretation of Lyman- $\alpha$  scattering from such hydrogen. (See Axford (1972) for additional references and a comprehensive review.) In the present context, all the forementioned work has suffered from the failing to incorporate both (1) a high temperature velocity distribution and (2) the effect (see below) of solar Lyman- $\alpha$  radiation pressure on the interstellar hydrogen gas.

Finally, Thomas (1972) brought to the field in modern context (but see also Brandt, 1960) the idea developed by Wilson (1960) that the radiation pressure of solar Lyman- $\alpha$  approximately cancels solar gravitation with respect to the transport of interstellar neutral hydrogen. Also incorporating an isotropically distributed velocity component to roughly simulate a temperature distribution for the hydrogen, Thomas was able to gain an estimate of the speed of the interstellar wind.

Using Thomas' estimate of the speed ( $\sim 6$  km/s) and the resulting estimates of the flowfield parameters based on the extended Parker solution (sections 2. and 3.), we now turn our attention to the physical processes mentioned above and to demonstrating the scale of their effects. Based on results obtained in the earlier sections, Table 4 collects nominal values for parameters of the solar wind regions and the interstellar wind.

a. Photoionization

A hydrogen atom exposed to solar ultraviolet radiation of wavelength at or below the Lyman edge 912 Å may absorb a photon and become

ionized. The process thus contributes one free proton and one free electron to the plasma of the flow regime in which the event occurs. If the absorbed photon has a wavelength less than 912 Å, corresponding to the hydrogen ionization threshold of 13.59 eV, the residual energy of the photon appears largely as kinetic energy of the freed electron.

The photoionization rate per atom of hydrogen is given by

$$\alpha_p = \int_{\nu_0}^{\infty} f(\nu) \sigma_p(\nu) d\nu \quad (1.4-1)$$

Table 4. Nominal values for parameters of solar wind and interstellar wind flow regimes

	SOLAR WIND		INTERSTELLAR WIND	
	SUPERSONIC	SUBSONIC	IONIZED	NEUTRAL
NUMBER DENSITY ( $\text{cm}^{-3}$ )	$\frac{5}{r^2}$	0.001	0.01	0.1
TEMPERATURE ( $^{\circ}\text{K}$ )	$\frac{10^5}{r^{0.4}}$	$10^6$	$10^4$	$10^4$
velocity (cm/s)	$4 \times 10^7$	$< 10^7$	$6 \times 10^5$	$6 \times 10^5$
MACH NUMBER	$> 7$	$< 0.5$	0.4	0.4

<sup>1</sup> distances r in astronomical units.

where  $\nu_0$  is the frequency at the Lyman edge,  $f(\nu)$  is the photon flux density, and  $\sigma_p(\nu)$  is photoionization cross section. As the

result of the approximate  $\nu^{-3}$  frequency dependence of the cross section above the Lyman edge, the integral is rapidly convergent; and the effective wavelength band is approximately  $\nu_0$  to  $2\nu_0$ . Using the solar u. v. flux measurements of Hinteregger, et al. (1965), Banks and Kockarts (1971) have computed the photoionization rate  $\alpha_p$  to be  $1.5 \times 10^{-7} \text{ s}^{-1}$  at 1 a. u. The integrated flux  $f_0$  over the effective wavelength band is  $2.8 \times 10^{10} \text{ photons cm}^{-2} \text{ s}^{-1}$  and the average photoionization cross section  $\bar{\sigma}_p$  is  $5.4 \times 10^{-18} \text{ cm}^2$  (Holzer, 1972).

Assuming the  $\nu^{-3}$  dependence for the cross section and uniform photon flux permits an easy estimate of the average kinetic energy of the photoelectrons, i.e. the average excess energy of the absorbed photons. When the integration is carried out over the interval  $\nu_0$  to  $2\nu_0$ , the average photon energy is  $4/3 h\nu_0$  where  $h\nu_0$  is the photon energy 13.59 eV at the Lyman edge.

Consequently the average energy residing in the photoelectrons is roughly  $1/3 h\nu_0$  or 4.5 eV. This number is only half the 10 eV figure adopted by Semar from Biermann's (1967) estimate for heavy molecules of cometary flow. Evidently the latter number is inappropriate for hydrogen.

The mean free path for photons is

$$\lambda_\nu = (N \bar{\sigma}_p)^{-1} \quad (1.4-2)$$

where  $N$  is the number density for hydrogen. At most,  $N$  has the interstellar number density  $N_0 = 0.1 \text{ cm}^{-3}$ ; and, consequently  $\lambda_\nu$  equals or exceeds  $1.85 \times 10^{18} \text{ cm}$  or roughly  $10^5 \text{ a. u.}$  Since the characteristic dimensions of the flowfield are less than  $10^{-3} \text{ a.u.}$ , attenuation of the ionizing flux is not a factor in the problem. With

the assumption of spherical symmetry, the flux then varies as  $r^{-2}$ . Hence from equation (1),  $\alpha$  may be represented in terms of the computed value  $\alpha_{pe}$  at earth by

$$\alpha_p = \alpha_{pe} \left( \frac{r_e}{r} \right)^2 \quad (1.4-3)$$

The mean free time  $\tau_p$  for hydrogen before photoionization is given by the reciprocal of  $\alpha_p$ . The characteristic speed for the transport of interstellar neutral hydrogen into the solar wind is the mean thermal speed at  $10^4$  °K. Then the mean free path against photoionization is the product of the characteristic speed  $1.5 \times 10^6$  cm/s with the mean free time, yielding  $\lambda_p^* \approx 0.6 r^{*2}$  where as before the asterisks signify quantities measured in astronomical units.

The differential relationship between hydrogen number density and mean free path is

$$dN = - \frac{d\lambda}{\lambda} N \quad (1.4-4)$$

Assuming for purposes of the present rough estimation that the hydrogen moves radially toward the sun we have  $d\lambda = -dr$ . Then with the approximate representation for the mean free path found above, equation (4) may be integrated to give  $N = N_0 \exp(-1.5/r^*)$ . Evidently a fraction on the order of 15% of the interstellar hydrogen is unable to survive photoionization to reach 10 a. u. while only 1% suffers photoionization in passing through the subsonic region to reach the (shock) boundary of the supersonic region.

The protons which are added thusly to the supersonic solar wind carry mass and, in conjunction with charge exchange, act through momentum



conservation to retard the velocity of the far supersonic solar wind. A needed parameter in a subsequent calculation of velocity retardation (subsection c.) is the amount by which the proton flux of the supersonic solar wind is augmented by photoionization.

The conservation law form of the equation governing proton number density  $n$  in the steady solar wind (Chapter II.) is

$$\operatorname{div} (n\mathbf{v}) = \dot{n}_p \quad (1.4-5)$$

where  $\dot{n}_p$  is the volume rate of photoionizations given by

$$\dot{n}_p = \alpha_p N = \alpha_{ep} r_e^2 \frac{N}{r^2} \quad (1.4-6)$$

With the assumption of spherically symmetric radial flow in the supersonic region, equations (5) and (6) may be expressed as

$$\frac{1}{r^2} \frac{d}{dr} (n v r^2) = \alpha_{ep} r_e^2 \frac{N}{r^2} \quad (1.4-7)$$

Recognizing the quantity under the differential operator to be the proton flux  $\varphi$ , we integrate equation (7) giving

$$\frac{\varphi - \varphi_e}{\varphi_e} = \frac{\alpha_{ep}}{n_e v_e} \int_{r_e}^r N dr \approx \frac{\alpha_{ep} N_0}{n_e v_e} (r - r_e) \quad (1.4-8)$$

#### b. Charge exchange

In the charge exchange reaction, a proton in passage of a hydrogen atom acquires the temporally shared electron. Since in the case of charge exchange between protons and hydrogen the product species are identical

in kind with the reactants, the process is said to be resonant. That is, the reaction requires no exchange of kinetic for chemical potential energy. As a consequence the reaction is more probable the longer the reactants are in proximity; and, accordingly, the cross sections are higher for lower relative velocities between the reacting particles.

The charge exchange cross section has been calculated over the energy range of our problem, 1 ev to 1 Kev by Dalgarno and Yadav (1953). At 1 ev, corresponding approximately to the case of protons and hydrogen interacting in the interstellar wind at  $10^4$  °K, Dalgarno and Yadav find the cross section to be  $47.3 \times 10^{-16} \text{ cm}^2$ . At 1 Kev, corresponding approximately to the case of supersonic solar wind protons colliding with interstellar neutral hydrogen, the calculated cross section is  $16.5 \times 10^{-16} \text{ cm}^2$ .

Over the subrange 20 ev to 1 Kev the charge exchange cross section has been determined experimentally by Fite, Smith and Stebbings (1962). The measurements are found to be about 10% higher but qualitatively fit the calculated cross sections very well. Indeed to accuracy well within that of the experimental measurements, Fite, et al. find the measurements fit the semi-empirical law for symmetric resonance cross sections (Dalgarno, 1957).

$$\sigma_c^{1/2} = 7.6 - 1.06 \log_{10} E \quad (1.4b-1)$$

where  $\sigma_c^{1/2}$  has units of  $10^{-8} \text{ cm}$  and  $E$  is in ev.

Expressing  $E$  in terms of the relative velocity of the particles, we find by squaring equation (1) the relation for the charge exchange

cross section

$$\sigma_c = 62.3 - 33.5 \log_{10} \bar{v} + 4.5 \log_{10}^2 \bar{v} \quad (1.4b-2)$$

In equation (2) the cross section has units of  $10^{-16} \text{ cm}^2$  and the velocity is in units of  $10^6 \text{ cm/s}$ . All charge exchange cross sections used in the thesis are derived from equation (2).

The charge exchange cross section plays its role in the reaction rate formulas. There the determining quantity is the product  $\bar{\alpha}$  of the cross section with the relative velocity of the reactants. Hence the quantity  $\bar{\alpha}$ , which we term the primitive rate coefficient is the thing for which we desire an effective mathematical representation.

In this connection it is noted that Axford, et al. (1963) suggested taking  $\bar{\alpha}$  constant, a choice that can lead to errors somewhat exceeding a factor of two when applied over the entire solar wind regime. But because the cross section is slowly varying with velocity, roughly like  $v^{-1/3}$  over the solar wind regime, recent authors (e.g., Semar, 1968; Holzer, 1972; Fahr, 1972) have taken the charge exchange cross section to be the constant appropriate to the solar wind velocity at earth. The latter choice of itself, implies errors of less than a factor of two. But taking  $\sigma_c$  constant implies the mathematical problem of treating the relative velocity, in the past with some approximation that introduces additional error into  $\bar{\alpha}$ . Whereas taking  $\bar{\alpha}$  constant obviates the necessity to prescribe the relative velocity. Using equation (2) we investigate analytically the question of making an effective formulation for  $\bar{\alpha}$ .

First it is noted that the coefficient of the last term in equation (2) is small offering the opportunity for effective linearization in  $\log_{10} \bar{v}$ . To this end we consider variations in velocity about some constant velocity  $v_o$ . Then equation (2) may be expressed as

$$\begin{aligned} \sigma_c &= 62.3 - 33.5 \log_{10} \bar{v}_o + 4.5 \log_{10}^2 \bar{v}_o & (1.4b-3) \\ &- (33.5 - 9.0 \log_{10} \bar{v}_o) \log_{10} \left(\frac{v}{v_o}\right) + 4.5 \log_{10}^2 \left(\frac{v}{v_o}\right). \end{aligned}$$

Taking  $\bar{v}_o = 40$  corresponding to the velocity of the supersonic solar wind at earth and expressing the result in natural logarithms we have from equation (3)

$$\sigma_{c1} = 20 - 8.25 \ln \frac{v}{v_e} + 0.85 \ln^2 \frac{v}{v_e} \quad (1.4b-4)$$

In the subsonic solar wind we base the cross section on  $\bar{v}_o = 10$  which is characteristic of both the post shock velocity and thermal speed. The choice yields

$$\sigma_{c2} = 33.3 - 10.6 \ln \left(\frac{4v}{v_e}\right) + 0.85 \ln^2 \left(\frac{4v}{v_e}\right). \quad (1.4b-5)$$

Lastly in the interstellar wind regime we base the cross section on the characteristic thermal speed for which  $\bar{v}_o = 2$ . In this case we get

$$\sigma_{cI} = 52.6 - 13.4 \ln \left(\frac{v}{2 \times 10^6}\right) + 0.85 \ln^2 \left(\frac{v}{2 \times 10^6}\right) \quad (1.4b-6)$$

Equation (4), (5), and (6) have the form

$$\sigma = \sigma_0 - \sigma_1 \ln \frac{v}{v_0} + \sigma_2 \ln^2 \frac{v}{v_0} \quad (1.4b-7)$$

Expanding in Taylor series about  $v_0$  gives, with  $\Delta v = v - v_0$ ,

$$\begin{aligned} \sigma &= \sigma_0 - \sigma_1 \frac{\Delta v}{v} + 2\sigma_2 \left( \ln \frac{v}{v_0} \right) \frac{\Delta v}{v} + \frac{\sigma_1}{2} \left( \frac{\Delta v}{v} \right)^2 + \dots \\ &= \sigma_0 - \sigma_1 \frac{\Delta v}{v} + \frac{(\sigma_1 + 4\sigma_2)}{2} \left( \frac{\Delta v}{v} \right)^2 + \dots \end{aligned} \quad (1.4b-8)$$

Finally multiplying equation (8) by  $v$  gives the series for the primitive rate coefficient

$$\bar{\alpha} = \alpha_0 + v_0 (\sigma_0 - \sigma_1) \frac{\Delta v}{v_0} + v_0 \frac{(\sigma_1 + 4\sigma_2)}{2} \left( \frac{\Delta v}{v_0} \right)^2 + \dots \quad (1.4b-9)$$

In the equation the symbol  $\bar{\alpha}_0$  represents the product  $v_0 \sigma_0$ .

Table 5. Parameters of formulae for primitive rate coefficients for charge exchange

Region	$\frac{1}{v_0}$	$\frac{2}{\sigma_0}$	$\sigma_1$	$\frac{3}{\bar{\alpha}_0}$	$(\sigma_0 - \sigma_1)v_0$	$\frac{(\sigma_1 + 4\sigma_2)}{2} v_0$
supersonic solar wind	40	20.0	8.25	8.04	4.70	2.33
subsonic solar wind	10	33.3	10.6	3.33	2.27	0.70
interstellar wind	2	52.6	13.4	1.05	0.784	0.17

$\frac{1}{v_0}$  velocity in units of  $10^6$  cm/s

$\frac{2}{\sigma_0}$  cross sections in units of  $10^{-16}$  cm<sup>2</sup>

$\frac{3}{\bar{\alpha}_0}$  products of cross section with velocity have units of  $10^{-8}$  cm<sup>3</sup> s<sup>-1</sup>

Table 5. is a compendium of parameters of the primitive rate coefficient for the three regions of flow. We note first that the terms in the last three columns decrease monotonically to the right. Then inspection of equation (9) reveals that in any sub region where  $\frac{\Delta v}{v_0} \ll 1$  the first term  $\bar{\alpha}_0$  in the series provides an excellent approximation to the primitive rate coefficient. But more to the point, in any region where  $\frac{\Delta v}{v_0} \approx 1$ , a good approximation is provided by the linear representation involving the first two terms. And in the context of the overall development of the subject, taking only the first term could be considered adequate. In the succeeding subsection c. we shall make use of the linear representation for  $\bar{\alpha}$  in a linear theory for the supersonic solar wind region.

The reaction rates per particle for protons and hydrogen atoms are given respectively by

$$\alpha_c^+ = \bar{\alpha} N \quad \text{and} \quad (1.4b-10)$$

$$\alpha_c = \bar{\alpha} n \quad (1.4b-11)$$

where for protons  $N$  is the number density of target hydrogen atoms and for hydrogen atoms  $n$  is the number density of target protons. The corresponding mean free times against charge exchange for a proton or a hydrogen atom are given respectively by the reciprocals of  $\alpha_c^+$  and  $\alpha_c$ . Finally the volume rates for charge exchange reactions for protons and hydrogen obey the symmetric relations

$$\dot{n}_c = \alpha_c^+ n = \bar{\alpha} N n \quad \text{and} \quad (1.4b-12)$$

$$\dot{N}_c = \alpha_c N = \bar{\alpha} n N \quad (1.4b-13)$$

For charge exchange in the interstellar wind region, the flow is subsonic and the characteristic speed  $2 \times 10^6$  cm/s is the square root of two times the mean square velocity for hydrogen at  $10^4$  °K. From Table 5. the primitive rate coefficient  $\bar{\sigma}_0$  has the value  $1 \times 10^{-8}$  cm<sup>3</sup>/s. From equation (10) the reaction rate and mean free time for protons against charge exchange in the interstellar wind are then  $1 \times 10^{-9}$  s<sup>-1</sup> and  $1 \times 10^9$  s respectively; and for hydrogen atoms,  $1 \times 10^{-10}$  s<sup>-1</sup> and  $1 \times 10^{10}$  s.

Based on the mean free times we can construct some revealing mean free paths for interactions. First for the protons in the ionized interstellar wind, the characteristic speed for bulk transport between charge exchange interactions is the bulk velocity  $6 \times 10^5$  cm/s. The mean free path  $\lambda^+$  for bulk transport of protons is given by the product of the bulk velocity with the mean free time. The result is  $\lambda^+ = 6 \times 10^{14}$  cm or 40 a.u.

The cross section for hydrogen atoms to scatter hydrogen atoms is given approximately by  $4\pi a_0^2$  where  $a_0$  is the first Bohr radius  $.529 \times 10^{-8}$  cm. The cross section is thus roughly  $3.5 \times 10^{-16}$  cm<sup>2</sup>. Taking the reciprocal of the product of the cross section with the hydrogen density  $0.1$  cm<sup>-3</sup> provides the self scattering mean free path  $\sim 3 \times 10^{16}$  cm or 2000 a.u.

Lastly taking the product of the characteristic thermal speed  $1.5 \times 10^6$  cm/s with the mean free time for charge exchange gives the mean free path  $\lambda_c$  for hydrogen to interact with the ionized interstellar wind as  $1.5 \times 10^{16}$  cm or 1000 a.u.

The characteristic dimension of the flowfield for the interstellar wind can be taken as the distance from the sun to the heliopause boundary, roughly 300 a.u. Comparing this value with the mean free paths for protons and hydrogen atoms we observe a striking dichotomy. Specifically, as was stated in section 2., the mean free path for hydrogen to collide with either itself or the protons of the interstellar wind is long compared to the dimensions of the flowfield. This result permits the use of collisionless kinetic theory to describe the transport of interstellar hydrogen into the solar wind.

On the other hand, the mean free path for charge exchange in the bulk transport of protons of the ionized interstellar wind is small compared to the characteristic dimension of the flowfield. Consequently the protons of the ionized interstellar wind frequently will be exchanged for new ones obtained from the neutral wind. But the ionized interstellar wind, flowing as a continuum fluid around the heliopause, does not have the same mean velocity as does the neutral hydrogen which is not significantly deflected by the flow of the ionized component. Hence each charge exchange event in the interstellar wind in the vicinity of the sun results in an exchange of momentum contributing to a net impulse on the ionized interstellar wind. Quite evidently the impulse is in the direction of the bulk velocity of the neutral hydrogen and results in pressure of the ionized interstellar wind on the heliopause.

The Mach number of the interstellar wind is low and the random velocities of the protons exceed their bulk speed. Consequently what small percentage of the primary neutral hydrogen does suffer charge exchange close to the sun will to a large extent be replaced by secondary hydrogen with nearly the same velocity distribution as that of



the primary hydrogen. Hence the flux of hydrogen across the heliopause into the subsonic solar wind is hardly altered by the presence of the ionized interstellar wind. Thus in evaluating the transport of neutral hydrogen into the solar wind (Chapter II.) we assume at the heliopause boundary the components of the differential flux of hydrogen directed into the solar wind region to be given by the Maxwellian distribution with temperature and density characteristic of the undistributed interstellar medium.

For charge exchange in the subsonic solar wind the characteristic speed of relative motion is the mean velocity  $10^7$  cm/s for the temperature  $10^6$  °K of the subsonic solar wind. From Table 5. the primitive rate coefficient is  $3.33 \times 10^{-8} \text{ cm}^3 \text{ s}^{-1}$ . Following equations (10) and (11) with densities from Table 4., we find the charge exchange rate and mean free time for protons to be  $3.33 \times 10^{-9} \text{ s}^{-1}$  and  $3 \times 10^8 \text{ s}$ ; for hydrogen,  $3.33 \times 10^{-11} \text{ s}^{-1}$  and  $3 \times 10^{10} \text{ s}$ .

Looking first at the numbers for hydrogen we see that the mean free time  $3 \times 10^{10} \text{ s}$  is the same while the characteristic speed is thrice as great in the subsonic solar wind as in the ionized interstellar wind. Thus the mean free path ( $\sim 3000$  a.u.) is three times as long in the subsonic solar wind as in the interstellar medium. Hence the presence of the subsonic solar wind also does not greatly effect the transport of interstellar neutral hydrogen into the supersonic solar wind.

Next considering the mean free time for subsonic solar wind protons, we have that the corresponding mean free path is  $3 \times 10^{15} \text{ cm}$  based on the post shock bulk speed of  $10^7$  cm/s. Since the mean free path ( $\sim 200$  a.u.) is comparable with the characteristic dimension

of the subsonic region, as measured by the thickness ( $\sim 180$  a.u.) for example, each solar wind proton has a significant probability of suffering a charge exchange event in the region.

For charge exchange in the supersonic solar wind the characteristic speed is the bulk velocity  $4 \times 10^7$  cm/s. From Table 5. the primitive rate coefficient is  $8 \times 10^{-8}$  cm<sup>3</sup>/s. From equation (10) with Table 4., the charge exchange rate and mean free time for protons are  $8 \times 10^{-9}$ s and  $1.2 \times 10^8$ s respectively. Similarly for hydrogen the rate per atom is  $4 \times 10^{-7} (r^*)^{-2} s^{-1}$  and the mean free time is  $2 \times 10^6 r^{*2}$  s.

Based on the mean thermal speed  $1.5 \times 10^6$  cm/s, the mean free path for hydrogen is  $3 \times 10^{12} r^{*2}$  cm or  $0.2 r^{*2}$  a.u. Virtually all of the hydrogen that passes within a few a.u. of the sun will suffer charge exchange while beyond ten a.u. hydrogen is not greatly affected.

Based on the bulk speed, the mean free path for protons is  $5 \times 10^{15}$  cm or 300 a.u. The radius of the supersonic region being half the mean free path, a significant fraction of the solar wind protons will undergo charge exchange in the supersonic region.

Table 6. Mean free paths for charge exchange and characteristic flowfield dimensions by region.

	supersonic solar wind <sub>1</sub>	subsonic solar wind	interstellar wind
proton mean free path	300	200	40
hydrogen mean free path	$0.2r^{*2}$	3000	1000
characteristic dimension	145	185	300

<sub>1</sub> lengths in astronomical units

A convenient comparison of mean free paths with characteristic lengths for the relevant regions can be made in Table 6, whose contents summarize the previous discussion. We now address the physical consequences of charge exchange in the solar wind regions.

Since (1) the mass of the electron is small, (2) the square root of the cross section for the reaction is large ( $\sim 5\text{\AA}$ ) compared to the size of the bound atom thereby providing for large separations of the nuclei in passage, (3) the electron acts to electrostatically shield the nuclei, and (4) the kinetic energy of relative motion is large compared to the potential energy of the electron in the neutral atom, the exchange of momentum between nuclei in the charge exchange encounter is very slight. Thus while exchanging the electron, the nuclei may be taken to change neither speed nor direction as a result of the encounter.

In the act of shocking the solar wind, as we have seen, exchanges momentum flux for pressure, a process which on the particle level serves to randomize direction of motion but leaves substantially unchanged the characteristic high velocities ( $\sim 10^7$  cm/s) of the protons. But in the same heliocentric reference frame, the characteristic speed of the interstellar neutral hydrogen is only  $10^6$  cm/s. Hence the result of a charge exchange event in either the supersonic or subsonic solar wind regions is the exchange of a high speed proton for a low speed one and the net loss of a lot of particle kinetic energy from the solar wind. The loss of energy per event of course resides in the secondary or "fast" hydrogen atom.

If the event takes place in the subsonic region, the loss in proton kinetic energy is primarily reflected in a reduction of bulk internal energy and temperature as the result of the random motion there. The pressure being roughly a conserved quantity in the subsonic solar wind, the loss of internal energy is balanced there by gains in density and magnetic field strength.

If the event takes place in the supersonic region, the net loss in particle momentum is reflected in a corresponding loss in bulk momentum flux due to the highly ordered nature of particle motion in the hypersonic radial flow. In the light of the shock termination model of section 3., the loss in momentum flux is seen to result in a reduction of the radial distance to the shock as previously estimated in the absence of this additional factor in the pressure - momentum flux balance. We estimate the effect and others due both to photoionization and charge exchange in the following.

c. Linear theory for the supersonic region

With the omission of magnetic stress and hydrodynamic pressure terms which together only amount to about 3% of the momentum flux of the supersonic wind at earth, the momentum equation in conservation law form for steady flow with sources (Chapter II) may be written

$$\operatorname{div} (\rho \mathbf{v} \mathbf{v}) = n_c \mathbf{p} \quad (1.4c-1)$$

where  $\mathbf{p}$  is the net momentum gain to the solar wind per charge exchange event. If we neglect the 1% momentum contribution of the primary hydrogen atom and assume spherically symmetric radial flow then from the previous discussion  $\mathbf{p} = -m v \mathbf{e}_r$  and equation (1) may be expressed

$$\frac{1}{r} \frac{d}{dr} (r^2 \rho v^2) = - n_c \dot{m} v \quad (1.4c-2)$$

Substituting equation (1.4b-12) for the volume rate of charge exchange and making the identification  $\rho v r^2 = m \varphi$  for the mass flux permits equation (2) to be cast

$$\frac{dv}{dr} + \frac{1}{\varphi} \frac{d\varphi}{dr} + \bar{\alpha} N = 0 \quad (1.4c-3)$$

From the results obtained in section 4a. (equation (8)) we express the proton flux in equation (3) by the approximate linear relation

$$\varphi = \varphi_e \left( + \frac{\Delta\varphi}{\varphi_e} \right) \simeq \varphi_e \left( 1 + \frac{\alpha_{ep} N_o}{n_e v_e} r \right). \quad (1.4c-4)$$

Evidently in the bracketed term of the linear expression we have dropped a quantity  $-\frac{\alpha_{ep} N_o}{n_e v_e} r_e$  which is small ( $\sim 0.001$ ) compared to unity. For  $\bar{\alpha}$ , use is made of the linear approximation

$$\bar{\alpha} = \sigma_o v_o + (\sigma_o - \sigma_1)(v - v_o) = \sigma_1 v_o + (\sigma_o - \sigma_1) v \quad (1.4c-5)$$

where the parameters are to be chosen from Table 5. for the supersonic region. Then equation (3) becomes

$$\frac{dv}{dr} + \left[ (\sigma_o - \sigma_1) N + \frac{\alpha_{ep} N}{n_e v_e} \left( 1 + \frac{\alpha_{ep} N_o}{n_e v_e} r \right)^{-1} \right] v + \sigma_1 v_e N = 0 \quad (1.4c-6)$$

Lastly we take  $N = N_o$  which is a good approximation over most of the supersonic region and treat equation (6) as a first order perturbation problem in the small quantities  $\frac{\alpha_{ep} N_o}{n_e v_e} r$ ,  $(\sigma_o - \sigma_1) N_o r$ , etc.

Accordingly, we expand the binomial expression  $(1 + \frac{\alpha_{ep} N_o}{n_e v_e} r)^{-1}$  in power series to first order and are left to solve an equation of the form

$$\frac{dv}{dr} + (a_1 - a_2^2 r) v = -a_3 v_e \quad (1.4c-7)$$

where  $a_1 = (\sigma_o - \sigma_1) N_o + \frac{\alpha_{ep} N_o}{n_e v_e}$ ,

$$a_2 = \frac{\alpha_{ep} N_o}{n_e v_e}, \quad \text{and} \quad a_3 = \sigma_1 N_o.$$

The solution of the zero order problem is

$$v = c_o e^{-a_1 r} + c_1. \quad (1.4c-8)$$

When the constant  $c_o$  is replaced by the variable function  $A(r)$  and the solution substituted in equation (7) there results

$$(A' - a_2^2 r A) e^{-a_1 r} + (a_1 - a_2^2 r) c_1 + a_3 v_e = 0. \quad (1.4c-9)$$

Finally, the quantity  $a_1 r$  being small in equation (9) we expand  $A$  (and  $A'$ ) and the exponential in power series and set the resulting coefficients of powers of  $r$  to zero. Through first order the result is

$$A_1 + a_1 c_1 + a_3 v_e = 0 \quad \text{and} \quad (1.4c-10)$$

$$a_1 A_1 + a_2^2 c_1 + a_2^2 A_o = 0 \quad (1.4c-11)$$

We have above only two equations in three unknowns  $A_0$ ,  $A_1$ , and  $c_1$ . The needed third relation is provided by the initial condition  $v = v_e$  which, consistent with the linearization of the problem, we apply at  $r = 0$  giving

$$A_0 + c_1 - v_e = 0 \quad (1.4c-12)$$

The solution of equation (10), (11), and (12) is

$$A_0 = v_e \left( 1 + \frac{a_3}{a_1} - \frac{a_2^2}{a_1^2} \right), \quad A_1 = -\frac{a_2^2}{a_1} v_e \quad (1.4c-13)$$

and  $c_1 = -v_e \left( \frac{a_3}{a_1} - \frac{a_2^2}{a_1^2} \right).$

Thence with expression (8) and the subsequent discussion, the solution of equation (7) is

$$v = v_e \left\{ \left[ 1 + \frac{a_3}{a_1} - \frac{a_2^2}{a_1^2} (1 + a_1 r) \right] (1 - a_1 r) - \frac{a_3}{a_1} + \frac{a_2^2}{a_1^2} \right\} \quad (1.4c-14)$$

to first order. When the binomial products are expanded the relation is seen to reduce to the exceedingly simple form

$$v = v_e [1 - (a_1 + a_3) r]$$

$$\equiv v_e \left[ 1 - \left( \sigma_0 N_0 + \frac{\alpha_{ep} N_0}{n_e v_e} \right) r \right]. \quad (1.4c-15)$$

The number density may now be obtained by dividing the proton flux, equation (4), by the product  $v r^2$  yielding

$$\begin{aligned}
n &= n_e \frac{r_e^2}{r_2^2} \left[ \frac{1 + a_2 r}{1 - (a_1 + a_3) r} \right] \\
&= n_e \frac{r_e^2}{r_e^2} [ 1 + (a_1 + a_2 + a_3) r ] \\
&\equiv n_e \frac{r_e^2}{r_e^2} [ 1 + (\sigma_o N_o + 2 \frac{\alpha_{ep} N_o}{n_e v_e}) r ] \quad (1.4c-16)
\end{aligned}$$

to first order.

Next multiplying the shock relation, equation (1.2-17) , by  $r^2$  provides the equivalent expression

$$\frac{\gamma + 3}{2(\gamma + 1)} M \varphi v = r^2 p_s \quad (1.4c-17)$$

In equation (17) the product  $\varphi v$  obtained from expression (4) and (15) is

$$\begin{aligned}
\varphi v &= \varphi_e v_e [ 1 + (a_2 - a_1 - a_3) r ] \\
&\equiv \varphi_e v_e [ 1 - \sigma_o N_o r ] \quad (1.4c-18)
\end{aligned}$$

to first order.

With numbers garnered from the previous discussion we have that

$$\sigma_o N_o = 20 \times 10^{-17} \text{ cm}^{-1} \quad \text{and} \quad \frac{\alpha_{ep} N_o}{n_e v_e} = 7.5 \times 10^{-17} \text{ cm}^{-1} .$$

These parameters are proportional to the charge exchange and photoionization rates used by other authors. Because the photoionization rate is only about  $3/8$  the rate for charge exchange, it has been



presumed Fahr (1972), Holzer (1972) Axford (1972) that photoionization is "relatively" unimportant but "qualitatively" has much the same influence on the system. Equation (15), with the numbers above, shows that the presumption is true for the velocity. Equation (16) shows that photoionization and charge exchange are of comparable importance in increasing the density, a fact that has been more or less understood. But equations (17) and (18) show that, in a different way, the presumption is not valid for the momentum flux and, therefore, the location of the shock transition. For in the latter case the first order effects of photoionization in decreasing the velocity are exactly cancelled by the increase in mass flux due to the added particles. Hence in so far as first order effects of any relative magnitude are concerned only the charge exchange process plays a role in determining the shock location.

There is additionally something to be learned here from Fahr's (1972) analysis viewed in the light of the foregoing. In part, the point we wish to make involves the desirability of employing to a consistent level of approximation the lowest order set of moment equations necessary to describe the phenomena in question.

In his analysis of the modified shock location Fahr assumed a priori that photoionization had negligible effect on the problem and took the mass flux to be conserved. As we have shown this assumption leads to no first order error in the computation of the shock location. Further Fahr assumed, as we have done, that temperature effects were negligible. He then described the variation of the velocity of the solar wind through an energy equation with a source term.

Though it is not specifically described as such, Fahr's equation is not a total energy equation in which thermal energy effects have been neglected; and his source term is not simply the net energy lost to the flow in the escape of the primary proton. Rather, his equation is the so called "mechanical energy equation" of fluid dynamics and his source term is twice the net energy lost to the flow. Fahr argues for his source term by adding to the net loss of energy to the flow the additional "work" done by the remaining fluid in accelerating the secondary proton. Fahr's result is correct but because of the complexity of the underlying mechanisms his method of getting the needed source term requires insight that as argued, at least, is not fully convincing.

By contrast in the momentum equation formulation the source term is the net momentum lost to the flow in the escape of the primary proton, while momentum is conserved in the interaction of the indistinguishable secondary proton and the remainder of the flow.

The connection between the two formulations which have yielded identical results is very simple. In fluid dynamics the mechanical energy equation is obtained from the momentum equation by multiplying the latter through by the velocity, a process which gives directly and unambiguously the source term used by Fahr.

Since Fahr's source term, the kinetic energy loss is twice the total energy loss of the flow, it is of interest to identify where the remaining kinetic energy goes. We recall that after the charge exchange event momentum was conserved in the interaction between the secondary proton and the remaining flow. The process terminates when the secondary proton reaches the bulk flow speed. But this scenario describes the "perfectly inelastic collision" of elementary mechanics. In such

collisions, we recall, momentum is conserved but kinetic energy is not; the process is dissipative, converting the lost kinetic energy to heat.

Thus without understanding the underlying mechanisms we also attribute the added loss of kinetic energy in the charge exchange interaction to dissipative heating of the flow. Indeed in a reference frame fixed in the flow, in which the initial velocity of the secondary proton is  $-v$ , Fahr's "work" may be seen as done against friction in slowing down the secondary proton to rest.

Returning to the computation of the reduced shock radius, we find that combining equations (17) and (18) results in the quadratic equation

$$r^2 + 2 \frac{\gamma + 3}{4(\gamma + 1)} \frac{m_p v_e \sigma_o N}{p_s} r - \frac{\gamma + 3}{2(\gamma + 1)} \frac{m_p v_e}{p_s} = 0 \quad (1.4c-19)$$

In the absence of the second term, the equation gives the classical solution  $r_{so}$  obtained previously, equation (1.2-18). Hence equation (19) may be written

$$r^2 + 2 r_{so}^2 \frac{\sigma_o N}{2} r - r_{so}^2 = 0 \quad (1.4c-20)$$

When  $r$  in equation (32) is normalized by  $r_{so}$ , the solution obtained from the quadratic formula is

$$\bar{r} = - \frac{\sigma_o N r_{so}}{2} \pm \left[ \left( \frac{\sigma_o N r_{so}}{2} \right)^2 + 1 \right]^{1/2} \quad (1.4c-21)$$

The quantity  $\frac{\sigma_o N r}{2}$  has the value 0.145 based on numbers developed to this point. Thus the radical may be expanded in a power series giving

$$\bar{R} \equiv \frac{R}{r_{so}} = 1 - \frac{\sigma_o N r}{2} + \frac{1}{2} \left( \frac{\sigma_o N r}{2} \right)^2 + \dots \quad (1.4c-22)$$

Thus the inclusion of particle processes in the model serves to reduce the estimate of the shock radius by some 14% to 125 a.u. from the previous estimate of 145 a.u.

d. Lyman-alpha scattering and radiation pressure on hydrogen

The chromosphere of the sun emits a strong, broad line of hydrogen Lyman- $\alpha$  radiation centered at 1215.67 Å in the ultraviolet. Reported rocket measurements (Purcell and Tousey, 1960; Bruner and Parker, 1969) place the integrated flux in the line at about 6 erg/cm<sup>2</sup> sec and the line width at roughly 0.8 Å.

Bruner and Rense (1969) have calibrated the flux spectral density profile over the line. The line profile features a broad solar absorption minimum of some 0.3 Å width about the line center. Based on twice the most probable thermal speed, the effective doppler width of the absorption spectrum for the bulk of the hot interstellar hydrogen is 0.1 Å, falling well within the self absorption notch in the emission spectrum. There the solar flux spectral density is  $4.2 \times 10^{11}$  photons cm<sup>-2</sup> s<sup>-1</sup> Å<sup>-1</sup>.

The rate  $g$  at which an atom of hydrogen scatters solar Lyman- $\alpha$  photons is given (e.g. Barth, 1969) by

$$g = (\pi F_{\lambda}) \frac{\lambda}{\nu} \frac{\pi e^2}{m_e c} f \quad (1.4d-1)$$

where  $\pi F_{\lambda}$  is the flux spectral density per unit wavelength,  $\lambda$  and  $\nu$  are the wavelength and frequency of the radiation, and  $f$  is the quantum mechanical oscillator strength 0.416. Using the quoted flux density we find  $g$  to have the value  $2.28 \times 10^{-3}$  s<sup>-1</sup> at 1 a.u.

The hydrogen absorbs momentum from an essentially plane wave propagating radially from the sun and scatters (emits) symmetrically as a dipole. Hence in each scattering event a hydrogen atom suffers an impulse that is directed radially outward and equal to the momentum of the photon  $h\nu/c$ . Thus the net force of radiation pressure in the Lyman- $\alpha$  line is the product of the scattering rate by the impulse per event

$$F_{\alpha} = \frac{h\nu}{c} g \quad (1.4d-2)$$

With the value found for  $g$ , the force of radiation pressure at 1 a.u. is estimated to be  $1.24 \times 10^{-24}$  dyne. Solar gravity contributes an opposing radial force  $0.99 \times 10^{-24}$  dyne at 1 a.u. The 25% difference between these two numbers falls within both experimental error in a single flux measurement (Bruner and Parker, 1969) and measured flux variation over the period of a solar rotation (Meir, 1969). The extent to which solar Lyman- $\alpha$  emission varies over a solar cycle is not known but there are indications it is within a factor of two and at least comparable with the variation over a rotation (see Banks and Kockarts, 1973 for related discussion).

Since interstellar hydrogen moves with a speed only on the order of 2 a.u. per year with respect to the sun, all solar flux variations including those over a solar cycle will be largely averaged out in the transport of hydrogen into the inner solar system. Thus in the absence of any more definitive information and for the compelling mathematical advantages the assumption affords, we assume the force of radiation pressure exactly balances solar gravitation in the transport of interstellar atomic hydrogen. In this connection we note that the Lyman- $\alpha$  flux varies as  $r^{-2}$  when the sun is assumed to be a point source scattering in an isotropic medium. Hence if we were to assume the forces of radiation pressure and gravity balance anywhere, we just as well assume they balance everywhere and the hydrogen particle trajectories become straight lines into the solar system.

The atomic absorption line width in scattering is given in terms of frequency interval by Stone (1963). Converted to wavelength interval by the relation  $\Delta\lambda = \frac{\lambda^2}{c} \Delta\nu$ , the absorption line width is

$$\Delta_{\lambda s} = \frac{8\pi}{3} \left( \frac{\pi e^2}{m_e c^2} \right) = 7.4 \times 10^{-4} \text{ \AA}. \quad (1.4d-3)$$

Hence the atomic absorption line width is very much narrower than the  $0.1 \text{ \AA}$  doppler broadened absorption band generated over the distribution of the scattering atoms.

The effective solar flux for scattering within an atomic absorption line is

$$\varphi_s = (\pi F_\lambda) \Delta_{\lambda s} \quad (1.4d-4)$$

And the definition of the atomic cross section  $\sigma_s$  for scattering is

$$g = \varphi_s \sigma_s \quad (1.4d-5)$$

With the relation  $\lambda = c/v$ , equations (1), (3), (4), and (5) can be combined to give

$$\sigma_s = \frac{3\lambda^2}{8\pi} f \quad (1.4d-6)$$

The cross section has the value  $7.35 \times 10^{-12} \text{ cm}^2$ .

For purposes of estimating the mean free path for scattering Lyman- $\alpha$  photons, we assume the hydrogen to be uniformly distributed over the  $0.1 \text{ \AA}$  doppler broadened absorption band. Then the density  $N_\Delta$  of hydrogen atoms occupying any absorption line in the band is roughly

$$N_\Delta = \frac{\Delta_{\lambda s}}{\Delta_{\text{dop}}} N \quad (1.4d-7)$$

Accordingly the mean free path for Lyman- $\alpha$  photons is

$$\lambda_s = \frac{1}{N \Delta \sigma_s} = \frac{\Delta_{\text{dop}}}{\Delta_{\lambda s}} \frac{1}{N \sigma_s} \quad (1.4b-8)$$

Assuming the hydrogen to have the undisturbed interstellar number density  $0.1 \text{ cm}^{-3}$ , the mean free path is found to be of the order 10 a.u. From the way in which the doppler bandwidth was defined, the above number is appropriate to photons scattered from the bulk of hydrogen under the peak of the distribution function. For hydrogen in the velocity tail of the distribution, the number density is considerably less and the mean free path is commensurately greater.

The volume rate of scattering is the product of the rate  $g$  per atom and the hydrogen number density  $N$ . Assuming the single scattering model, we get the contribution to the observed intensity from sources in  $dr$  at  $r$  to be

$$dI = \frac{gN}{4\pi} dr \quad (1.4d-9)$$

The total intensity is then given by the integral of equation (9) taken over the line of sight. Neglecting the effect of aspherically symmetric multiple scattering, we assume the solar flux and, hence,  $g$  to decrease as  $r^{-2}$  and

$$I = \frac{g_e r_e^2}{4\pi} \int \frac{N}{r^2} dl \quad (1.4d-10)$$

Equation (10) finds use in Chapter III where we calculate the intensity of Lyman- $\alpha$  backscatter from the distribution of interplanetary hydrogen



that we find. We now turn our attention to completing the mathematical model including the problem of the transport of hot interstellar neutral hydrogen into the solar wind.

## Chapter II. A Mathematical Model

In chapter I. we have seen that the mean free paths for protons to interact with hydrogen in either flow regime are short compared to characteristic flowfield dimensions. This fact and other plasma properties involving short characteristic lengths lead us ultimately to treat the ionized fraction of the gas through a continuum model.

On the other hand, except very near the sun, the mean free paths for hydrogen to interact with either itself or the ionized fraction in either flow regime are very large compared to characteristic flowfield dimensions. This fact leads us to treat the transport of hydrogen through a single particle description.

But the state of the two gases are interdependent through the photoionization and charge exchange processes. The global formulation including the interaction between the two gases is best understood if we begin the discussion where the two descriptions make contact, at their foundations in the kinetic theory.

### 1. Distribution Functions, Boltzmann's Equations, and the Plasma Transport Equations.

The state of the partially ionized gas in either flow regime, solar wind or interstellar wind, is specified by the set of distribution functions  $f_e$ ,  $f_i$ ,  $f_n$  for the three species comprising the gas - electrons, ions (protons), and neutral hydrogen atoms. The distribution functions which are the locally averaged particle density functions in the six dimensional phase space of position and velocity are solutions of Boltzmann's equation

$$\frac{\partial f}{\partial t} + \frac{\partial}{\partial x_\beta} (v_\beta f) + \frac{\partial}{\partial v_\beta} (a_\beta f) = C + S . \quad (2.1-1)$$

We emphasize for the sake of the subsequent discussion that for each species of particle there is a separate equation of the type described by equation (1).

In equation (1) the summation convention is invoked for repeated subscript indices. The quantities  $a_\beta$  are the cartesian components of particle acceleration due to macroscopic fields - gravitation, radiation, electric, and magnetic. The symbols  $\underline{C}$  and  $\underline{S}$  represent functions describing discontinuous additions and subtractions of particles from unit volume of phase space.

The symbol  $\underline{C}$  stands for collisions in which particles of the given species interact with particles of either the same or different species, all particles being changed in velocity but unchanged in kind by the interaction. In fact only Coulomb collisions within and between the population of electrons and protons are important in the problem, and for hydrogen  $\underline{C}_N$  is effectively zero.

The symbol  $\underline{S}$  represents particle processes in which changes of kind do occur. Here the processes are photoionization and charge exchange. The interactions between hydrogen and the ionized species are described by the functions  $S_e, S_i, S_N$ . These are intimately mathematically related and provide the basis for the source terms of the continuum equations for the plasma.

The macroscopic quantities number density  $n$ , bulk velocity  $\underline{V}$ , and total specific kinetic energy  $\epsilon$  are given by the first three velocity moments of the distribution function

$$n = \int f d^3v \quad (2.1-2)$$

$$\bar{v} = \frac{1}{n} \int \bar{v} f d^3v \equiv \langle \bar{v} \rangle \quad (2.1-3)$$

$$\epsilon = \frac{1}{n} \int \frac{\bar{v} \cdot \bar{v}}{2} f d^3v \equiv \frac{1}{2} \langle \bar{v} \cdot \bar{v} \rangle . \quad (2.1-4)$$

When the distributed velocity  $\bar{v}$  is written in terms of the bulk velocity by

$$\bar{v} = \bar{V} + \bar{v}' \quad (2.1-5)$$

then  $\langle \bar{v}' \rangle = 0$  and

$$\epsilon = \frac{1}{2} \bar{V}^2 + \frac{1}{2} \langle \bar{v}' \cdot \bar{v}' \rangle . \quad (2.1-6)$$

Equation (6) shows the decomposition of the total specific kinetic energy into the sum of the bulk specific kinetic energy  $\frac{1}{2} \bar{V}^2$  and the specific internal energy, the latter to which we give the standard symbol  $\underline{e}$ .

The moment equations for a species result from taking successive velocity moments of the associated Boltzmann equation. The continuum transport equations in conservation law form for the macroscopic quantities  $n$ ,  $\bar{V}$ ,  $\epsilon$  derive from the first three moment equations which are

$$\frac{\partial n}{\partial t} + \frac{\partial}{\partial x_\beta} (n \langle v_\beta \rangle) = \int C d^3v + \int S d^3v \quad (2.1-7)$$

$$\begin{aligned} \frac{\partial}{\partial t} (n \langle v_\alpha \rangle) + \frac{\partial}{\partial x_\beta} (n \langle v_\beta v_\alpha \rangle) &= n \langle a_\alpha \rangle \\ &+ \int v_\alpha C d^3v + \int v_\alpha S d^3v \end{aligned} \quad (2.1-8)$$

$$\begin{aligned} \frac{\partial}{\partial t} \left( \frac{n}{2} \langle v_{\alpha} v_{\alpha} \rangle \right) + \frac{\partial}{\partial x_{\beta}} \left( \frac{n}{2} \langle v_{\alpha} v_{\alpha} v_{\beta} \rangle \right) = \\ n \langle a_{\beta} v_{\beta} \rangle + \int \frac{1}{2} v_{\alpha} v_{\alpha} C d^3 v \\ + \int \frac{1}{2} v_{\alpha} v_{\alpha} S d^3 v \end{aligned} \quad (2.1-9)$$

In equation (8) for the mathematical convenience we have represented the vector equation by the set of scalar cartesian component equations for  $\alpha = 1, 2, 3$ .

By virtue of the conservation of particles in collisions, by definition, the first integral on the right hand side of equation (7) is identically zero. Then from equations (7) and (9) multiplied by the particle mass  $m$  and by using equations (3), (4), (5), and (6) we get the continuum transport equations for a plasma species.

$$\frac{\partial \rho}{\partial t} + \frac{\partial}{\partial x_{\beta}} (\rho v_{\beta}) = \dot{m} \quad (2.1-10)$$

$$\frac{\partial}{\partial t} (\rho v_{\alpha}) + \frac{\partial}{\partial x_{\beta}} (\rho v_{\beta} v_{\alpha} + p \delta_{\beta\alpha} - \sigma_{\beta\alpha}) = n F_{\alpha} + \dot{P}_{C\alpha} + \dot{P}_{S\alpha} \quad (2.1-11)$$

$$\begin{aligned} \frac{\partial}{\partial t} \left[ \rho \left( \frac{v^2}{2} + e \right) \right] + \frac{\partial}{\partial x_{\beta}} \left[ \rho v_{\beta} \left( \frac{v^2}{2} + e \right) + p v_{\beta} - \sigma_{\beta\alpha} v_{\alpha} + q_{\beta} \right] \\ = n F_{\alpha} v_{\alpha} + \dot{\epsilon}_C + \dot{\epsilon}_S \end{aligned} \quad (2.1-12)$$

where the mass density  $\rho = mn$ .

In accord with the standard definitions from kinetic theory, in equations (10), (11), and (12) the pressure  $p$ , deviatoric stress tensor components  $\sigma_{\beta\alpha}$ , and conduction heat flux vector components  $q_{\beta}$  are represented by

$$p = \frac{\rho}{3} \langle v'_\alpha v'_\alpha \rangle \quad (2.1-13)$$

$$\sigma_{\beta\alpha} = p \delta_{\beta\alpha} - \rho \langle v'_\beta v'_\alpha \rangle \quad (2.1-14)$$

$$q_\beta = \rho \langle \frac{v'^2}{2} v'_\beta \rangle \quad (2.1-15)$$

With equation (13) and the definition of the specific internal energy, equation (6), we get the state equation

$$e = \frac{3}{2} \frac{p}{\rho} \quad (2.1-16)$$

Lastly a temperature can be defined for the species by

$$T = \frac{2}{3} \frac{m}{k} e \quad (2.1-17)$$

When  $n$ ,  $\underline{V}$ , and  $T$  are sufficiently slowly varying in space and time, the distribution function will approximate a Maxwellian as guaranteed by the Boltzmann H- Theorem for the relaxation process. Under such conditions the distribution function may be represented by a first order perturbation expansion the first, zeroth order, term of which is the Maxwellian distribution. By the method of Chapman and Enskog the Boltzmann equation can be solved approximately for the first order perturbation which is linear in the space derivatives of  $n$ ,  $\underline{V}$ , and  $T$ . The approach permits the integration of relations (14) and (15) to give approximate expressions for the components of the deviatoric shear stress tensor and conduction heat flux vector that are linear respectively in the derivatives of the velocity and the temperature.

In the absence of a magnetic field the components of shear stress and heat flux take the form

$$\sigma_{\beta\alpha} = \mu \left( \frac{\partial v_{\beta}}{\partial x_{\alpha}} + \frac{\partial v_{\alpha}}{\partial x_{\beta}} - \frac{2}{3} \delta_{\beta\alpha} \frac{\partial v_{\epsilon}}{\partial x_{\epsilon}} \right) \quad (2.1-18)$$

and

$$q_{\beta} = \kappa \frac{\partial T}{\partial x_{\beta}} \quad (2.1-19)$$

in which the single (scalar) coefficients  $\mu$  and  $\kappa$  are termed the viscosity and thermal conductivity, respectively. Using the method suggested above, Chapman (1954) has obtained coefficients which may be expressed

$$\mu_i = \frac{5}{16A_i} \left( \frac{m_i K T_i}{\pi} \right)^{1/2} \left( \frac{2K T_i}{e^2} \right)^2 \quad (2.1-20)$$

$$\mu_e = \frac{5}{16A_e} \left( \frac{m_e K T_e}{\pi} \right)^{1/2} \left( \frac{2K T_e}{e^2} \right)^2 \quad (2.1-21)$$

$$\kappa_e = \frac{75K}{64A_e} \left( \frac{K T_e}{\pi m_e} \right)^{1/2} \left( \frac{2K T_e}{e^2} \right)^2 \quad (2.1-22)$$

$$\kappa_i = \frac{75K}{64A_i} \left( \frac{K T_i}{\pi m_i} \right)^{1/2} \left( \frac{2K T_i}{e^2} \right)^2 \quad (2.1-23)$$

where  $A \approx \ln \left( \frac{4KT}{e^2 n^{1/3}} \right) - 1$

for  $\frac{4KT}{e^2 n^{1/3}} \gg 1$  as occurs everywhere in our problem.

When the plasma contains a magnetic field such that the gyro radii of particle orbits in the field are short compared to the characteristic mean free path for Coulomb collisions, a great deal of anisotropy is found in the medium. Then the heat flux vector and shear stress tensor

are not described by single scalar coefficients but by sets of coefficients that can differ markedly according to direction relative to the magnetic field vector. Braginskii (1965) has derived expressions for the transport coefficients in the presence of such a magnetic field.

When written in terms of our definition of shear stress components and the components  $h_\alpha$  of the unit vector  $\underline{h}$  in the direction of the magnetic field, Braginskii's expressions become

$$\sigma_{\alpha\beta} = \mu_0 W_{0\alpha\beta} + \mu_1 W_{1\alpha\beta} + \mu_2 W_{2\alpha\beta} - \mu_3 W_{3\alpha\beta} - \mu_4 W_{4\alpha\beta}$$

$$W_{0\alpha\beta} = \frac{3}{2} (h_\alpha h_\beta - \frac{1}{3} \delta_{\alpha\beta}) h_\mu h_\nu w_{\mu\nu}$$

$$W_{1\alpha\beta} = (\delta_{\alpha\mu}^\perp \delta_{\beta\nu}^\perp + \frac{1}{2} \delta_{\alpha\beta}^\perp h_\mu h_\nu) w_{\mu\nu}$$

(2.1-24)

$$W_{2\alpha\beta} = (\delta_{\alpha\mu}^\perp h_\beta h_\nu + \delta_{\beta\nu}^\perp h_\alpha h_\mu) w_{\mu\nu}$$

$$W_{3\alpha\beta} = \frac{1}{2} (\delta_{\alpha\mu}^\perp \epsilon_{\beta\gamma\nu} + \delta_{\beta\nu}^\perp \epsilon_{\alpha\gamma\mu}) h_\gamma w_{\mu\nu}$$

$$W_{4\alpha\beta} = (h_\alpha h_\mu \epsilon_{\beta\gamma\nu} + h_\beta h_\nu \epsilon_{\alpha\gamma\mu}) h_\gamma w_{\mu\nu}$$

where  $w_{\alpha\beta} = \frac{\partial v_\alpha}{\partial x_\beta} + \frac{\partial v_\beta}{\partial x_\alpha} - \frac{2}{3} \delta_{\alpha\beta} \frac{\partial v_\epsilon}{\partial x_\epsilon}$ ,  $\delta_{\alpha\beta}^\perp = \delta_{\alpha\beta} - h_\alpha h_\beta$

$\delta_{\alpha\beta}$  is the Kronecker delta, and  $\epsilon_{\alpha\beta\gamma}$  is the unit antisymmetric tensor.

For protons the coefficients are given by

$$\mu_0^i = 0.96 n_i^{KT} \tau_i$$

$$\mu_2^i = \left( \frac{6}{5} \chi_1^2 + 2.23 \right) \frac{n_i^{KT} \tau_i}{\Delta_1}$$



$$\begin{aligned}\mu_4^i &= \chi_i (\chi_i^2 + 2.38) \frac{n_i K T_i \tau_i}{\Delta_i} \\ \mu_1^i &= \left(\frac{24}{5} \chi_i^2 + 2.23\right) \frac{n_i K T_i \tau_i}{\Delta_{2i}} \\ \mu_3^i &= 2\chi_i (4\chi_i^2 + 2.38) \frac{n_i K T_i \tau_i}{\Delta_{2i}}\end{aligned}\quad (2.1-25)$$

where  $\tau_i$  is the mean free time between coulomb collisions for protons with protons,  $\chi_i = \omega_i \tau_i$  is identically the ratio of gyro radius to mean free path for coulomb collisions and  $\omega_i = \frac{eB}{m_i c}$  is the Larmor or cyclotron frequency. Then the parameters  $\Delta_i$  and  $\Delta_{2i}$  are given by

$$\begin{aligned}\Delta_i &= \chi_i^4 + 4.03 \chi_i^2 + 2.33 \quad \text{and} \\ \Delta_{2i} &= 16 \chi_i^4 + 16.12 \chi_i^2 + 2.33 .\end{aligned}$$

Finally the mean free time is

$$\tau_i = \frac{3\sqrt{2\pi m_i} (K T_i)^{3/2}}{8\pi e^4 n_i \Lambda} \quad (2.1-26)$$

where, Spitzer (1962),  $\Lambda = \frac{3}{2\sqrt{\pi n_e}} \left(\frac{K T_i}{e}\right)^{3/2}$

is the ratio of the Debye shielding distance to the impact parameter for  $90^\circ$  coulomb collisions. The Debye shielding distance

$$h = \left(\frac{K T_e}{4\pi n_i e}\right)^{1/2} \quad (2.1-27)$$

is the characteristic length over which thermal energy can support local fluctuations in electrical charge density in the plasma and is used as the effective cutoff distance for coulomb collisions.

For the electron gas the coefficients of viscosity are given by

$$\begin{aligned} \mu_0^e &= 0.733 n_e K T_e \tau_e, \quad \mu_1^e = (8.2 \chi_e^2 + 8.50) \frac{n_e K T_e \tau_e}{\Delta_{2e}} \\ \mu_2^e &= (2.05 \chi_e^2 + 8.50) \frac{n_e K T_e \tau_e}{\Delta_e}, \quad \mu_3^e = - (4 \chi_e^2 + 7.91) \frac{n_e K T_e \tau_e}{\Delta_{2e}} \\ \mu_4^e &= - (\chi_e^2 + 7.91) \frac{n_e K T_e \tau_e}{\Delta_e} \end{aligned} \quad (2.1-28)$$

where very similarly to the case for protons  $\chi_e = \omega_e \tau_e$ ,  $\omega_e = \frac{eB}{m_e c}$ ,

$$\begin{aligned} \Delta_e &= \chi_e^4 + 13.8 \chi_e^2 + 11.6 \quad \text{and} \\ \Delta_{2e} &= 16 \chi_e^2 + 55.2 \chi_e^2 + 11.6. \end{aligned}$$

The electron collision time is

$$\tau_e = \frac{3\sqrt{2\pi m_e} (K T_e)^{3/2}}{8\pi e^4 n_e \Lambda} \quad (2.1-29)$$

Similarly, for the heat flux conducted by the electron gas,

Braginskii's expressions may be represented

$$\underline{\underline{q}}^e = \underline{\underline{q}}^{eT} + \underline{\underline{q}}^{ev} \quad \text{with} \quad (2.1-30)$$

$$\underline{\underline{q}}^{eT} = - \kappa_{||}^e \underline{\underline{h}} \cdot \underline{\underline{\nabla}} T_e + \kappa_{\perp}^e \underline{\underline{h}} \times (\underline{\underline{h}} \times \underline{\underline{\nabla}} T_e) - \kappa_{\Lambda}^e \underline{\underline{h}} \times \underline{\underline{\nabla}} T_e$$

$$\underline{\underline{q}}^{ev} = \{ \beta_{||} \underline{\underline{h}} \cdot (\underline{\underline{v}}^e - \underline{\underline{v}}^i) - \beta_{\perp} \underline{\underline{h}} \times [\underline{\underline{h}} \times (\underline{\underline{v}}^e - \underline{\underline{v}}^i)] \}$$

$$+ \beta_{\Lambda} \underline{\underline{h}} \times (\underline{\underline{v}}^e - \underline{\underline{v}}^i) \} n_e K T_e$$

In the above expressions, the coefficients of thermal conductivity are

$$\begin{aligned}\kappa_{\parallel}^e &= 3.2 \frac{n_e K T_e \tau_e}{m_e} \\ \kappa_{\perp}^e &= (4.66 \chi_e^2 + 11.9) \frac{n_e K T_e \tau_e}{\Delta_e^{\prime m_e}} \\ \kappa_{\Lambda}^e &= \chi_e \left( \frac{5}{2} \chi_e^2 + 21.7 \right) \frac{n_e K T_e \tau_e}{\Delta_e^{\prime m_e}}\end{aligned}\tag{2.1-31}$$

and the coefficients for the additional transport due to collisions between electrons and ions are

$$\beta_{\parallel} = 0.7, \quad \beta_{\perp} = (5.1 \chi_e^2 + 2.68) \frac{1}{\Delta_e^{\prime}}$$

(2.1-32)

$$\beta_{\Lambda} = \chi_e \left( \frac{3}{2} \chi_e^2 + 3.05 \right) \frac{1}{\Delta_e^{\prime}}, \quad \text{with}$$

$$\Delta_e^{\prime} = \chi_e^4 + 14.8 \chi_e^2 + 3.77.$$

For the proton gas Braginskii gives

$$\tilde{q}_{\parallel}^i = -\kappa_{\parallel}^i \tilde{h} \cdot \nabla T_i + \kappa_{\perp}^i \tilde{h} \times (\tilde{h} \times \nabla T_i)$$

$$- \kappa_{\Lambda}^i \tilde{h} \times \nabla T_i$$

(2.1-33)

where

$$\begin{aligned} \kappa_{||}^i &= 3.9 \frac{n_i K^2 T_i \tau_i}{m_i} \\ \kappa_{\perp}^i &= (2\chi_i^2 + 2.65) \frac{n_i K^2 T_i \tau_i}{\Delta_i' m_i} \\ \kappa_{\Lambda}^i &= \chi_i \left( \frac{5}{2} \chi_i^2 + 4.65 \right) \frac{n_i K^2 T_i \tau_i}{\Delta_i' m_i} \end{aligned} \quad (2.1-34)$$

$$\text{and } \Delta_i' = \chi_i^4 + 2.7 \chi_i^2 + 0.68$$

The exposition of terms in the plasma transport equations is continued now with considerations of the body force  $\underline{F} = m \langle \underline{a} \rangle$  which appears in equations (11) and (12). For the protons the force is given by

$$\underline{F}^i = e \underline{E} + e \frac{\underline{v}^i}{c} \times \underline{B} - GM_o m_i \frac{\underline{r}}{r^3} \quad (2.1-35)$$

where  $\underline{E}$  and  $\underline{B}$  are the macroscopic electric field and magnetic induction respectively and  $e$  is the charge of the electron and  $c$  the speed of light, Gaussian units being employed. Similarly, for the electron gas the force is

$$\underline{F}^e = -e \underline{E} - e \frac{\underline{v}^e}{c} \times \underline{B} - GM_o m_e \frac{\underline{r}}{r^3} \quad (2.1-36)$$

From equations (7), (8) and (9) the source terms of the plasma transport equations are defined by

$$\dot{m} = \int m s d^3v \quad (2.1-37)$$

$$\dot{\underline{P}}_c = \int m \underline{v} C d^3v \quad (2.1-38)$$

$$\dot{\underline{P}}_s = \int m \underline{v} S d^3v \quad (2.1-39)$$

$$\dot{\epsilon}_c = \int \frac{m}{2} v^2 C d^3v \quad (2.1-40)$$

$$\dot{\epsilon}_s = \int \frac{m}{2} v^2 S d^3v \quad (2.1-41)$$

The source term  $\dot{m}$  represents the time rate of adding new mass bearing particles to unit volume of the plasma. In charge exchange the number of plasma particles is conserved and only photoionization contributes to the source term. Since there is one proton and one electron contributed per event the source term is given by the product  $m \dot{n}$  where  $\dot{n}$  is the photoionizations rate for hydrogen (section 1.4a)

$$\dot{n} = \int \alpha_p f_N d^3v = \alpha_p N \quad (2.1-42)$$

The source term  $\dot{\underline{P}}_c$  is the time rate of change of momentum per unit volume due to coulomb collisions. Since total momentum is conserved in such collisions, there is no contribution to the source term from collisions between members of the given species. For the same reason, the sum of the source terms for ions and electrons is identically zero or

$$\dot{\underline{P}}_c^i = - \dot{\underline{P}}_c^e \quad (2.1-43)$$

Representing the transfer of momentum between the electron and ion gases, the source term gives rise to the electrical resistivity of the

plasma in the one-fluid description. Where common parameters are the same as in the similar representation for the heat flux, Braginski finds

$$\begin{aligned} \dot{\tilde{P}}_c^e = & -b_{\parallel} \tilde{h} \cdot (\tilde{v}^e - \tilde{v}^i) - \beta_{\parallel} n_e K (\tilde{h} \cdot \tilde{\nabla} T_e) \\ & + b_{\perp} \tilde{h} \times [\tilde{h} \times (\tilde{v}^e - \tilde{v}^i)] + \beta_{\perp} n_e K [\tilde{h} \times (\tilde{h} \times \tilde{\nabla} T_e)] \\ & - b_{\Lambda} \tilde{h} \times (\tilde{v}^e - \tilde{v}^i) - \beta_{\Lambda} n_e K (\tilde{h} \times \tilde{\nabla} T_e) \end{aligned} \quad (2.1-44)$$

In the relations the coefficients of dynamical friction are

$$\begin{aligned} b_{\parallel} &= 0.51 \frac{m_e n_e}{\tau_e} \\ b_{\perp} &= (\Delta_e' - 6.4 \chi_e^2 + 1.84) \frac{m_e n_e}{\Delta_e' \tau_e} \\ b_{\Lambda} &= \chi_e (1.7 \chi_e^2 + 0.78) \frac{m_e n_e}{\Delta_e' \tau_e} \end{aligned} \quad (2.1-45)$$

The source term  $\dot{\tilde{P}}_s$ , equation (39), is the time rate of change of momentum per unit volume due to photoionization and, in the case of protons only, charge exchange. The source term for electrons, due to their small mass relative to the protons, does not contribute significantly to the formulation and is omitted here. The source term for protons is given by

$$\dot{P}_s^i = \int m_i v (\alpha_p + \alpha_c) f_N d^3v - \int m_i v \alpha_c^+ f_i d^3v . \quad (2.1-46)$$

In the equation the first integral evidently represents the addition of momenta of the new protons arising from photoionization and charge exchange with hydrogen. The second integral represents the loss of momenta of solar wind protons which undergo charge exchange with hydrogen. Retaining only the first term in the expansion for  $\bar{\alpha}$ , we get the useful approximate relation (see equations (1.4b-9, 10, and 11)) .

$$\dot{P}_s^i \approx \int m_i v (\alpha_p + \bar{\alpha}_o n_i) f_N d^3v - \bar{\alpha}_o N \rho_i v^i . \quad (2.1-47)$$

The source term  $\dot{\epsilon}_c$  defined by equation (37) is the time rate of change of total kinetic energy per unit volume due to coulomb collisions. Since total kinetic energy is conserved among the particles in such collisions, there is no contribution to the source term from collisions between members of the given species. For the same reason, the sum of the source terms for ions and electrons is identically zero or

$$\dot{\epsilon}_{ce} = - \dot{\epsilon}_{ci} . \quad (2.1-48)$$

Representing the exchanges of energy between the electron and proton gases, the source terms play no explicit role in the one-fluid formulation and will not be given here. However the processes which the terms represent do play an important implicit role in keeping the temperature of the two gases comparable in circumstances where the one-fluid formulation is most effective.

Lastly the source term  $\dot{\epsilon}_s$  is the time rate of change of total kinetic energy per unit volume due to photoionization and charge exchange. For the electron gas photoionization contributes the excess energy of the ionizing photons. As we found in section 1.4a, the average excess energy per event amounts to roughly  $\frac{1}{3} h \nu_0$  or 4.5 e. v. and the source term is given by

$$\dot{\epsilon}_s^e = \frac{1}{3} h \nu_0 \dot{n}_i \equiv \frac{1}{3} h \nu_0 \alpha_p N. \quad (2.1-49)$$

Similarly to the case for the corresponding momentum source term, the energy source term for the proton gas is evidently

$$\begin{aligned} \dot{\epsilon}_s^i &= \int \frac{m_i}{2} v^2 (\alpha_p + \alpha_c) f_N d^3v - \int \frac{m_i}{2} v^2 \alpha_c^+ f_i d^3v \\ &\approx \int \frac{m_i}{2} v^2 (\alpha_p + \bar{\alpha}_o n_i) f_N d^3v - \bar{\alpha}_o N n_i \left( \frac{m_i}{2} \bar{v}_i^2 + \frac{3}{2} K T_i \right) \quad (2.1-50) \end{aligned}$$

Having laid much of the groundwork for the global formulation, we now direct our attention in the next section to the one-fluid or magnetohydrodynamic formulation of the plasma flow problem. Following that, a formulation of the hydrogen transport problem as an approximate solution of the Boltzmann equation concludes the chapter.



## 2. The Magnetohydrodynamic Description

The magnetohydrodynamic description of the plasma flow problem is a synthesis of Maxwell's equations, the plasma transport equations, and equations of state into a reduced set of equations for the state of a single ionized fluid and the embedded magnetic field.

### a. Maxwell's equations and the MHD approximation

The presence of the rarefied hydrogen gas contributing no significant effect, the electric and magnetic fields which appear in the body force terms, equations (2.1-35 and 36), of the plasma transport equations are governed by Maxwell's equations for charges in a vacuum

$$\nabla \times \underline{\underline{B}} = \frac{1}{c} \frac{\partial \underline{\underline{E}}}{\partial t} + \frac{4\pi}{c} \underline{\underline{j}} \quad (2.2a-1)$$

$$\nabla \cdot \underline{\underline{B}} = 0 \quad (2.2a-2)$$

$$\nabla \times \underline{\underline{E}} = - \frac{1}{c} \frac{\partial \underline{\underline{B}}}{\partial t} \quad (2.2a-3)$$

$$\nabla \cdot \underline{\underline{E}} = 4\pi(n_i - n_e) \quad (2.2a-4)$$

In the equations, written for Gaussian units,  $\underline{\underline{j}}$  is the current density given by

$$\underline{\underline{j}} = e(n_i \underline{\underline{V}}^i - n_e \underline{\underline{V}}^e) \quad (2.2a-5)$$

The principal assumption of magnetohydrodynamics is that the plasma is electrically quasi neutral over the volume element of mathematical interest, i.e. one whose dimension is large compared to the scale of

charge density fluctuations as measured by the Debye shielding distance but small compared to characteristic flowfield dimensions. Debye lengths being short, on the order of kilometers, the assumption is applicable in our problem and we take the state variable for particle density

$$n = n_i \approx n_e \quad (2.2a-6)$$

Then from equation (5) we understand the density of electrical current flowing in the plasma to be given approximately by

$$\underline{j} = e n (\underline{v}^i - \underline{v}^e) \quad (2.2a-7)$$

We now and henceforth explicitly assume a steady flow problem in the heliocentric reference frame and ignore the unsteady terms in Maxwell's equations and the plasma transport equations. Accordingly, the latter combined with the state equation we now write in vector form explicitly for each species

$$\text{div} (\rho_i \underline{v}^i) = m_i \dot{n}_i \quad (2.2a-8)$$

$$\text{div} (\rho_i \underline{v}^i \underline{v}^i + p_i \underline{I} - \underline{\sigma}_i) = n_i e \underline{E} + \frac{n_i e}{c} (\underline{v}^i \times \underline{B}) \quad (2.2a-9)$$

$$- \frac{GM_o \rho_i}{r^3} \underline{r} + \dot{p}_c^i + \dot{p}_s^i$$

$$\text{div} \left[ \rho_i \underline{v}^i \left( \frac{v^i}{2} + \frac{5}{2} \frac{p_i}{\rho_i} \right) - \underline{\sigma}_i \cdot \underline{v}^i + \underline{q}^i \right] = n_i e \underline{E} \cdot \underline{v}^i \quad (2.2a-10)$$

$$- \frac{GM_o \rho_i}{r^3} \underline{r} \cdot \underline{v}^i + \dot{e}_c^i + \dot{e}_s^i$$

$$\operatorname{div} (\rho_{e\sim} \mathbf{V}^e) = m_e \dot{n}_e \quad (2.2a-11)$$

$$\operatorname{div} (\rho_{e\sim} \mathbf{V}^e \mathbf{V}^e + p_e \tilde{\mathbf{I}} - \tilde{\boldsymbol{\sigma}}_e) = -n_e e \mathbf{E} - \frac{n_e e}{c} (\mathbf{V}^e \times \mathbf{B}) \quad (2.2a-12)$$

$$- \frac{GM_o \rho_e}{r^3} \mathbf{r} + \dot{P}_c^e + \dot{P}_s^e$$

$$\operatorname{div} [\rho_{e\sim} \mathbf{V}^e (\frac{V_e^2}{2} + \frac{5}{2} \frac{P_e}{\rho_e}) - \tilde{\boldsymbol{\sigma}}_e \cdot \mathbf{V}^e + \mathbf{q}^e] = -n_e e \mathbf{E} \cdot \mathbf{V}^e \quad (2.2a-13)$$

$$- \frac{GM_o \rho_e}{r^3} \mathbf{r} \cdot \mathbf{V}^e + \dot{\epsilon}_c^e + \dot{\epsilon}_s^e$$

The one-fluid hydrodynamic equations are obtained by adding the corresponding plasma transport equations for electrons and protons.

Thus the continuity equation is

$$\operatorname{div} (\rho \mathbf{V}) = \dot{m} \quad (2.2a-14)$$

where  $\rho = \rho_i + \rho_e$ ,  $m = m_i + m_e$ , and the bulk velocity of the plasma is defined by  $\mathbf{V} = \frac{1}{\rho} (\rho_i \mathbf{V}^i + \rho_e \mathbf{V}^e)$ . Since  $m_e \ll m_i$  and  $n_e \approx n_i$ ,  $\rho_e \ll \rho_i$  and for all intents and purposes  $\rho = m n = \rho_i$  and  $\mathbf{V} = \mathbf{V}^i$ .

With the above definitions, approximations, and assumptions, the one-fluid momentum equation is effectively

$$\operatorname{div} (\rho \mathbf{V} \mathbf{V} + p \tilde{\mathbf{I}} - \tilde{\boldsymbol{\sigma}}) = \frac{1}{c} \mathbf{j} \times \mathbf{B} - \frac{GM_o \rho}{r^3} \mathbf{r} + \dot{P} \quad (2.2a-15)$$

where  $p = p_e + p_i$ ,  $\tilde{\boldsymbol{\sigma}} = \tilde{\boldsymbol{\sigma}}_e + \tilde{\boldsymbol{\sigma}}_i$ , and  $\dot{P} = \dot{P}_c^e + \dot{P}_s^e + \dot{P}_c^i + \dot{P}_s^i$ .

In equation (15) the omission of a body force term involving the electric field introduces an error only of order  $(V/c)^2$ . Again since  $m_e \ll m_i$  and the coefficients of viscosity (section 2.1) are proportional to the masses of the plasma species, it is evident that only the protons contribute significantly to the shear stress and  $\tilde{\sigma} = \tilde{\sigma}_i$ . From equations (2.1 - 43 and 46) and the accompanying discussion we have also  $\dot{\tilde{p}} = \dot{\tilde{p}}_s^i$ .

Similarly the one-fluid energy equation is obtained as

$$\text{div} \left[ \rho \mathbf{V} \left( \frac{V^2}{2} + \frac{5}{2} \frac{p}{\rho} \right) - \tilde{\sigma} \cdot \mathbf{V} + \mathbf{q} \right] = \mathbf{E} \cdot \mathbf{j} - \frac{GM_o \rho}{r^3} \mathbf{r} + \dot{\epsilon} \quad (2.2a-16)$$

where  $\mathbf{q} = \mathbf{q}^e + \mathbf{q}^i$  and  $\dot{\epsilon} = \dot{\epsilon}_s^e + \dot{\epsilon}_s^i$  (see equation 2.1-48.).

When it is assumed finally that the plasma is in local thermodynamic equilibrium at temperature  $T = T_i = T_e$ , there results the state equation

$$p = 2nRT = 2\rho RT \quad (2.2a-17)$$

where  $R$  is the universal gas constant.

The set of six equations (1), (3), (14), (15), (16), and (17) are now found to involve the seven unknowns  $\mathbf{E}$ ,  $\mathbf{B}$ ,  $\mathbf{j}$ ,  $\rho$ ,  $\mathbf{V}$ ,  $p$ , and  $T$ . The equation needed to form a closed set is obtained by combining equations (6), (7), and (17) with the equations of motion for the electrons equation (12). As the result of the small mass of the electron, the viscous and inertia terms, except the source term involving dynamic friction from Coulomb collisions, may be dropped in the latter equation. Since in our problem  $\chi_e \equiv \omega \tau_e$  is always several orders of magnitude greater than unity, the source term for dynamic friction, equation (2.1-44), greatly simplifies to

$$\begin{aligned}
 \dot{p}_c^e &= - \frac{m_e n_e}{\tau_e} (\vec{v}^e - \vec{v}^i) & (2.2a-18) \\
 &+ 0.49 \frac{m_e n_e}{\tau_e} h \cdot (\vec{v}^e - \vec{v}^i) \\
 &- 0.7 n_e K h \cdot \nabla T_e
 \end{aligned}$$

Then the final result we seek may be expressed as a relation for the electric field

$$\begin{aligned}
 \vec{E} &= - \frac{1}{c} \vec{v} \times \vec{B} + \frac{1}{nec} \vec{j} \times \vec{B} - \frac{1}{2ne} \nabla p + \eta \vec{j} & (2.2a-19) \\
 &- 0.49 \frac{\eta}{B^2} \vec{j} \cdot \vec{B} \vec{B} - 0.7 \frac{K}{eB^2} (\nabla T) \cdot \vec{B} \vec{B} .
 \end{aligned}$$

Equation (19) is regarded as the generalized Ohm's law for the plasma; the electrical resistivity  $\eta$  appearing therein is given by

$$\eta = \frac{m_e}{ne^2 \tau_e} . \quad (2.2a-20)$$

The terms on the right hand side of equation (19) are ordered from the left roughly according to importance as determined from dimensional analysis based on characteristic parameters of the flowfield from Chapter I. Except in the immediate vicinity of the stagnation point where the velocity is very small, the first term is orders of magnitude larger than the others. The second and third terms are of comparable importance followed with lesser importance by the remainder. Then as a matter of mathematical convenience that introduces no inordinate error we drop the last two small terms that involve anisotropy.

For steady flow, the first of Maxwell's equations, equation (1), implies

$$\operatorname{div} \underline{j} = 0 \quad (2.2a-21)$$

Then substituting equation (19) in (3) and using equations (1), (2) and (21) we get

$$\begin{aligned} \frac{c^2 \eta}{4\pi} \nabla^2 \underline{B} - \frac{mc}{4\pi \rho e} [(\underline{B} \cdot \nabla) \nabla \times \underline{B} - (\nabla \times \underline{B}) \cdot \nabla \underline{B} \\ + \frac{1}{\rho} \nabla \rho \times \nabla \frac{B^2}{2} - \frac{1}{\rho} \nabla \rho \times (\underline{B} \cdot \nabla \underline{B})] \\ - (\underline{V} \cdot \nabla) \underline{B} - (\nabla \cdot \underline{V}) \underline{B} + (\underline{B} \cdot \nabla) \underline{V} = 0 \end{aligned} \quad (2.2a-22)$$

The last three terms in equation (22) derive from the generally dominant first term of equation (19) and taken alone describe the apparent transport of the magnetic field lines with the fluid in the so called frozen field approximation. Where the approximation is valid the equation may be written succinctly

$$\nabla \times (\underline{V} \times \underline{B}) = 0$$

Finally, from Maxwell's equations the vector identities for steady flow

$$\frac{1}{c} \underline{j} \times \underline{B} = \frac{1}{4\pi} \operatorname{div} (\underline{B} \underline{B} - \frac{B^2}{2} \underline{I})$$

and

$$\underline{E} \cdot \underline{j} = - \frac{c}{4\pi} \operatorname{div} (\underline{E} \times \underline{B})$$

permit the momentum and energy equations, equations (15) and (16), to be cast

$$\operatorname{div} \left[ \rho \underline{\underline{V}} \underline{\underline{V}} + \left( p + \frac{B^2}{8\pi} \right) \underline{\underline{I}} - \frac{B \underline{\underline{B}}}{4\pi} - \underline{\underline{\sigma}} \right] = - \frac{GM_o \rho}{r^3} \underline{\underline{r}} + \underline{\underline{P}} \quad (2.2a-24)$$

$$\begin{aligned} \operatorname{div} \left[ \rho \underline{\underline{V}} \left( \frac{v^2}{2} + \frac{5}{2} \frac{p}{\rho} \right) + \frac{c}{4\pi} \underline{\underline{E}} \times \underline{\underline{B}} - \underline{\underline{V}} \cdot \underline{\underline{\sigma}} + \underline{\underline{q}} \right] \\ = - \frac{GM_o \rho}{r^3} \underline{\underline{r}} \cdot \underline{\underline{V}} + \underline{\underline{e}} \end{aligned} \quad (2.2a-25)$$

Equations (1) and (19) can be used to eliminate  $\underline{\underline{j}}$  and  $\underline{\underline{E}}$  from the momentum and energy equations. Then collecting from section 2.1 transport and source terms appropriate to strong magnetic fields ( $\chi \gg 1$ ), we have the hydrodynamic equations.

$$\operatorname{div} (\rho \underline{\underline{V}}) = m \underline{\underline{n}} \quad (2.2a-26)$$

$$\underline{\underline{n}} = \alpha_{pe} \frac{r^2}{r} \underline{\underline{e}} N \quad (2.2a-26a)$$

$$\operatorname{div} \left[ \rho \underline{\underline{V}} \underline{\underline{V}} + \left( p + \frac{B^2}{8\pi} \right) \underline{\underline{I}} - \underline{\underline{\sigma}} - \frac{B \underline{\underline{B}}}{4\pi} \right] = - \frac{GM_o \rho}{r^3} \underline{\underline{r}} + \underline{\underline{P}} \quad (2.2a-27)$$

$$\underline{\underline{\sigma}} = \sigma_{ij} \hat{e}_i \hat{e}_j \quad (2.2a-27a)$$

$$\sigma_{ij} = \mu_o W_{oij}$$

$$W_{oij} = \frac{3}{2} B^{-4} (B_i B_j - \frac{B^2}{3} \delta_{ij}) B_\alpha B_\beta W_{\alpha\beta}$$

$$W_{ij} = \frac{\partial V_i}{\partial x_j} + \frac{\partial V_j}{\partial x_i} - \frac{2}{3} \delta_{ij} \frac{\partial V_k}{\partial x_k}$$

$$\mu_o = \frac{\rho K T \tau}{m}$$

$$\chi = \frac{eB}{mc} \tau$$

$$\tau = \frac{3\sqrt{2\pi}(mKT)^{3/2}}{8\pi \lambda n \Lambda \rho}, \quad \Lambda = \frac{3}{2} \left(\frac{\pi\rho}{m}\right)^{-1/2} \left(\frac{KT}{e}\right)^{3/2}$$

$$\dot{\tilde{P}} = \int m v \left( \alpha_{pe} \frac{r_e^2}{r^2} + \frac{\bar{\alpha}_o \rho}{m} \right) f_N d^3 v - \bar{\alpha}_o N \rho v \quad (2.2a-27b)$$

$$\text{div} \left[ \rho v \left( \frac{v^2}{2} + \frac{5}{2} \frac{p}{\rho} + \frac{B^2}{4\pi\rho} \right) - v \cdot \left( \bar{\sigma} + \frac{1}{4\pi} \bar{B} \bar{B} \right) \right. \quad (2.2a-28)$$

$$+ \frac{c}{8\pi n e} \bar{B} \times \nabla \left( p + \frac{B^2}{4\pi} \right) - \frac{c}{(4\pi)^2 n_e} \bar{B} \times (\bar{B} \cdot \nabla) \bar{B}$$

$$\left. - \frac{c^2 \eta}{4\pi} \nabla \frac{B^2}{8\pi} + \frac{c^2 \eta}{(4\pi)^2} \bar{B} \cdot \nabla \bar{B} + \bar{q} \right] = - \frac{GM_o \rho}{r^3} \bar{r} \cdot \bar{v} + \epsilon$$

$$\bar{q} = - \frac{\kappa_{||}}{B^2} \bar{B} \bar{B} \cdot \nabla T - \frac{0.7c}{4\pi e B^2} \bar{B} \bar{B} \cdot (\nabla \times \bar{B}) KT \quad (2.2a-28a)$$

$$\kappa_{||} = 3.2 \frac{\rho KT \tau}{m^{3/2} m_e^{1/2}}$$

$$\dot{\epsilon} = \int \frac{m}{2} v^2 \left( \alpha_{pe} \frac{r_e^2}{r^2} + \frac{\bar{\alpha}_o \rho}{m} \right) f_N d^3 v \quad (2.2a-28b)$$

$$- \bar{\alpha}_o N \rho \left( \frac{v^2}{2} + \frac{3KT}{2m} \right) + \frac{1}{3} h \nu_o \alpha_{pe} \frac{r_e^2}{r^2} N$$

When the distribution function  $f_N$  for hydrogen is regarded as known, equations (22) or (23), (26), (27), and (28) with the equation of state, equation (17), form a complete set in the unknowns  $\bar{B}$ ,  $\rho$ ,  $\bar{v}$ ,  $p$ , and  $T$ . We refer to the set as the magnetohydrodynamic equations.

#### b. Discontinuity relations of the MHD formulation

The Maxwell's equations (2) and (3) and the hydrodynamic equations (14), (24), and (25) admit respectively the following integral relations



across a surface of discontinuity

$$[B_n]_1^2 = 0 \quad (2.2b-1)$$

$$[E \times n]_1^2 = 0 \quad (2.2b-2)$$

$$[\rho V_n]_1^2 = 0 \quad (2.2b-3)$$

$$[\rho V V_n + (P + \frac{B^2}{8\pi}) n - \frac{BB_n}{4\pi} - \sigma \cdot n]_1^2 = 0 \quad (2.2b-4)$$

$$[\rho V_n (\frac{v^2}{2} + \frac{5}{2} \frac{P}{\rho}) + \frac{c}{4\pi} (E \times B) \cdot n - V \cdot \sigma \cdot n + q_n]_1^2 = 0 \quad (2.2b-5)$$

In the relations,  $n$  is a unit vector normal to the surface of discontinuity and  $B_n = B \cdot n$ , etc.

When only the first term is retained in equation (19), i.e. take

$$E = -\frac{1}{c} V \times B, \quad (2.2b-6)$$

the substitution made in equations (2) and (5), and the viscous terms in equations (4) and (5) dropped, there results the set of approximate relations

$$[B_n]_1^2 = 0 \quad (2.2b-7)$$

$$[B_{n\sim} v - v_{n\sim} B]_1^2 = 0 \quad (2.2b-8)$$

$$[\rho V_n]_1^2 = 0 \quad (2.2b-9)$$

$$\left[ \rho V_n \tilde{V} + \left( p + \frac{B^2}{8\pi} \right) \tilde{n} - \frac{B_n B}{4\pi} \right]_1^2 = 0 \quad (2.2b-10)$$

$$\left[ \rho V_n \left( \frac{v^2}{2} + \frac{5}{2} \frac{p}{\rho} + \frac{B^2}{4\pi\rho} \right) - \frac{1}{4\pi} B_n B \cdot \tilde{V} \right]_1^2 = 0 \quad (2.2b-11)$$

The normal component of equation (8) vanishes identically leaving for the component tangential to the surface

$$\left[ B_{n\tilde{t}} \tilde{V}_t - V_{n\tilde{t}} B_t \right]_1^2 = 0 \quad (2.2b-12)$$

For the normal component of equation (10) we have

$$\left[ \rho V_n^2 + p + \frac{B_t^2}{8\pi} - \frac{B_n^2}{8\pi} \right]_1^2 = 0 \quad (2.2b-13)$$

while for the tangential component,

$$\left[ \rho V_n \tilde{V}_t - \frac{1}{4\pi} B_n B_t \right]_1^2 = 0 \quad (2.2b-14)$$

Two classes of solutions of equations (7), (9), (11), (12), (13), and (14) are of interest. The tangential discontinuity relations and the quasi-normal shock relations. The former class of solutions is able to describe conditions across the surface of contact between flows of independent character and origin. Evidently in our problem such relations should be applied at the boundary between the solar and interstellar winds. The latter class of solutions apply to conditions across the shock in the supersonic solar wind.

For the tangential discontinuity relations, as a matter of definition

$$V_n \equiv 0. \quad (2.2b-15)$$

Then from equations (7), (12) and (14) we demand

$$B_n \equiv 0 \quad (2.2b-16)$$

since the alternative demands (of the "contact" discontinuity relations)

$$[V_t]_1^2 = 0 \text{ and } [B_t]_1^2 = 0$$

would be too restrictive to describe the phenomena of interest. Equation (11) is then satisfied identically by equations (15) and (16). Lastly, equation (13) provides a total pressure balance condition

$$\left[ p + \frac{B_t^2}{8\pi} \right]_1^2 = 0 \quad (2.2b-17)$$

Retrospectively and for consistency with the foregoing, the viscous terms omitted from the analysis should be small and therefore approximately satisfy the compatibility conditions

$$\sigma_{nn1} = \sigma_{nn2} = 0 \quad (2.2b-18)$$

$$[\sigma_{tn}]_1^2 = 0 \quad (2.2b-19)$$

$$[V_t \sigma_{tn} + q_n]_1^2 = 0 \quad (2.2b-20)$$

or they should be retained with the other terms. In the light of equation (16) and Braginskii's finding (section 2.2a) that the viscous shear stress is greatly reduced in directions along and across strong magnetic

field lines and similarly for the conduction heat flux normal to field lines, the terms in equations (19) and (20) are indeed small and their omission from the ensuing development is warranted. But if viscous terms are to be retained in the overall formulation then equation (18) is not justified and instead equation (17) is replaced by

$$\left[ p + \frac{B_t^2}{8\pi} + \sigma_{nn} \right]_1 = 0. \quad (2.2b-21)$$

The relations that we shall now derive and term the quasi-normal shock relations hold when the momentum flux greatly exceeds the stresses of the magnetic field ( $\rho v^2 \gg \frac{B^2}{4\pi}$ ) in the supersonic region and the flow approaches the surface of discontinuity at nearly normal incidence. Such is believed to be the case in the solar wind. We begin the development with relations (7), (9), (12), (14), (13), and (11) which can be written respectively

$$B_n = \text{const} \quad (2.2b-22)$$

$$\rho v_n = \text{const} \quad (2.2b-23)$$

$$\rho v_n \left[ \frac{1}{\rho} B_t \right]_1^2 \equiv [v_n B_t]_1^2 = B_n [v_t]_1^2 \quad (2.2b-24)$$

$$\rho v_n [v_t]_1^2 = \frac{B_n}{4\pi} [B_t]_1^2 \quad (2.2b-25)$$

$$\left[ \rho v_n^2 + p + \frac{B_t^2}{8\pi} \right]_1 = 0 \quad (2.2b-26)$$

$$\rho v_n \left[ \frac{v^2}{2} + \frac{5}{2} \frac{p}{\rho} + \frac{B_t^2}{4\pi\rho} \right]_1 = \frac{B_n}{4\pi} [v_t \cdot B_t]_1^2 \quad (2.2b-27)$$

By hypothesis the right hand sides of equations (24), (25), and (27) are second or higher order small quantities. Accordingly, we seek as an approximate solution a solution to the set

$$[V_{n\sim t} B]_1^2 \equiv \rho V_n [\frac{1}{\rho} B_{\sim t}]_1^2 = 0 \quad (2.2b-28)$$

$$[\rho V_n^2 + p + \frac{B_t^2}{8\pi}]_1 = 0 \quad (2.2b-29)$$

$$[\frac{V_n^2}{2} + \frac{5}{2} \frac{p}{\rho} + \frac{B_t^2}{4\pi\rho}]_1 = 0 \quad (2.2b-30)$$

along with relations (22) and (23). Within the scheme equation (25) is now regarded as providing the jump in  $V_{\sim t}$  after  $B_{\sim t}$  is found from equations (28), (29), and (30).

When  $u \equiv V_n$ ,  $J \equiv \rho u$ , and  $\Phi \equiv u B_{\sim t}$ , then equations (28), (29), and (30) may be expressed explicitly in the form

$$\Phi = \text{const} \quad (2.2b-31)$$

$$p_2 = p_1 + (1 - \beta) J u_1 + \frac{\Phi^2}{8\pi u_1} \left( \frac{\beta^2 - 1}{\beta} \right) \quad (2.2b-32)$$

$$\frac{\beta^2 u_1^2}{2} + \frac{5}{2} \frac{\beta p_2 u_1}{J} + \frac{\Phi^2}{4\pi J \beta u_1} = \frac{u_1^2}{2} + \frac{5}{2} \frac{p_1 u_1}{J} + \frac{\Phi^2}{4\pi J u_1} \quad (2.2b-33)$$

where the parameter  $\beta$  is defined

$$\beta \equiv u_2/u_1 \quad (2.2b-34)$$

Substituting equation (32) in (33) provides the equation

$$\frac{\beta^2 - 1}{2} + \frac{5}{2} \beta (1 - \beta) + \frac{5}{2} (\beta - 1) \frac{P_1}{J u_1} + \quad (2.2b-35)$$

$$\frac{1}{\beta} \left[ \frac{5}{4} (\beta^2 - 1) + (1 - \beta) \right] \frac{\phi^2}{4\pi J u_1^3}$$

Equation (35) has two roots  $\beta = 1$  and

$$\beta = \frac{1}{8} \left[ 1 + 5 \left( \frac{P_1}{J u_1} + \frac{\phi^2}{8\pi J u_1^3} \right) \right] \quad (2.2b-36)$$

$$+ \frac{1}{8} \left\{ \left[ 1 + 5 \left( \frac{P_1}{J u_1} + \frac{\phi^2}{8\pi J u_1^3} \right) \right]^2 + \frac{16 \phi^2}{8\pi J u_1^3} \right\}^{1/2}$$

The former solution represents continuous flow and is of no interest here. For the latter solution in the supersonic solar wind region both

$$\frac{P_1}{J u_1} \equiv \frac{P_1}{\rho_1 u_1^2} \ll 1 \quad \text{and} \quad \frac{\phi^2}{8\pi J u_1^3} \equiv \frac{B_t^2}{8\pi \rho_1 u_1^2} \ll 1 .$$

Then expanding equation (36) in the appropriate convergent power series and retaining only terms to first order yields the strong shock solution

$$\beta = \frac{1}{4} \left[ 1 + 5 \frac{P_1}{\rho_1 u_1^2} + 9 \frac{B_t^2}{8\pi \rho_1 u_1^2} \right] \equiv \frac{1}{4} \left[ 1 + \frac{3}{M_1^2} + \frac{9}{2M_{At1}^2} \right] \quad (2.2b-37)$$

In the latter representation of the solution  $M_1$  and  $M_{At1}$  are respectively the ordinary preshock Mach number and the preshock Alfvén Mach number based on the transverse component of the magnetic field.

Thus from equations (34), (22), (23), (28), (25), and (29) with  $\beta$  given by equation (37) we have the complete approximate solution

$$V_{n2} = \beta V_{n1} \quad (2.2b-38)$$

$$B_{n2} = B_{n1} \quad (2.2b-39)$$

$$\rho_2 = \frac{1}{\beta} \rho_1 \quad (2.2b-40)$$

$$B_{t2} = \frac{1}{\beta} B_{t1} \quad (2.2b-41)$$

$$V_{t2} = V_{t1} + \frac{(1-\beta)}{\beta} \frac{B_{n1}}{4\pi\rho_1 V_{n1}} B_{t1} \quad (2.2b-42)$$

$$P_2 = P_1 + (1 - \beta) \rho_1 V_{n1}^2 - \frac{(1-\beta^2)}{\beta^2} \frac{B_{t1}^2}{8\pi} \quad (2.2b-43)$$

As was the case for the tangential discontinuity relations, if viscous terms are to be retained in the formulation then it should be sufficient to add the normal stresses to either side of equation (43). It is expected that the omission of shearing stresses is appropriate in the region of nearly normal flow where the above relations apply.

c. Equations of quasi-one-dimensional compressible flow

With certain assumptions it is possible to construct an essentially one dimensional flow problem that embodies major features of the termination of the solar wind. With certain approximations the resulting mathematical formulation involves an equation which in the absence of magnetic fields reduces to the one-dimensional compressible flow equation of gas dynamics.

In the interstellar wind region, the assumptions are that in the uniform flow far upstream of the sun the velocity vector is parallel to the solar equatorial plane and the magnetic field is orthogonal to the velocity. In the solar wind region, symmetry is assumed with respect to

the solar equatorial plane. Then the regimes of quasi-one-dimensional flow are about the upstream and downstream axes through the sun.

The approximations are that  $\underline{E} = -\frac{1}{c} \underline{V} \times \underline{B}$  and the viscous terms in the hydrodynamic equations can either be ignored or treated as prescribed functions in the solution of the equations by iterative methods.

Then the mass equation (2.2a-26)

$$\text{div} (\rho \underline{V}) = \dot{m} n \quad (2.2c-1)$$

with the familiar vector identities permits the momentum and energy equations (2.2a-27 and 28) to be cast respectively

$$\begin{aligned} \rho \underline{V} \cdot \underline{\nabla} \frac{V^2}{2} - \rho \underline{V} \times (\underline{\nabla} \times \underline{V}) + \underline{\nabla} \cdot \left( p + \frac{B^2}{8\pi} \right) - \frac{1}{4\pi} \text{div} \underline{B} \underline{B} \\ = \rho \underline{g} + \text{div} \underline{\sigma} + \dot{P} - \dot{m} n \underline{V} \end{aligned} \quad (2.2c-2)$$

$$\begin{aligned} \rho \underline{V} \cdot \underline{\nabla} \frac{V^2}{2} + \underline{V} \cdot \underline{\nabla} \left( p + \frac{B^2}{4\pi} \right) - \frac{1}{4\pi} (\text{div} \underline{B} \underline{B}) \cdot \underline{V} \\ - \left( \frac{p}{\rho} + \frac{B^2}{4\pi\rho} \right) \underline{V} \cdot \underline{\nabla} \rho + \frac{3}{2} \rho \underline{V} \cdot \underline{\nabla} \left( \frac{p}{\rho} \right) - \frac{1}{4\pi} \underline{B} \underline{B} : \underline{\nabla} \underline{V} \\ = \rho \underline{g} \cdot \underline{V} + (\text{div} \underline{\sigma}) \cdot \underline{V} + \underline{\sigma} : \underline{\nabla} \underline{V} \\ + \dot{e} + \dot{Q} - \dot{m} n \left( \frac{V^2}{2} + \frac{5}{2} \frac{p}{\rho} + \frac{B^2}{4\pi\rho} \right) \end{aligned} \quad (2.2c-3)$$

where  $\underline{g} = -\frac{GM_0}{r^3} \underline{r}$  and  $\dot{Q} = -\text{div} \underline{q}$ . When equation (2) is dotted with the velocity and the result subtracted from equation (3) the difference is the generalized heat equation



$$\begin{aligned} \frac{3}{2} \rho \mathbf{v} \cdot \nabla \left( \frac{p}{\rho} \right) + \mathbf{v} \cdot \nabla \frac{B^2}{8\pi} - \left( \frac{p}{\rho} + \frac{B^2}{4\pi\rho} \right) \mathbf{v} \cdot \nabla \rho - \frac{1}{4\pi} \mathbf{B} \cdot \nabla \mathbf{v} \\ = \dot{\epsilon} + \dot{Q} - \dot{P} \cdot \mathbf{v} + mn \left( \frac{v^2}{2} - \frac{5}{2} \frac{p}{\rho} - \frac{B^2}{4\pi\rho} \right) + \dot{\sigma} : \nabla \mathbf{v} \end{aligned} \quad (2.2c-4)$$

Finally with equation (2.2a-2), equation (2.2a-23) may be written

$$\mathbf{B} \cdot \nabla \mathbf{v} - \mathbf{v} \cdot \nabla \mathbf{B} - (\nabla \cdot \mathbf{v}) \mathbf{B} = 0 \quad (2.2c-5)$$

For one dimensional flow equations (1), (2), (4), and (5) find expression

$$\lim_{\Delta s \rightarrow 0} \frac{1}{\Delta s} \frac{d}{dx} (\rho u \Delta s) = mn \quad (2.2c-6)$$

$$\rho u \frac{du}{dx} + \frac{dp}{dx} + \frac{1}{8\pi} \frac{dB^2}{dx} + \frac{1}{4\pi} \frac{B^2}{r_B} = -g\rho + \dot{P}_x - mn u + \frac{d\sigma_{xx}}{dx} \quad (2.2c-7)$$

$$\begin{aligned} \frac{3}{2} \rho u \frac{d}{dx} \left( \frac{p}{\rho} \right) + \frac{u}{8\pi} \frac{dB^2}{dx} - u \left( \frac{p}{\rho} + \frac{B^2}{4\pi\rho} \right) \frac{d\rho}{dx} - \frac{B^2}{4\pi} \frac{u}{r_V} \\ = \dot{\epsilon} + \dot{Q} - \dot{P}_x u + mn \left( \frac{u^2}{2} - \frac{5}{2} \frac{p}{\rho} - \frac{B^2}{4\pi\rho} \right) + \sigma_{xx} \frac{du}{dx} \end{aligned} \quad (2.2c-8)$$

$$\mathbf{B} \frac{u}{r_V} - u \frac{dB}{dx} - \lim_{\Delta s \rightarrow 0} \frac{1}{\Delta s} \frac{d}{dx} (u \Delta s) \mathbf{B} = 0 \quad (2.2c-9)$$

In the equation  $\Delta s$  is a differential element of area normal to the axis of flow and  $r_B$  and  $r_V$  are the local radii of curvature of the magnetic field lines and the normal surfaces to the velocity field respectively.

We approximate both  $r_V$  and  $r_B$  by  $\lim_{\Delta s \rightarrow 0} \frac{1}{2\Delta s} \frac{d\Delta s}{dx}$ . Then ceasing the repetitious writing of the limit  $\Delta s \rightarrow 0$ , we can rewrite equations (6)-(9) in the forms

$$\frac{1}{\rho} \frac{dp}{dx} = -\frac{1}{u} \frac{du}{dx} - \frac{1}{\Delta s} \frac{d\Delta s}{dx} + \frac{mn}{\rho u} \quad (2.2c-10)$$

$$\begin{aligned} u \frac{du}{dx} &= \frac{1}{\rho} \frac{dp}{dx} + \frac{1}{8\pi\rho} \frac{dB^2}{dx} + \frac{B^2}{8\pi\rho} \frac{1}{\Delta s} \frac{d\Delta s}{dx} \\ &= -g + \frac{\dot{p}_x}{\rho} - mn \frac{u}{\rho} + \frac{1}{\rho} \frac{d\sigma_{xx}}{dx} \end{aligned} \quad (2.2c-11)$$

$$\begin{aligned} \frac{3}{2} \frac{d}{dx} \left( \frac{p}{\rho} \right) + \frac{1}{8\pi\rho} \frac{dB^2}{dx} - \left( \frac{p}{\rho} + \frac{B^2}{4\pi\rho} \right) \frac{1}{\rho} \frac{dp}{dx} - \frac{B^2}{8\pi\rho} \frac{1}{\Delta s} \frac{d\Delta s}{dx} \\ = \frac{1}{\rho u} \left\{ \dot{\epsilon} + \dot{Q} - \dot{p}_x u + mn \left( \frac{u^2}{2} - \frac{5}{2} \frac{p}{\rho} - \frac{B^2}{4\pi\rho} \right) + \sigma_{xx} \frac{du}{dx} \right\} \end{aligned} \quad (2.2c-12)$$

$$\frac{1}{\Delta s^{1/2}} \frac{d}{dx} (uB\Delta s^{1/2}) = 0 \quad (2.2c-13)$$

Equation (13) provides an immediate integral which squared and then differentiated yields

$$\frac{1}{8\pi} \frac{dB^2}{dx} = -\frac{B^2}{4\pi} \frac{1}{u} \frac{du}{dx} - \frac{B^2}{8\pi} \frac{1}{\Delta s} \frac{d\Delta s}{dx} \quad (2.2c-14)$$

Differentiating  $p = \left( \frac{p}{\rho} \right) \rho$  we have

$$\frac{1}{\rho} \frac{dp}{dx} = \frac{d}{dx} \left( \frac{p}{\rho} \right) + \left( \frac{p}{\rho} \right) \frac{1}{\rho} \frac{d\rho}{dx} \quad (2.2c-15)$$

In equations (11) and (12) we substitute for the quantities on the left hand sides of equations (10), (14), and (15). In the resulting

equations we then replace  $\frac{p}{\rho}$  by  $\frac{3}{5} a^2$  and  $\frac{B^2}{4\pi\rho}$  by  $A^2$  where  $a^2$  and  $A^2$  are the squares of the speeds of sound and Alfvén waves respectively.

The results of doing the above are

$$u \frac{du}{dx} + \frac{3}{5} \frac{da^2}{dx} - \frac{3}{5} \frac{u}{M^2} \frac{du}{dx} - \frac{3}{5} \frac{a^2}{\Delta s} \frac{d\Delta s}{dx} + \frac{3}{5} \frac{a^2}{\rho u} \dot{m} \quad (2.2c-16)$$

$$- \frac{u}{M_A^2} \frac{du}{dx} = -g + \frac{P_x}{\rho} - \frac{u}{\rho} \dot{m} + \frac{1}{\rho} \frac{d\sigma_{xx}}{dx}$$

$$\frac{9}{10} \frac{da^2}{dx} + \frac{3}{5} \frac{u}{M^2} \frac{du}{dx} + \frac{3}{5} \frac{a^2}{\Delta s} \frac{d\Delta s}{dx} - \frac{3}{5} \frac{a^2}{\rho u} \dot{m} \quad (2.2c-17)$$

$$= \frac{1}{\rho u} \left\{ \dot{e} + \dot{Q} - \dot{P}_x u + \dot{m} \left( \frac{u^2}{2} - \frac{3}{2} a^2 \right) + \sigma_{xx} \frac{du}{dx} \right\}$$

where  $M \equiv \frac{u}{a}$  is the Mach number and  $M_A \equiv \frac{u}{A}$  is the Alfvén Mach number.

Finally when equation (17) is multiplied by  $\frac{2}{3}$ , subtracted from equation (16), and the resulting difference divided by  $u^2$ , we arrive at the equation for quasi-one-dimensional compressible flow

$$\left( 1 - \frac{1}{M^2} - \frac{1}{M_A^2} \right) \frac{1}{u} \frac{du}{dx} = \frac{1}{M^2} \frac{1}{\Delta s} \frac{d\Delta s}{dx} - \frac{g}{u^2} \quad (2.2c-18)$$

$$- \frac{4}{3} \frac{\dot{m}}{\rho u} + \frac{5}{3} \frac{\dot{P}_x}{\rho u^2} - \frac{2}{3} \frac{\dot{e} + \dot{Q}}{\rho u^3} + \frac{1}{\rho u^2} \left( \frac{d\sigma_{xx}}{dx} - \frac{2}{3} \frac{\sigma_{xx}}{u} \frac{du}{dx} \right)$$

### 3. Transport of Hydrogen of Interstellar Origin and Moments of the Distribution Function

The transport of interstellar atomic hydrogen into the solar wind is governed by Boltzmann's equation (2.1-1). In the equation the self collision term  $C_N$  can be neglected as the result of the associated large mean free path compared to the characteristic dimension of the solar wind cavity (section 1.4b). In section 1.4d we have provided a rationale for omitting from the equation the forcing term involving macroscopic fields. Finally in the heliocentric reference frame in which the problem is regarded as steady, the Boltzmann equation for hydrogen is reduced to

$$\text{div} (\mathbf{v} f_N) = S_N \quad (2.3-1)$$

Since the fast secondary hydrogen that is the product of charge exchange has been shown by Hundhausen (1968) and Holzer (1972) to be unimportant in the problem, the source term  $S_N$  involves only losses of primary interstellar hydrogen as the result of both photoionization and charge exchange. Then the source term is

$$S_N = - (\alpha_p + \bar{\alpha}_c n) f_N \quad (2.3-2)$$

$$\approx - (\alpha_{pe} \frac{r_e^2}{r^2} + \bar{\alpha}_o n) f_N$$

with rate constants defined in sections 1.4a and 1.4b.

We note that equation (2) depends on the proton number density  $n$  of the plasma flow problem. Since the hydrodynamic equations of the latter problem depend on  $f_N$  through their source terms, the two problems

are coupled. But the solution of the plasma flow problem is at the forefront of computational capability even to the extent the distribution of hydrogen is known. Thus hope of solving the combined problem hinges on the separation of the two.

We have seen in section 1.4c that the source terms represent only a first order perturbation on the plasma flow problem. Hence the approach we adopt (at least for a first iteration) is to assume the unperturbed, extended Parker solution for  $n$ . That solution we recall as

$$n = \left\{ \begin{array}{l} n_e \frac{r_e^2}{r^2} \text{ in the supersonic region} \\ 4 n_e \frac{r_e^2}{r_s^2} \text{ in the subsonic region.} \end{array} \right\} \quad (2.3-3)$$

Finally because the peculiar velocity is an independent variable we have

$$\text{div } \tilde{v} = 0 \quad (2.3-4)$$

Thus the hydrogen transport is governed by

$$\tilde{v} \cdot \nabla \tilde{f}_N = S_N \quad (2.3-5)$$

with the approximations (2) and (3).

As the result of the assumptions, the trajectories of hydrogen into the solar wind are straight lines and equation (5) may be interpreted

$$\frac{df_N}{dl} = \frac{S_N}{v} \quad (2.3-6)$$

where  $v = \frac{d\ell}{dt}$  and  $d\ell$  is an infinitesimal element of length along a trajectory.

In the light of equations (2) and (3), calling  $S_N = -\alpha f_N$  and dropping the subscript  $N$  we have

$$\frac{df}{f} = -\frac{\alpha}{v} d\ell. \quad (2.3-7)$$

Formally the solution of equation (7) is

$$f = f_0 \exp - \int \frac{\alpha}{v} d\ell \quad (2.3-8)$$

where  $f_0$  is the unattenuated distribution function which in the rest frame of the gas is Maxwellian.

In order to carry out the integrations implied by equation (8) with approximations (2) and (3) we now take up some geometrical considerations. As in the case of the extended Parker solution, we take the positive  $x$  axis of a heliocentric cartesian reference frame  $(x, y, z)$  to have the same direction and sense as the velocity vector  $\underline{V}_0$  of the sun with respect to the local interstellar gas. Without loss of generality we consider a point in the  $x, y$  plane, the point being described by the conventional polar coordinates  $r, \theta$ . Some geometric relations governing linear trajectories of primary interstellar hydrogen atoms passing through such a point follow.

The peculiar velocities of the hydrogen atoms with respect to their mean velocity -  $\underline{V}_0$  is the vector field  $\underline{c}$  represented in conventional spherical polar coordinates as  $c, \eta, \xi$  based on the positive  $x$  direction. The velocity  $\underline{v}$  of a hydrogen atom relative to the sun is

then given by

(2.3-9)

$$\vec{v} = \vec{c} - \vec{V}_0 \quad (2.3-9)$$

$$= (c \cos \eta - V_0) \vec{n}_x + c \sin \eta \cos \xi \vec{n}_y + c \sin \eta \sin \xi \vec{n}_z$$

If  $\beta$  is the elevation angle the trajectory of a hydrogen atom makes with the x direction in passing through the point  $r, \theta$  then (Figure 2.)

$$\tan \beta = \frac{c \sin \eta}{V_0 - c \cos \eta} \quad (2.3-10)$$

The trajectory vector  $\vec{r}$  of such an atom is described by the coordinates

$$\begin{aligned} \bar{x} &= r \cos \theta + \bar{R} \cos \beta \\ \bar{y} &= r \sin \theta + \bar{R} \sin \beta \cos \xi \\ \bar{z} &= \bar{R} \sin \beta \sin \xi \end{aligned} \quad (2.3-11)$$

where  $\bar{R}$  is the distance of a point on the trajectory from the point  $r, \theta$  and, in terms of the angle coordinate  $\xi$  of the peculiar velocity of an atom describing the trajectory, the azimuthal trajectory angle  $\bar{\xi}$  is given by

$$\bar{\xi} = \xi - \pi \quad (2.3-12)$$

The distance of the sun from a point on the trajectory is

$$\bar{r} = (\bar{R}^2 + 2r\bar{R} \cos \gamma + r^2)^{1/2} \quad (2.3-13)$$





In equation (13) the angle  $\gamma$  lies at the apex between the incoming trajectory to the point  $r, \theta$  and the prolongation of the line from the sun to the point  $r, \theta$ . Finally, in obtaining the magnitude  $\bar{r}$  from equation (11), one arrives at the useful identity

$$\cos \gamma = \cos \theta \cos \beta + \sin \theta \sin \beta \cos \bar{\xi} \quad (2.3-14)$$

As a practical matter we do not compute  $f(r, \theta)$  in the heliocentric reference frame since we need only its moments for the source terms (section 2.2a) of the hydrodynamic equations. Rather we compute the contributions to the moments of  $f(r, \theta)$  from atoms in the distribution expressed in the rest frame of the hydrogen gas. Then to get the moments we sum the contributions over the coordinates  $c, \eta, \xi$  of the distribution expressed in the rest frame.

For atoms in the differential velocity space element  $\delta c, \delta \eta, \delta \xi$  the contribution  $\delta N_0$  to the zeroth moment or number density  $N_0$  at large distances from the sun is given according to hypothesis by the Maxwellian distribution as

$$\delta N_0 = N_0 \pi^{-3/2} c^2 / c_s^3 \exp(-c^2 / c_s^2) \sin \eta \delta c \delta \eta \delta \xi \quad (2.3-15)$$

In the heliocentric reference frame such atoms have the velocity given by equation (9) and the associated speed

$$v = (c^2 - 2c V_0 \cos \eta + V_0^2)^{1/2} \quad (2.3-16)$$

along the trajectory whose parameters in the heliocentric frame are given by equations (10), (11), (12), (13), and (14). Then in the

vicinity of the sun where there has been some perturbing effect due to photoionization and (if the trajectory has intersected the solar wind cavity, section 1.4) charge exchange, the contribution of the remaining atoms  $\delta N$  to  $N$  will be given, from equation (8), by

$$\delta N = \delta N_0 \exp - \int_{\ell} \frac{\alpha}{v} d\ell' \quad (2.3-17)$$

Evidently from the discussion above the parameters of the line integral over the attenuating path  $\ell$  are all functions of  $c$ ,  $\eta$ ,  $\xi$  as is  $\delta N_0$  and, hence,  $\delta N$ . Substituting for  $\alpha \equiv \alpha_p + \alpha_c$  from equation (2), we have

$$- \int_{\ell} \frac{\alpha}{v} d\ell' = - \int_{\ell} \frac{\alpha_{pe} r_e^2}{v} \frac{d\ell'}{r^2} - \int_{\ell} \frac{\bar{\alpha}_0 n}{v} d\ell' \quad (2.3-18)$$

with  $n$  given by equation (3).

To carry out the integrations explicitly we choose as the dummy variable of integration the distance  $\bar{R}$  of the trajectory point from the end point  $r, \theta$ . Then, since photoionization acts everywhere, we have for the first integral on the right hand side, from equation (13),

$$\begin{aligned} - \int_{\ell} \frac{\alpha_{pe} r_e^2}{v} \frac{d\ell'}{r^2} &= \frac{\alpha_{pe} r_e^2}{v} \int_{\infty}^0 \frac{d\bar{R}}{\bar{R}^2 + 2r\bar{R} \cos \gamma + r^2} \\ &= \frac{-\alpha_{pe} r_e^2 \gamma}{vr \sin \gamma} \end{aligned} \quad (2.3-19)$$

In the integrated expression  $\gamma$  in the numerator may be seen to be the angle subtended at the sun by the entire trajectory to the end point  $r, \theta$ ; and in the denominator  $r \sin \gamma$  is the closest approach of the trajectory (or its prolongation beyond  $r, \theta$ ) to the sun.

The second integral in equation (18) in general may contain integrations over segments of the trajectory intersecting both the subsonic and supersonic domains of the solar wind. In the case of the subsonic region (II), the solar wind proton number density  $n$  is constant, from equation (3); and the contribution to the integral involves simply the total geometric path length  $PL$  II in the region

$$- \int_{\text{II}} \frac{\bar{\alpha}_o n}{v} d\ell' = - \frac{4\bar{\alpha}_o n_e r_e^2}{v r_s^2} \text{ (PLII) .} \quad (2.3-20)$$

In the supersonic region (I), the solar wind proton density varies as  $r^{-2}$  as has been the case treated for photoionization and the contribution to the integral (18) is

$$- \int_{\text{I}} \frac{\bar{\alpha}_o n}{v} d\ell' = \frac{\bar{\alpha}_o n_e r_e^2}{v r \sin \gamma} \text{ (\Delta I)} \quad (2.3-21)$$

where  $\Delta I$  is the angle subtended at the sun by the segment of the trajectory intersecting the supersonic region. The angle is given by

$$\Delta I = \left\{ \begin{array}{l} \cos^{-1} \frac{r \sin \gamma}{r_s} + \gamma - \frac{\pi}{2} \quad | \quad r < r_s \\ 2 \cos^{-1} \frac{r \sin \gamma}{r_s} \quad | \quad r \geq r_s \end{array} \right\} \quad (2.3-22)$$

To summarize the integrations we have

$$\delta N(c, \eta, \xi) = \delta N_o(c, \eta, \xi) \exp - \left[ \frac{\alpha_{pe} r_e^2 \gamma}{v r \sin \gamma} \right. \quad (2.3-23)$$

$$\left. + \frac{4\bar{\alpha}_o n_e r_e^2}{v r_s^2} \text{ (PLII)} + \frac{\bar{\alpha}_o n_e r_e^2}{v r \sin \gamma} \text{ (\Delta I)} \right] .$$

With equation (23), the moments of  $f(r, \theta)$  required for the mass, momentum, and energy source terms in the hydrodynamic equations, see equations (2.2a-26a, 27b, 28b), are

$$N = \int f d^3v \equiv \iiint \delta N(c, \eta, \xi) \quad (2.3-24)$$

$$\int \underline{v} f d^3v \equiv \iiint \underline{v}(c, \eta, \xi) \delta N(c, \eta, \xi) \quad (2.3-25)$$

$$\int v^2 f d^3v \equiv \iiint v^2(c, \eta, \xi) \delta N(c, \eta, \xi) \quad (2.3-26)$$

Chapter III. Numerical Results -  
Interplanetary Neutral Hydrogen and the Speed  
of the Interstellar Wind

In this chapter we describe and present some particular results from a numerical algorithm developed to compute the moments of the distribution of primary neutral hydrogen and the associated source terms in the hydrodynamic equations. Specifically, from computed neutral hydrogen number density profiles on the upstream and downstream axes of flow we further compute the intensity of backscattered solar Lyman- $\alpha$  radiation expected to be observed at 1 a.u. The computations have been carried out for a varied set of conditions with respect to number density, temperature, and velocity of the local interstellar gas. Finally the theoretical predictions represented by our computations are compared with measurements of Lyman- $\alpha$  radiation from earth satellites. Given current estimates of the temperature of the interstellar gas, the comparison suggests a meaningful estimate of the speed of the interstellar wind.

1. Algorithm for Computing Moments of the Hydrogen Distribution Function.

The algorithm described in this section implements the approach described in section 2.3. We retain here the geometry and notation previously defined.

The algorithm makes use of the fact that hydrogen atoms whose trajectories pass through the point  $r, \theta$  and that have the same peculiar velocity coordinate all have trajectories lying in the same plane  $\xi = \bar{\xi} - \pi$  that contains a line through  $r, \theta$  parallel to the  $x$  axis. The given line is viewed as a polar axis of rotation and the azimuthal

angles  $\bar{\xi}$  are measured with the  $y$  axis in the  $y, z$  plane. For evident reason the planes  $\bar{\xi}$  constant for  $\xi$  constant are termed trajectory planes for the point  $r, \theta$ . Within a trajectory plane a given trajectory line is described by the angle  $\beta$ , Figure 2.

From equations (2.3-10 and 16) both the angle of the trajectory line and the speed of an atom along the line depend jointly on the peculiar velocity coordinates  $c$  and  $\eta$ , i.e. a multiplicity of pairs  $c, \eta$  find trajectories along the same trajectory line. For a given trajectory characterized by  $c$  and  $\eta$ , the attenuation path length — the argument of the exponential attenuation factor in equation (2.3-23) — is seen to be the product of the reciprocal of the speed  $v$  and a function composed solely of geometric factors depending only on  $r, \theta, \beta$ , and  $\bar{\xi}$ , the geometry of the plasma flowfield being given. The geometric function which we term the velocity path length contains the essence of the problem and is costly to compute. Accordingly, since the velocity path length is the same for the multiplicity of trajectories that can fall along a given trajectory line, for each point  $r, \theta$  and computational plane  $\bar{\xi}$  the velocity path length is pretabulated at appropriately fine  $\beta$  intervals for later look-up and interpolation as a function of  $\beta(c, \eta)$  during integration.

The computation of the moments of the distribution function is performed by integrating equations (2.3-24, 25, and 26) with equation (2.3-23), in order over  $\eta, c, \xi (\bar{\xi})$ . These independent variables are of course quantized and the integrations are performed using Simpson's rule with the output of the present level of integration being tabulated as arguments for the next.

For each  $\bar{\xi}$  plane, in the process of integrating the contributions to the moments of  $f$  the speed  $v$  and the velocity  $\underline{v}$  are computed for each coordinate pair  $\eta$  and  $c$  from equations (2.3-9 and 16). The angle  $\beta$  is computed from equation (2.3-10) and the velocity path length obtained from the interpolation table as suggested above. The attenuation path length for the trajectory is then simply the velocity path length divided by the speed  $v$  and the associated exponential attenuation factor is computed.

The initial unattenuated number density element  $\delta N_0$  which appears as the coefficient of the attenuation factor in equation (2.3-23) is given by equation (2.3-15) where it is seen to involve only the product of a function of  $c$  by a function of  $\eta$ , both functions independent of  $\bar{\xi}$ . For the evident economy of computation, these homogeneous functions have also been precomputed and tabulated for the quantized values of their arguments  $c$  and  $\eta$  used in the integration.

In computing the interpolation table for velocity path length, the figure of the heliopause boundary is approximated by an ellipsoid - cylinder, Figure 3. The sun is at the focus of the ellipsoid which fits the extended Parker solution exactly at the stagnation point and again in a plane that includes the sun and is normal to the axis of flow. Downstream of the sun, the cylinder terminates the ellipsoid smoothly at the semiminor axis providing another fit to the extended Parker solution asymptotically.

Making available the analytical geometric power of quadratic surfaces, the ellipsoid cylinder approximation permits closed analytic expressions for a number of geometric parameters including the length of the trajectory segment in the subsonic solar wind region, equation

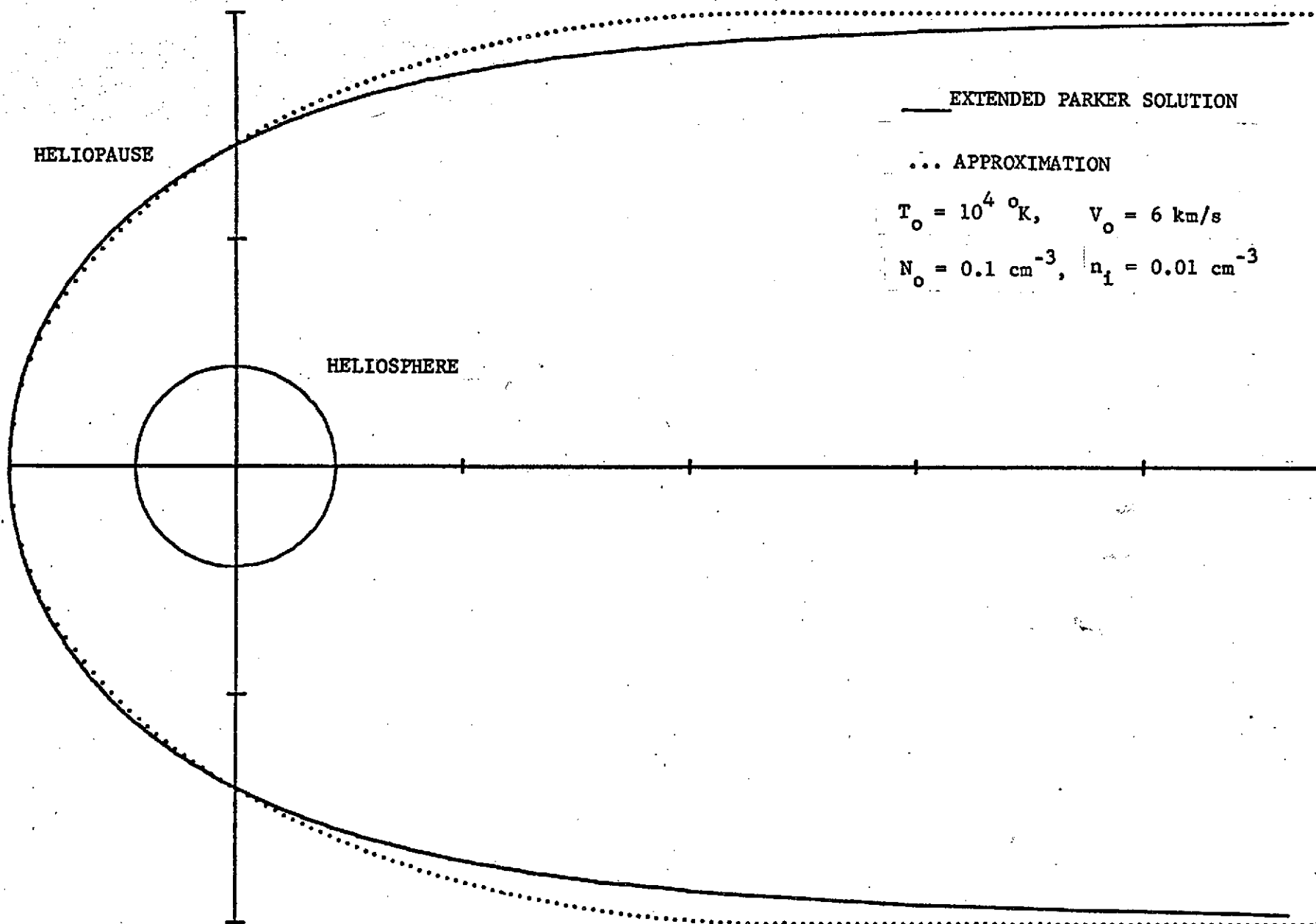


Figure 3. Ellipsoid cylinder approximation to the figure of the heliopause boundary.



(2.3-20). In toto the approach results in closed analytic expressions for the velocity path length and obviates otherwise prohibitively costly numerical integration along trajectories, such integration involving searches for intersections with the heliopause boundary surface.

## 2. Axial Profiles of Hydrogen Number Density

With reference to the algorithm of the previous section, the results presented below were computed with the angles  $\eta$  and  $\xi$  each quantized in  $3^\circ$  increments over the interval  $0^\circ$  to  $180^\circ$  (converted to radians). The speeds  $c$  were quantized in  $0.1 c_s$  increments over the interval 0 to  $3.5 c_s$  where  $c_s$  is the most probable thermal speed in the Maxwellian distribution. The velocity path length table had 129 entries spaced equally over the interval 0 to  $\pi$ .

Figures 4 and 5 show profiles of Hydrogen number density computed on the upstream and downstream axes of flow in the solar wind. In both figures the results shown are for  $N_o = 0.1 \text{ cm}^{-3}$  and  $T_o = 10^4 \text{ }^\circ\text{K}$ . Figure 4 is for  $V_o = 16.6 \text{ km/sec}$  and Figure 5, for  $8 \text{ km/s}$ . The former speed is sonic with respect to the ionized component of the interstellar wind. The latter subsonic speed is typical of the estimate we determine in the next section from comparing additional computed results with experimental measurements of Rayleigh backscatter of solar Lyman- $\alpha$  radiation. Also plotted for comparison in Figures 4 and 5 are curves derived from an analytical formula for the case of zero temperature hydrogen penetrating along the upstream axis of flow.

The flowfield described by the extended Parker solution (section 1.2) and to which Figure 4 refers has the shock at 123 a.u. and the stagnation point at 182 a.u. Similarly for Figure 5 the respective numbers are 142 a.u. and 282 a.u.

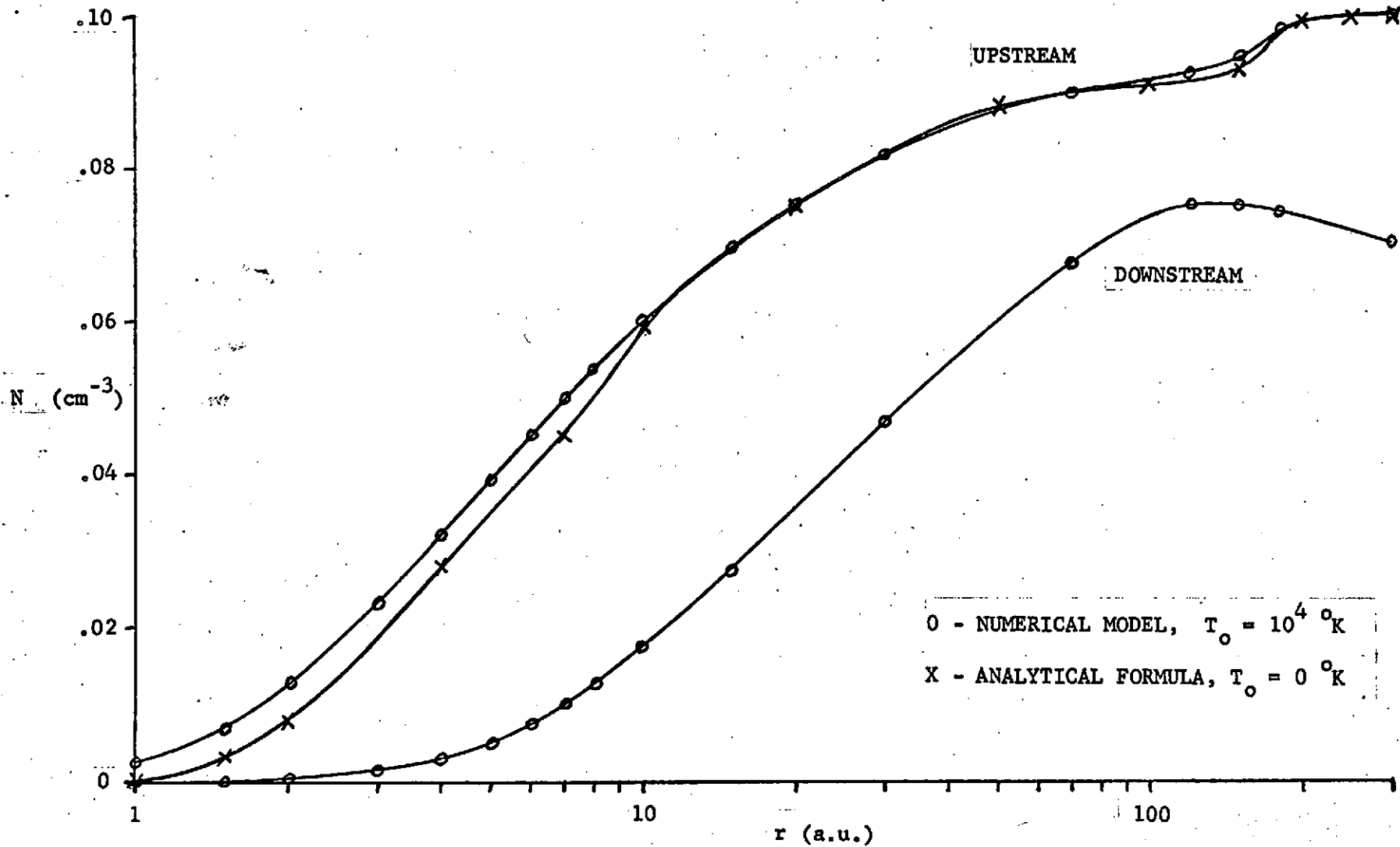


Figure 4. Hydrogen number density profiles computed on the upstream and downstream axes of flow for  $N_0 = 0.1 \text{ cm}^{-3}$ ,  $V_0 = 16.6 \text{ km/s}$ .

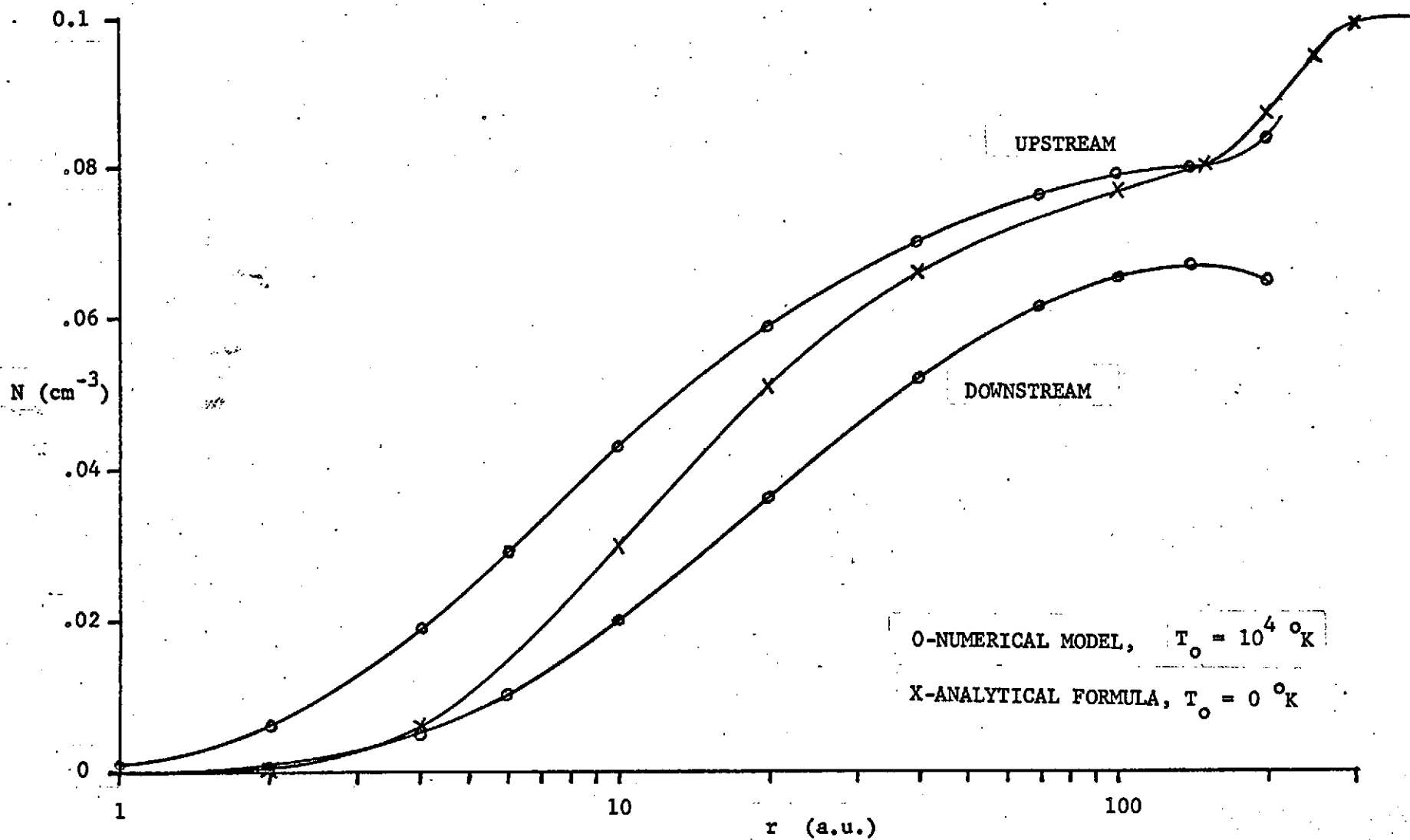


Figure 5. Hydrogen number density profiles computed on the upstream and downstream axes of flow for  $N_0 = 0.1 \text{ cm}^{-3}$ ,  $V_0 = 8 \text{ km/s}$ .

Looking first at Figure 4 and comparing the number density profiles for hot and cold hydrogen on the upstream axis, we find close quantitative as well as qualitative agreement for distances beyond 10 a.u. from the sun. Within 10 a.u., however, the predicted surviving density of hot hydrogen is systematically higher than for cold.

The trend within 10 a.u. is easily understood particularly when one notes that the bulk speed and most probable thermal speed are comparable and where the trend becomes pronounced the surviving number density has fallen to roughly half the far field value. The interpretation is based on the fact that the peculiar velocity components for the fraction of hot hydrogen in the forward  $\eta$  cone ( $\eta < \frac{\pi}{2}$ ) of the distribution tend to reduce the speed  $v$  of penetration along the trajectory and thus increase the attenuation while the converse is true in the rearward  $\eta$  cone. Thus after much of the slower hot hydrogen in the forward cone has been lost to attenuation the surviving hot hydrogen is penetrating relatively faster than the surviving cold hydrogen and thence penetrating deeper into the solar wind before suffering photoionization or charge exchange. The same trend is apparent in Figure 5 but there because the peculiar velocities are relatively higher than the bulk speed the effect is considerably enhanced.

In Figure 6 we observe the steep drop in hydrogen number density in passing through the relatively proton dense subsonic solar wind region on the upstream axis. Between the two curves for the upstream axis, the drop in number density is greater through the thicker subsonic region associated with the slower bulk velocity  $V_0 = 8 \text{ km/s}$ .

On the downstream axis the existence of any neutral hydrogen is the result of the transverse peculiar velocity components associated with

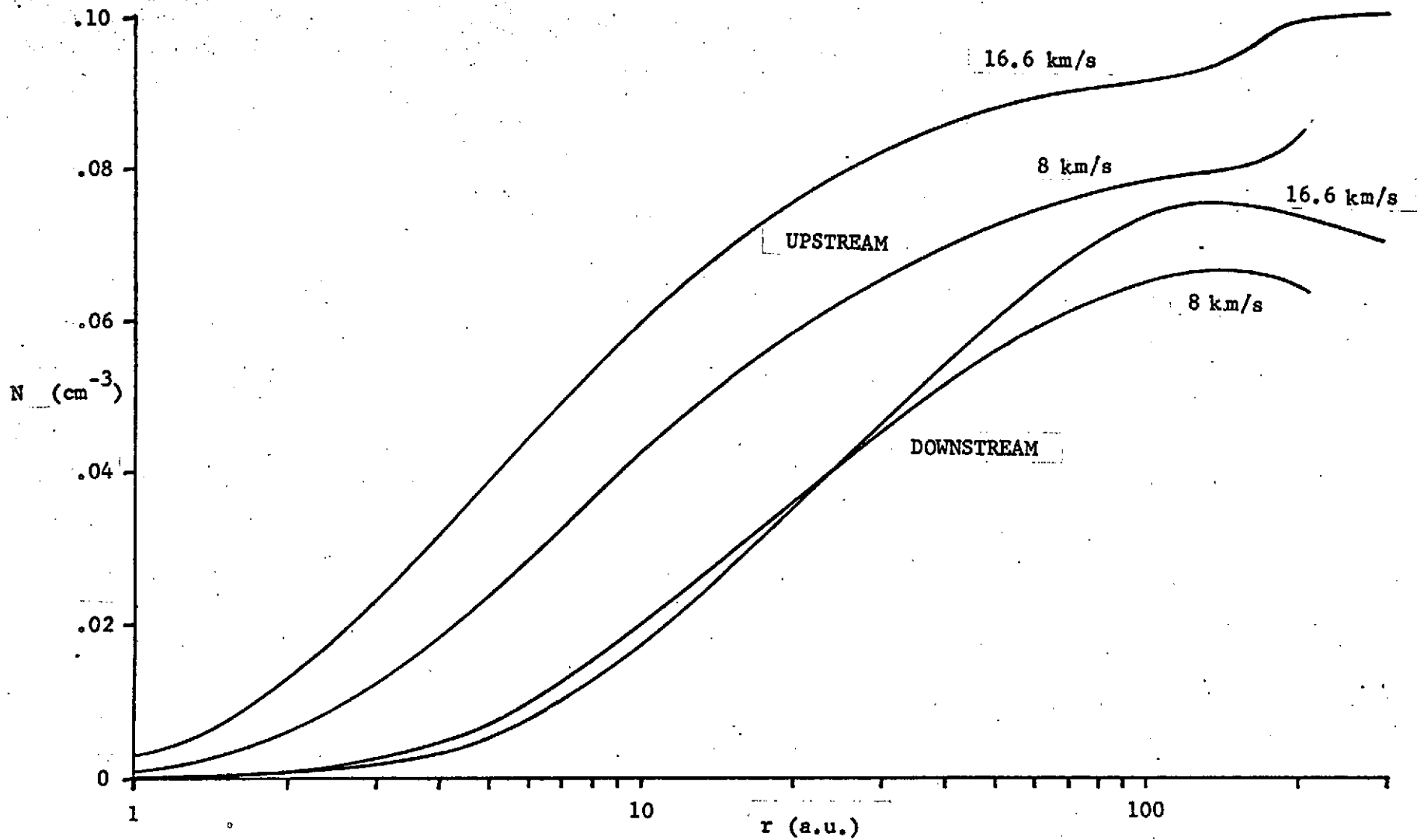


Figure 6. Comparison of profiles of hydrogen number density for  $N_0 = 0.1 \text{ cm}^{-3}$ ,  $T_0 = 10^4 \text{ }^\circ\text{K}$ , and  $V_0 = 8 \text{ km/s}$  and  $16.6 \text{ km/s}$ .

temperature. The higher the thermal speed relative to the bulk speed the steeper the angles  $\beta$  for trajectories and the closer to the sun can hydrogen atoms fill in the cavity on the downstream axis. Farther from the sun on the downstream axis the mean penetration distance through the subsonic region and the mean penetration speed govern the surviving number density jointly. The former decreases while the latter increases with  $V_0$  leading to increased penetration of the solar wind and in Figure 6 the result that the two number density profiles for the rearward axis eventually cross. The existence of maxima and subsequent decline in both profiles with distance on the rearward axis is associated with the evasion of the denser solar wind regions near the sun on the one hand and the progressive lengthening of attenuation paths through the subsonic solar wind region on the other.

Finally in Figure 6 we observe that for hydrogen at the same temperature a difference in assumed bulk speed has a considerably greater impact on predicted surviving number density on the forward axis than on the rearward.

### 3. Predicted Intensity of Solar Lyman- $\alpha$ Backscatter from Hydrogen

When the intensity of solar Lyman- $\alpha$  backscatter at 1 a.u. is measured in Rayleighs (1 Rayleigh  $\sim \frac{10^6}{4\pi}$  photons  $\text{cm}^{-2} \text{sec}^{-1} \text{ster}^{-1}$ ) the derivative of the intensity and the intensity (section 1.4d) are represented on the axis of flow by

$$\frac{dI}{dr} = \frac{g_e r_e}{10^6} \frac{N}{r^2} \quad (3.3-1)$$

$$I = \frac{g_e r_e}{10^6} \int_1^{\infty} \frac{N}{r^2} dr \quad (3.3-2)$$

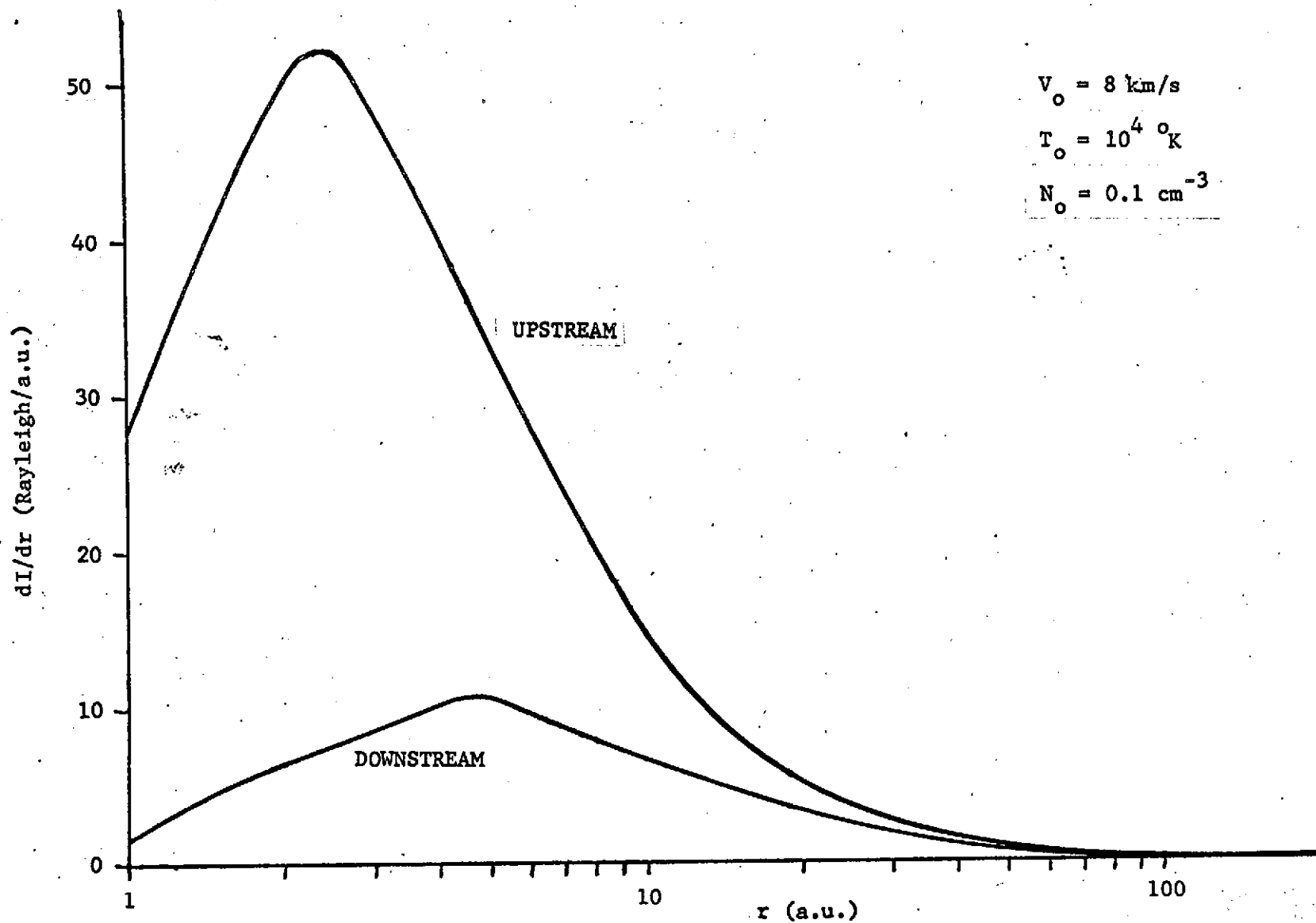


Figure 7. Derivative of the Lyman- $\alpha$  backscatter intensity function for line of sight along upstream and downstream axes of flow.

where  $N$  is the hydrogen number density,  $g_e$  the single atom scattering rate at 1 a.u. has the value  $2.28 \times 10^{-3} \text{ s}^{-1}$ ,  $r_e$  is  $1.5 \times 10^{13} \text{ cm}$ , and  $r$  is measured in a.u. For the number density profiles shown in Figure 5 for hot hydrogen, the profiles of the derivative of the intensity are plotted in Figure 7. We note that the largest contributions to the predicted intensity come from distances closer to 1 a.u. on the upstream axis than on the downstream axis and that the intensity integrals in both directions find effective convergence in the vicinity of 100 or 200 a.u.

Table 7 contains relevant parameters and results from a varied set of computer runs made with the model. In the table U and D stand respectively for the predicted intensities at 1 a.u. on the upstream and downstream axes of flow and U/D stands for the ratio of these intensities. Inspection of the table reveals the following qualitative trends

$$\begin{aligned} \frac{\partial U}{\partial T_0} > 0, & \quad \frac{\partial D}{\partial T_0} \gg 0, & \quad \frac{\partial U/D}{\partial T_0} < 0 \\ \frac{\partial U}{\partial v_0} \gg 0, & \quad \frac{\partial D}{\partial v_0} < 0, & \quad \frac{\partial U/D}{\partial v_0} \gg 0 \\ \frac{\partial U}{\partial N_0} \gg 0, & \quad \frac{\partial D}{\partial N_0} \gg 0, & \quad \frac{\partial U/D}{\partial N_0} \approx 0 \end{aligned} \quad (3.3-3)$$

The trends evident in the last column in relations (3) make the ratio U/D an attractive estimator of the interstellar wind velocity from satellite measurements of Lyman- $\alpha$  backscatter. The ratio of measurements is independent of error in the absolute calibration of the measuring instruments. And the ratio of predicted intensities are



Table 7. Synopsis of computer runs with model predicting solar Lyman- $\alpha$  backscatter on upstream and downstream axes of flow

$T_o$ ( $^{\circ}K$ )	$N_o$ ( $cm^{-3}$ )	$V_o$ (km/s)	U (Rayleigh)	D	U/D	INT. LIM. (a.u.)	$R_s$ (a.u.)	$X_o$ (a.u.)
$10^4$	0.2	16.6	1510	339	4.45	100	98	129
"	"	6	788	374	2.11	"	124	256
"	"	0.6	312	205	1.52	"	129	779
$10^5$	"	6	1604	1187	1.35	"	55	161
$4 \times 10^4$	"	"	1256	827	1.52	"	80	195
$10^4$	"	"	788	374	2.11	"	124	256
$5 \times 10^3$	"	"	666	259	2.57	200	139	257
$10^3$	"	8	636	84	7.57	"	150	231
$5 \times 10^3$	0.2	6	666	259	2.57	"	139	257
"	0.15	"	497	194	2.56	"	147	282
$5 \times 10^3$	0.2	8	803	255	3.15	"	134	218
"	"	6	666	259	2.57	"	139	257
"	"	4	530	254	2.09	"	144	319
$10^4$	0.1	12	580	176	3.29	100	133	223
"	"	10	516	181	2.85	"	138	248
"	"	8	454	185	2.45	"	142	281
"	"	10	531	193	2.75	200	138	248
"	"	8	468	197	2.38	"	142	281

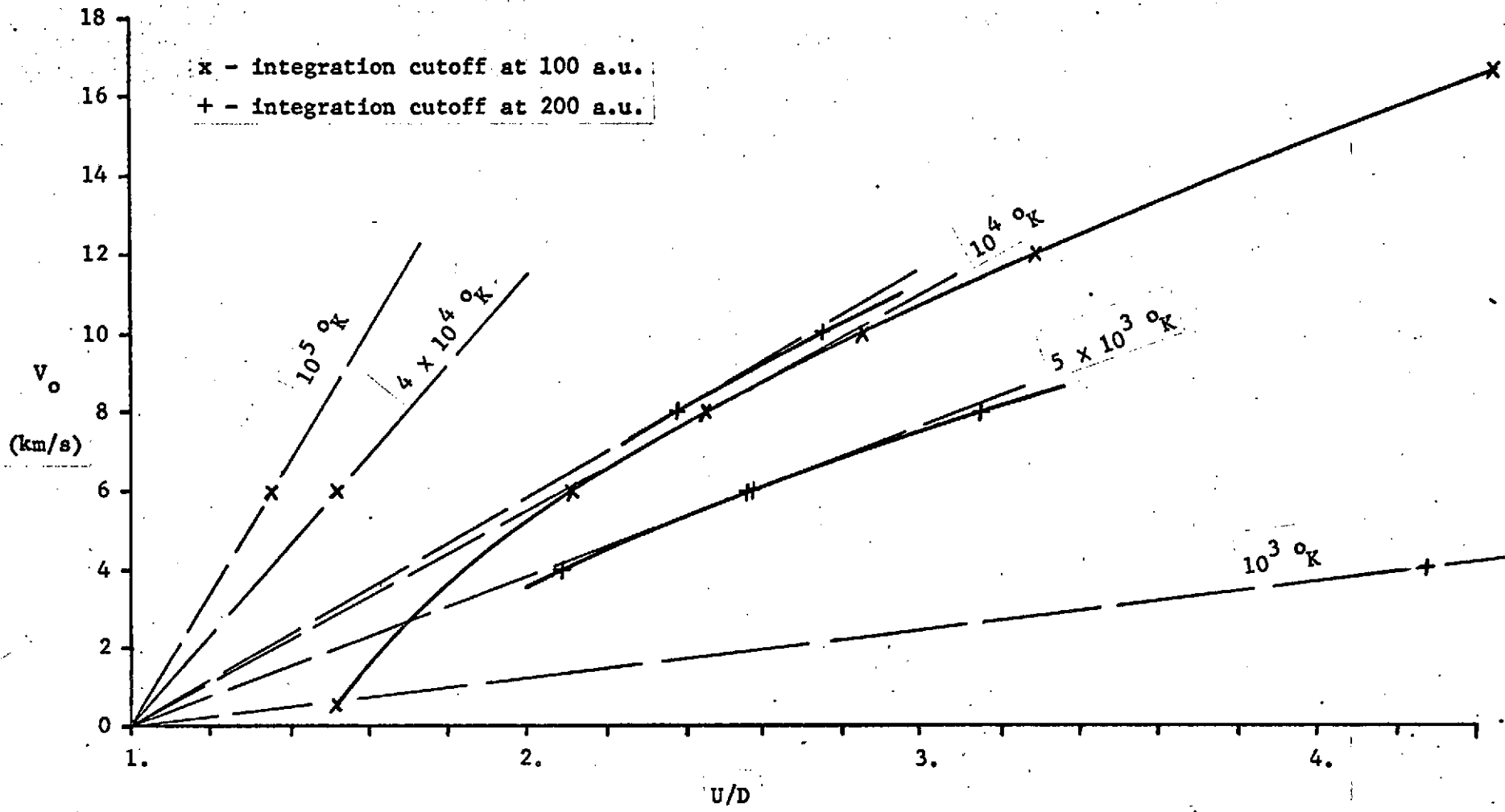


Figure 8. Plot of velocity of the interstellar wind vs. computed upstream to downstream Lyman- $\alpha$  backscatter intensity ratio for parameter temperature.

insensitive to the estimate of the density of the interstellar gas. Thus the estimator of the interstellar wind velocity from the  $U/D$  ratio is sensitive mostly to the estimate of the temperature of the interstellar gas.

From the data of Table 7 the predicted ratios  $U/D$  are plotted versus interstellar wind speed in Figure 8. The points plotted with an x are for integrations cut off at 100 a.u. and with a + at 200 a.u. Where two or more points are for the same temperature, curves of constant temperature are drawn. Evidently substantial portions of the constant temperature curves for  $T_0 = 10^4 \text{ }^\circ\text{K}$  and  $T_0 = 5 \times 10^3 \text{ }^\circ\text{K}$  approximate straight lines which intercept the point (1,0). Theoretically the point (1,0) would be occupied in the instance of the spherically symmetric flowfield that would obtain were the sun at rest in the interstellar gas. Straight lines to indicate both the trend of the constant temperature curves and the spatial organization of the data with temperature have been drawn through the points - even single ones - for all temperatures represented in the set of computations.

Because the angles that trajectory lines make for different  $V_0$  and  $c_s$  are geometric invariants for constant ratio  $V_0/c_s$  (or equivalently  $V_0/\sqrt{T_0}$ ), it is of interest to replot the data of Table 7 and Figure 8 as the ratios  $V_0/c_s$  vs  $U/D$ . Figure 9 shows the data so plotted. With the exception of one point the data so organized describe a universal curve for which  $V_0/\sqrt{T_0}$  can be regarded as the independent variable.

For the points which fall on the curve, the dashed line indicates the curve is highly linear for  $V_0/c_s < 1$ . The point for  $V_0 = 0.6 \text{ km/s}$ ,  $T_0 = 10^4 \text{ }^\circ\text{K}$  falls off the curve but in the region of the graph ( $V_0/c_s \ll 1$ ,  $U/D \sim 1$ ) where the curve is linear. The point for

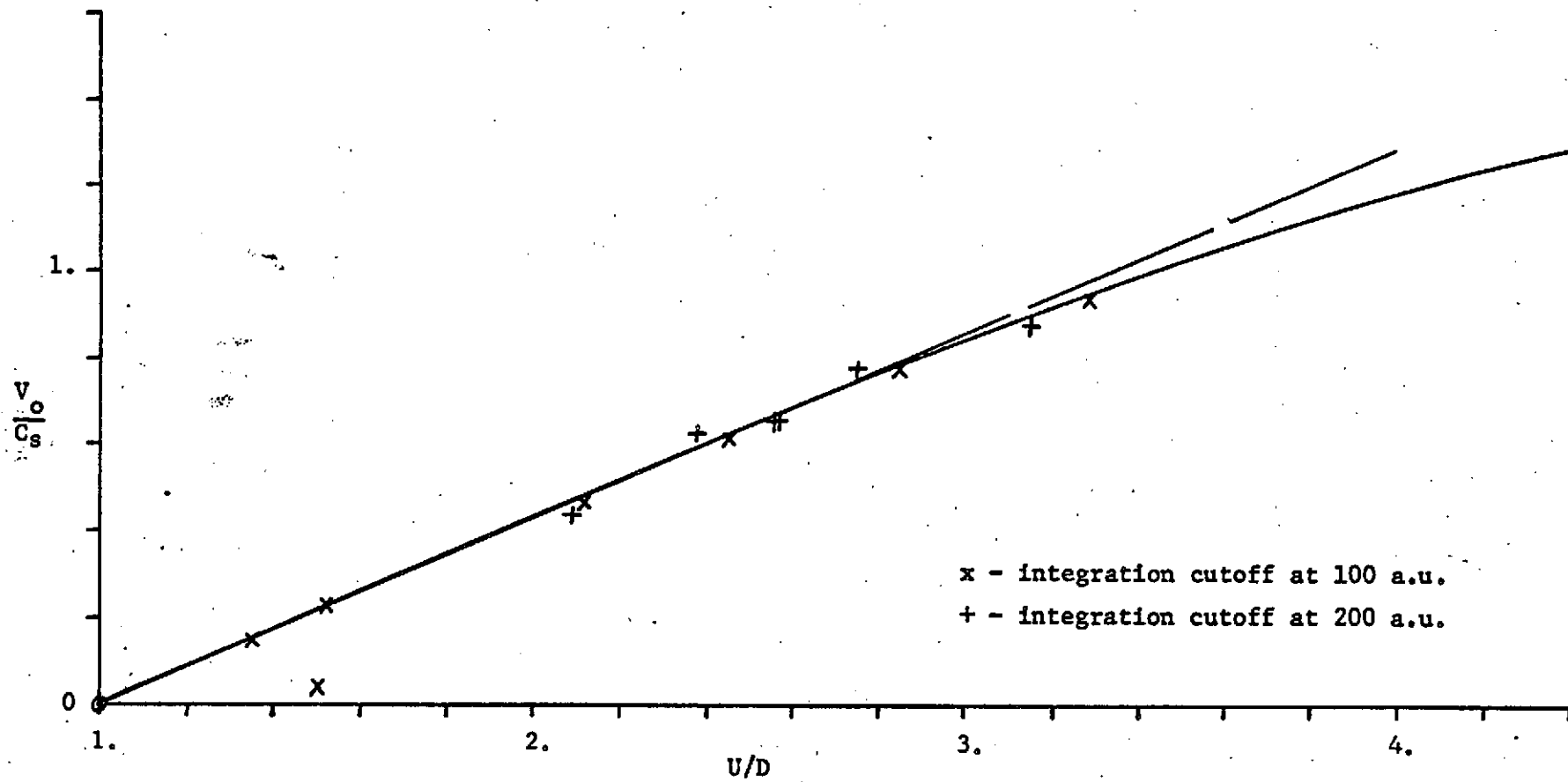


Figure 9. Universal plot of ratio of interstellar wind velocity to most probable thermal speed vs. ratio of computed upstream to downstream Lyman- $\alpha$  backscatter intensities.

$V_0 = 16.6$  km/s,  $T_0 = 10^4$  °K falls on the curve but out of the region of linearity ( $V_0/c_s > 1$ ). The evidence is that the model predicts results that describe a curve that is linear and will occupy the point (1,0) only in the limit  $T_0 \rightarrow \infty$ ,  $V_0$  large and finite but that such a curve is not described for  $T_0$  finite and  $V_0$  small approaching the limit  $V_0 \rightarrow 0$ . As can be seen in the model for the extended Parker solution, the conditions securing the domain of linearity above have to do physically with restricting the size and relative importance of the subsonic region of the solar wind in favor of the supersonic region. For small  $V_0$  the aspherical subsonic region becomes enormous (Table 7).

#### 4. Estimate of the Mach Number and Speed of the Interstellar Wind

Table 8 contains intensity ratios  $I_{\max}/I_{\min}$  obtained from satellite measurements reported by Bertaux and Blamont (1971, 1972) and Thomas and Krassa (1971). (See Thomas, 1972.) The authors cited have argued the correspondence of their observations to the physical model to which we have given the mathematical representation and from which computed the predicted intensity ratios U/D above. In particular and in conformity with the predictions of our model, they have inferred that the maximum and minimum intensities should be observed respectively when the observational lines of sight are along the upstream and downstream axes of flow.

Table 8 - Maximum and minimum intensity<sup>1</sup>  
of solar Lyman- $\alpha$  backscatter measured  
by earth satellite at 1 a.u.

Maximum	Minimum	Ratio	Instrument
580	240	2.42	LASP
570	250	2.28	LASP
460	180	2.55	Paris
525	200	2.62	Paris

<sup>1</sup> data extracted from Figure 3 of Thomas (1972)

We note that the measured intensity ratios fall in the linear portion of our universal curve which accordingly we may represent by the expression

$$V_o/c_s = \frac{1}{2.4} (U/D - 1) . \quad (3.4-1)$$

Since the speeds of sound in either the neutral or ionized components of the interstellar gas and the most probable thermal speed in the neutral gas are all proportional to  $\sqrt{T_o}$ , the left hand side of equation (3.4-1) is proportional to the Mach number in the continuum flow of the ionized fraction. Thus from equation (3.4-1) with the inferred correspondence between  $I_{\max}/I_{\min}$  and U/D and from measurements of  $I_{\max}/I_{\min}$  we derive the direct estimator of the Mach number of the sun in the interstellar wind

$$\hat{M} = \frac{1}{3.1} \left[ \left( \frac{\hat{I}_{\max}}{\hat{I}_{\min}} \right) - 1 \right] \quad (3.4-2)$$

The mean of the intensity ratios in Table 8 is 2.47 for which equation (2) gives the Mach number 0.475. Rounding off meaningless digits, we take 0.5 as our estimate for the Mach number of the sun in the local interstellar medium.

Further taking  $10^4$  °K for the estimate of  $T_o$  we have 12.8 km/s for  $\hat{c}_s$ . Then from equation (3.4-1) with U/D replaced by the estimate 2.47 for  $I_{\max}/I_{\min}$  we get 7.84 km/s for  $\hat{V}_o$ . Thus we take 8 km/s as our estimate of the speed of the sun with respect to the local interstellar gas.

This number differs substantially but not radically from the earlier estimate of 6 km/s found for the same assumed temperature ( $10^4$  °K) by Thomas, 1972 with a less detailed model. Thomas' model featured an interstellar wind having a single constant speed, isotropically distributed thermal component traversing a constant speed supersonic solar wind of infinite extent.

## Chapter IV - Summary and Discussion

The termination of the solar wind has been described from the theoretical point of view as the problem of finding a model for the extended solar corona such that admissible boundary conditions match conditions in the perturbed local interstellar medium

As a prelude to formulating a mathematical model, certain theoretical foundations of our understanding of the problem have been reexamined in Chapter I. in the light of most recent findings concerning the states of the solar wind and the local interstellar medium. In particular, the findings that have had the greatest impact on the present exposition and have served in considerable measure to distinguish it from earlier work are that the local interstellar medium has a high temperature  $\sim 10^4$  °K, is partially ionized  $\sim 10\%$ , and blows past the sun with subsonic velocity  $\sim$  Mach 0.5.

Given these findings, investigation of Parker's early (1961) analytical model for the termination of the solar wind suggested that a simple reinterpretation or extension of the model provides a useful approximate description of the adjacent flows of the solar wind and the ionized interstellar wind.

An investigation of solar wind temperature along lines of the one dimensional compressible flow equation and heating associated with polytropic solutions brought to light additional evidence that either or both the classical coefficient of thermal conductivity is too high — perhaps by as much as a factor of five — and the associated classical inhibition of heat conduction by the embedded transverse magnetic field is overstated for the bulk of low temperature ( $\sim 10^5$  °K) electrons comprising the quiet solar wind in the vicinity of earth.

The scale of effects of photoionization and charge exchange are investigated both for protons and neutral hydrogen atoms in the three regimes of

plasma flow — supersonic solar wind, subsonic solar wind, and ionized interstellar wind. In the analysis the properties of the plasma flow regimes were taken from the extended Parker solution. The results suggest that in the ionized interstellar wind region photoionization and charge exchange may be ignored in the solution of the hydrogen transport problem but that charge exchange does contribute a significant drag on the flow of the ionized component of the interstellar wind around the heliopause. In the subsonic solar wind region photoionization is not important; charge exchange, however, while having only small effect on the transport of hydrogen, acts significantly to cool the flow of the solar wind. In the supersonic solar wind both photoionization and charge exchange have an impact on the transport of hydrogen and on the flow of the solar wind.

In the latter region a linear perturbation solution has been found that adequately describes the effects of both processes on the solar wind flow. The solution exhibits the point that as the result of photoionization of hydrogen the addition of mass and associated decrease of velocity of the supersonic solar wind has no first order effect on the momentum flux and thus the location of the shock surface. The effect of charge exchange was found to decrease by 14% the estimate of the shock radius as given by the extended Parker solution.

The preliminary investigation concluded with the finding that within experimental uncertainties the opposing forces of solar gravitation and radiation pressure from solar Lyman- $\alpha$  scattering are in balance for hydrogen. Then, in view also of the large mean free paths for collisions of all kinds, the assumption was made that the trajectories of interstellar hydrogen atoms are straight lines into the solar system.



In Chapter II, a mathematical model was formulated to describe the transport of interstellar hydrogen into the solar wind and the adjacent flow of the solar wind with the ionized component of the interstellar wind. The global formulation begins with the Boltzmann's equations for both neutral and plasma species.

Ultimately the flow of the plasma species is described through a model on the level of one-fluid magnetohydrodynamics. The model is developed through the plasma transport equations in the manner of and with the transport terms given by Braginskii (1965). Source terms for the mass, momentum, and energy equations in conservation law form derive from the interaction of the neutral component of the interstellar wind with the solar wind and ionized interstellar wind plasmas. Except in the immediate vicinity of the stagnation point singularity, the frozen magnetic field approximation has validity. In the solar wind, quasi-normal, strong shock relations apply on a closed surface surrounding the sun. Tangential discontinuity relations apply at the free surface (heliopause) between the solar wind and ionized interstellar wind flows.

We note that the latter relations demand that the normal component of magnetic field vanish at the heliopause. Except in the unlikely case of purely field aligned flow, the vanishing of the normal field component will lead to an imbalance of magnetic field strength around the perimeter of the intersection of the heliopause with any plane normal to the axis of flow. The associated imbalance in the Lorentz forces of pressure normal to the perimeter and tension along the perimeter must then progressively push in the perimeter where the field is concentrated and permit the perimeter to squish out where the field is weakened, the motion taking place in time as the plane and the perimeter are convected downstream with the flow.

Thus the shape of the heliopause downstream of the sun is not expected to be axisymmetric as described by the extended Parker solution but, rather, to be "delta winged", tapering from more or less circular cross sections near the sun to thin ellipse-like sections far downstream. Of course, the asphericity of the near interplanetary magnetic field embedded in the solar wind must also contribute to the departure of the heliopause from axisymmetry. To describe in some quantitative fashion the scale of the departure of the heliopause from axisymmetry must be regarded as one of the outstanding theoretical problems associated with the termination of the solar wind.

In the field free, single collision approximation adopted for the transport of neutral hydrogen, the Boltzmann equation reduces to a continuity equation for the distribution function. Since the fast secondary hydrogen products of charge exchange have been shown by Holzer (1972) to have negligible importance, the continuity equation has only source terms for removal of hydrogen through photoionization and charge exchange. But the source term for the neutrals to suffer charge exchange depends on the density of ions and the source terms of the hydrodynamic equations for the plasma flow depend on the density of neutrals. Thus the two formulations are coupled. To resolve the impasse at least for the first iteration of solution, the extended Parker solution was assumed for the plasma and the hydrogen transport problem solved in the approximation afforded.

To the latter end, an efficient semianalytical numerical algorithm (Chapter III.) has been developed to carry out the solution on the needed level of moments of the hydrogen distribution function. The algorithm depends on approximating the figure of the heliopause by a prolate ellipsoid - cylinder which is fit to the heliopause, first, at the stagnation point; secondly, in a plane that includes the sun and is normal to the axis of flow; and, finally, asymptotically far downstream.

The algorithm has been used to compute profiles of hydrogen number density on the upstream and downstream axes of flow. Using the single scattering model developed at the end of Chapter I., we have computed intensities of backscattered solar Lyman- $\alpha$  radiation predicted to be observed at 1 a.u. as the result of scatter from hydrogen distributed according to the previously computed axial profiles. The results of computations for a varied set of parameters of the interstellar wind has been found over a substantial range to exhibit a strong linear dependence between predicted ratios of upstream to downstream backscatter intensity and the ratios of the independent variables bulk velocity and most probable thermal speed of the interstellar hydrogen.

Bertaux and Blamont (1972) and Thomas (1972) have provided the interpretation that the maximum and minimum backscatter intensities found in satellite observations occur respectively when the lines of sight are along the upstream and downstream axes of flow. Since the ratios of maximum to minimum intensity observed by satellite fall in the linear range of our predictive model for upstream to downstream intensity ratios and given the inferred correspondence between these ratios, we inferred that observation of maximum to minimum backscatter intensity provides a sensitive measure of the ratio of the speed of the sun through the local interstellar gas to the most probable thermal speed of the gas. Further, since the most probable thermal speed and the speed of sound are in constant ratio, the observation of Lyman- $\alpha$  backscatter provides a sensitive measure of the Mach number of the sun through the interstellar gas. Based on the ratios of observed maximum to minimum backscatter intensity reported by Bertaux and Blamont (1971) and Thomas and Krassa (1971) the Mach number that we found is 0.5 with respect to the ionized component of the interstellar wind.

Given the estimate  $10^4$  °K for the temperature of the interstellar medium, the corresponding estimate for the speed of the interstellar wind is 8 km/s. We note that with respect to Mach number, consistency has been found between the predictions of the model and the assumption that the flow is subsonic as required by the extended Parker solution. While being fully cognizant it is only an approximation, the latter solution we have represented as being a useful approximation for the analytical purposes we have made of it. In particular since the backscatter intensity integral finds effective convergence well within the distance to the stagnation point and most of the scattering comes from within the supersonic region, we do not expect anticipated departures of the solution from that used here to greatly affect the estimate of the Mach number.

However, as Holzer (1972) and Axford (1972) have discussed, the strengthening of the magnetic field lines by stretching and curvature in both the subsonic region of the solar wind and in the interstellar wind and by cooling of the subsonic solar wind through charge exchange introduces additional compression in the region beyond that predicted by the Bernoulli equation. To assess the scale of these additional, highly nonlinear, three dimensional effects on the dimensions of the flowfield really requires a full numerical solution of a model on the order of that developed here. Given present uncertainty in the measurement of astrophysical quantities, such a solution may not provide measurably greater information than we currently possess about the absolute state of the system. And obtaining such a solution will be a formidable and costly task, but having a solution for even one set of nominal conditions — hopefully with a transverse interstellar magnetic field — would constitute a most fascinating contribution in structural detail.

## References

- Allen, C. W. (1963) Astrophysical Quantities, 2nd ed., p. 18, Athlone Press, University of London.
- Axford, W. I.; Dessler, A.J. and Gottlieb, B. (1963) Termination of solar wind and solar magnetic field, Astrophys. J., 137, 1268.
- Axford, W. I. (1972) Interaction of the solar wind with the interstellar medium, in Solar Wind, NASA SP-308, p. 609, Washington, D. C.
- Banks, P. M. and Kockarts, G. (1973) Aeronomy, Part A, Academic Press, New York, N. Y.
- Barnes, A. and Hartle, R. E. (1972) Model for energy transfer in the solar wind: model results, in Solar Wind, NASA SP-308, p. 219, Washington, D.C.
- Barth, C. A. (1969) Planetary ultraviolet spectroscopy, Appl. Opt., 8, 1295.
- Bertaux, J. L. and Blamont, J. E. (1971) Evidence for source of an extra-terrestrial hydrogen Lyman-alpha emission: the interstellar wind, Astron. Astrophys., 11, 200.
- Bertaux, J. L. and Blamont, J. E. (1972) Observation of Lyman- $\alpha$  emission in interplanetary space, in Solar Wind, NASA SP-308, p. 661, Washington, D. C.
- Biermann, I.; Brosowski, B. and Schmidt, H. U. (1967) The interaction of the solar wind with a comet, Solar Physics, 1, 254.
- Blum, P. W. and Fahr, H. J. (1970) Interaction between interstellar hydrogen and the solar wind, Astron. and Astrophys., 4, 280.
- Blum, P. W. and Fahr, H. J. (1971) Interpretation of extraterrestrial Lyman-alpha observations, Nature, 231, 171.
- Bondi, H. (1952) On spherically symmetrical accretion, M. N. Royal Astron. Soc., 112, 195.
- Braginskii, S. I. (1965) Transport Processes in a Plasma, in Reviews of Plasma Physics, M. A. Leontovich ed., vol. 1, p. 205, Consultants Bureau, New York, N. Y.
- Brandt, J. C. (1961) Interplanetary gas. IV. Neutral hydrogen in a model solar corona, Astrophys. J., 133, 688.
- Bruner, E. C., Jr., and Parker, R. W. (1969) Hydrogen geocorona and solar Lyman-alpha line, J. Geophys. Res., 74, 107.
- Bruner, E. C., Jr., and Rense, W. A. (1969) Rocket observations of profiles of solar U. V. emission lines, Astrophys. J., 157, 417.

- Chamberlain, J. W. (1960) Interplanetary gas. II. Expansion of a model corona, Astrophys. J., 131, 47.
- Chamberlain, J. W. (1961) Interplanetary gas. III. A hydrodynamic model of the corona, Astrophys. J., 133, 675.
- Chapman, Sydney (1954) The viscosity and thermal conductivity of a completely ionized gas, Astrophys. J., 120, 151.
- Chapman, S. (1957) Smithsonian Contributions to Astrophys., 2, No. 1, p. 1, Washington, D. C.
- Clauser, F. (1960) 4th Symposium on Cosmical Gas Dynamics, Varenna, Italy.
- Cuperman, S. and Harten, A. (1972) Some physical implications of recent solar wind measurements, in Solar Wind, NASA SP-308, p. 244, Washington, D. C.
- Dalgarno, A. and Yadav, H. N. (1953) Proc. Phys. Soc. A, 66, 173.
- Dalgarno, A. (1957) in The Threshold of Space, M. Zelikoff ed., p. 186, Pergamon Press, London.
- Fahr, H. J. (1972) Influence of neutral interstellar matter on the expansion of the solar wind, in Cosmic Plasma Physics, p. 81, Plenum Press, New York, N. Y.
- Fite, W. L.; Smith, A. C. H. and Stebbings, R. F. (1962) Charge transfer in collisions involving symmetric and asymmetric resonance, Proc. Roy. Soc. A, 268, 527.
- Gosling, J. T. (1972) Temporal evolution of velocity structures in the solar wind, in Solar Wind, NASA SP-308, p. 202, Washington, D. C.
- Hinteregger, H. E.; Hall, L. A. and Schmidtke, G. (1965) Solar XUV radiation and neutral particle distribution in July 1963 thermosphere, Space Res., 5, 1175.
- Holzer, T. E. and Axford, W. I. (1970 a) The theory of stellar winds and related flows, Ann Rev. Astron. Astrophys., 8, p. 31.
- Holzer, T. E. and Axford, W. I. (1970 b) Solar wind ion composition, J. Geophys. Res., 75, 6354.
- Holzer, T. E. (1972) Interaction of the solar wind with the neutral component of the interstellar gas, J. Geophys. Res., 77, 5407.
- Hundhausen, A. J. (1968) Interplanetary neutral hydrogen and the radius of the heliosphere, Planet. Space Sci., 16, 783.
- Meier, R. R. (1969) Temporal variations of solar Lyman-Alpha, J. Geophys. Res., 74, 6487.
- Montgomery, M. D. (1972) Average thermal characteristics of solar wind electrons, in Solar Wind, NASA SP-308, P. 208, Washington, D. C.

- Parker, E. N. (1958) Dynamics of the interplanetary gas and magnetic fields, Astrophys. J., 128, 664.
- Parker, E. N. (1960) The hydrodynamic theory of solar corpuscular radiation and stellar winds, Astrophys. J., 132, 821.
- Parker, E. N. (1961) The stellar-wind regions, Astrophys. J. 134, 20.
- Parker, E. N. (1963) Interplanetary Dynamical Processes, vol. VIII of Interscience Monographs and Texts in Physics and Astronomy, R. E. Marshak, ed., Interscience, New York, N. Y.
- Patterson, T. N. L.; Johnson, F. S. and Hanson, W. B. (1963) The distribution of interplanetary hydrogen, Planet. Space Sci., 11, 767.
- Purcell, J. D. and Tousey, R. (1960) The profile of solar hydrogen-Lyman- $\alpha$ , J. Geophys. Res., 65, 370.
- Schatten, K. H. (1972) Large-scale properties of the interplanetary magnetic field, in Solar Wind, NASA SP-308, p. 65, Washington, D. C.
- Scudder, J. D. (1972) Comments to the paper "Average thermal Characteristics of solar wind electrons" by M. D. Montgomery, in Solar Wind, NASA SP-308, p. 211, Washington, D. C.
- Semar, C. L. (1970) Effect of interstellar neutral hydrogen on the termination of the solar wind, J. Geophys. Res., 75, 6892.
- Silk, J. (1973) Heat and ionization sources in the interstellar medium, Pub. Astron. Soc. Pacific, 85, 704.
- Spitzer, L., Jr. (1962) Physics of Fully Ionized Gases, No. 3 of Interscience Tracts on Physics and Astronomy, R. E. Marshak ed., Interscience Publishers, New York, New York.
- Stone, J. M. (1963) Radiation and Optics, McGraw-Hill, New York, N. Y.
- Thomas, G. E. and Krassa, R. F. (1971) OGO 5 measurements of the Lyman alpha sky background, Astron. Astrophys., 11, 218.
- Thomas, G. E. (1972) Properties of nearby interstellar hydrogen deduced from Lyman- $\alpha$  sky background measurements, in Solar Wind, NASA SP-308, p. 668, Washington, D. C.
- Whang, Y. C. (1972) Conversion of magnetic field energy into kinetic energy in the solar wind, in Solar Wind, NASA SP-308, p. 236, Washington, D. C.
- Wentzel, D. G. (1972) Interstellar motions: minuet or rock, Pub. Astron. Soc. Pacific, 84, 225.
- Weymann, R. (1960) Coronal Evaporation as a possible mechanism for mass loss in red giants, Astrophys. J., 132, 380.
- Wilson, O. C. (1960) A suggested mechanism for the ejection of matter from M-type stars, Astrophys. J., 131, 75.
- Wolfe, J. H. (1972) Large-scale structure of the solar wind, in Solar Wind, NASA SP-308, p. 170, Washington, D. C.